Calcium i valleprocesser. Teknologi og produkter

Final report

for collaborative projects funded via the Danish Dairy Research Foundation (DDRF)

1. Title of the project

Calcium during whey processing. Technology and products.

2. Project manager

Leif H. Skibsted, professor, Department of Food Science, University of Copenhagen, Rolighedsvej 30, DK-1958 Frederiksberg, +45 35 33 32 21, ls@food.ku.dk

3. Other project staff

Martina Vavrusova, post doc, Department of Food Science, University of Copenhagen, Rolighedsvej 30, DK-1958 Frederiksberg, mava@food.ku.dk

André C. Garcia, Ph.D. student, Department of Food Science, University of Copenhagen, Rolighedsvej 30, DK-1958 Frederiksberg, andregarcia@food.ku.dk

Hong Cheng, post doc, Department of Food Science, University of Copenhagen, Rolighedsvej 30, DK-1958 Frederiksberg, hong.cheng@food.ku.dk

4. Sources of funding

5. Project period

Project period with DDRF funding: Project start: 01/01/2014

                                                                              Project end: 30/06/2018

6. Project summary

Det er dokumenteret at den tungtopløselige mineralfraktion fra inddampning af valle kan opløses i nærvær af citrat. Citrat kan danne stærkt overmættede opløsninger af amorft calciumphosphat. Herved kan et rest-produkt fra produktion af laktose og valleproteiner anvendes i nye højværdiprodukter til forebyggelse af knogleskørhed. Sacchararat og isocitrat fra brombær synes at gøre overmætningen mere robust. En skånsom og miljøvenlig metode til rensning af procesanlæg på samme kemiske principper er udviklet.

Calcium from the insoluble mineral fractions from whey has been shown to solubilize in aqueous citrate forming strongly supersaturated solutions. The supersaturated calcium citrate/phosphate solutions may

form the basis for formulation of novel fortified foods and beverages with perspectives of improved calcium bioavailability. Saccharate and isocitrate from blackberry seems to increase the robustness of supersaturation.

Citric acid has been found to be an efficient cleaning agent for scale deposits in whey evaporator and processing equipment forming supersaturated solutions of calcium citrate. Flushing with cold water is recommended due to inverse solubility of calcium citrate tetrahydrade. Citric acid is environmentally friendlier and may replace the commonly used nitric acid in the dairy industry, with the benefit of producing calcium citrate from this process with acceptable purity for further technical use.

7. Project aim

Projektet vil kvantificere calciums binding til vallens proteiner og mindre molekyler med henblik på at beskrive tungtopløselige calciumsaltes udfældningskinetik under valles fraktionering og oprensning af værdistoffer fra valle. På baggrund af en skelnen mellem total-calcium, fri calcium-koncentration og calciumaktivitet under forskellige betingelser af temperatur, pH og ionstyrke, som forekommer under vallens fraktionering ved filtrering, justering af pH og inddampning af vallefraktioner, vil en forståelse af udfældningskinetik og overmætning for calciumphosphat, calciumcitrat og calciumlactat blive tilstræbt. Formålet er endvidere at kunne anvise procesbetingelser, der (i) styrer calcium-indhold i valleproteiner, (ii) forhindrer udfældning af calciumcitrat og calciumlactat i procesudstyr og af calciumphosphat i lactose, samt (iii) minsker tab af calcium og phosphat til spildevand.

1. Utilization of calcium in whey for future development of new products with increased calcium bioavailability.

2. Reduction of calcium and phosphate loss from whey processing to waste water.

3. Prevention of unintended precipitation of calcium salts in process lines

8. Background for the project

Whey proteins and lactose are valuable sidestreams from cheese production. The dairy industry may also utilize the mineral fraction from whey processing better. Calcium and phosphate are often wasted, but may be transformed into high-valuable mineral products for food supplements or for functional foods, with high calcium bioavailability. Calcium phosphate and calcium citrate scale today even present a problem for the processing lines.

9. Sub-activities in the entire project period

	2014				2015				2016				2017				2018		
Solubility of calcium salts	▓	▓	▓	▓	▓	▓												-	-
Supersaturation of calcium hydroxycarboxylates					▓	▓	▓	▓	▓	▓	▓	▓	▓	▓	▓	▓		-	-
Cleaning methods for processing equipment (scale)						▓	▓											-	-

	2014			2015			2016			2017			2018		
Calcium phosphate mobility							▓	▓	▓	▓	▓	▓		-	-
Pilot plant experiments at Arla Food Ingredients		▓					▓							-	-
Theoretical modeling of supersaturation						▓	▓	▓	▓	▓	▓	▓		-	-
Defense of PhD-thesis													▓	-	-

10. Project results

New information about the basic chemistry of calcium salts and mixtures of these salts, focusing on thermodynamics and kinetics, especially of supersaturation phenomena were obtained during the execution of this project.
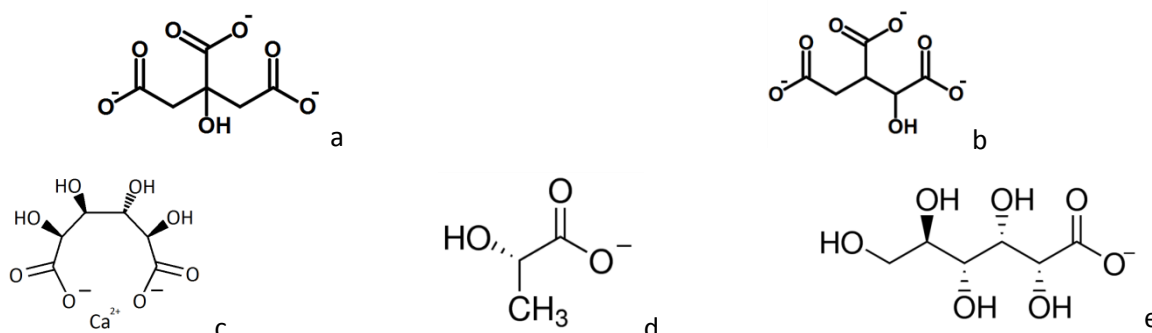

Figure 1. Structures of citrate ion (a), isocitrate ion (b), calcium saccharate (c), lactate ion (d), and gluconate ion (e).

Inverse solubility of calcium citrate and isocitrate

Aqueous solubility of calcium citrate tetrahydrate was found to decrease with increasing temperature, while the solubility of calcium citrate hexahydrate increased, with a transition temperature of 51.6 $^\circ$C between these two hydrates. The so-called reverse solubility is the result of the exothermic complex formation, but only for the tetrahydrate form with the moderate endothermic dissolution. It was also verified that citrate increases the solubility of calcium citrate with initial solubility overshooting resulting in supersaturated solutions, due to complex formation between calcium and citrate, as verified by the decrease in calcium ion activity. The tetrahydrate form of calcium citrate was found to precipitate at ambient temperature from moderate supersaturated solutions rather than calcium citrate hexahydrate, the less soluble form. Calcium isocitrate, a new compound synthetized in the project also precipitates as a tetrahydrate, which also shows reverse solubility. The complex formation between calcium and citrate and calcium isocitrate was fully characterized thermodynamically together with the dissolution equilibrium for temperature interval of relevance for whey processing as ΔH^o and ΔS^o.

3
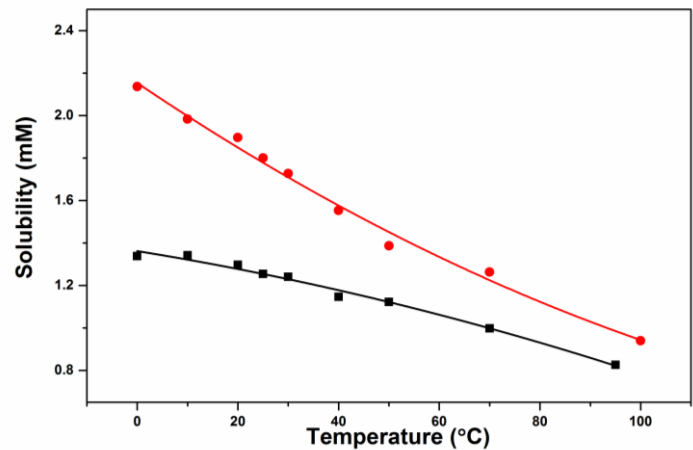
Figure 2. Solubility of calcium citrate tetrahydrate (in red) and calcium isocitrate tetrahydrate (in black).

≪======≫
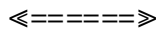
Calcium saccharate as a stabilizer of supersaturation

Calcium D-saccharate has low solubility, but stabilizes supersaturation of other calcium salts of biological importance. It was verified that the complex formation between calcium and D-saccharate ions is strongly exothermic and seems to be stabilized through ring formation. The complex formation is stronger than the endothermic and weaker complex formation between calcium and other hydroxycarboxylates, like L-lactate, D-gluconate, and D-lactobionate. It was also verified that in supersaturated solutions of calcium D-saccharate, free calcium concentration, monitored by calcium ion activity, is temperature independent and seems to be only slowly adjusted, which could explain the low driving force for precipitation of calcium D-saccharate from supersaturated solutions. From the experiments with combinations of calcium D-gluconate and D-saccharate, it seems that the exothermic complex formation between calcium and D-saccharate ions assists the dissolution of calcium D-gluconate, which is endothermic. The slow adjustment of calcium D-saccharate complexes formed leads to a supersaturated solution both with respect to calcium D-saccharate and calcium D-gluconate. The paradox that an even less soluble calcium salt may increase robustness of su-persaturated solutions of more soluble calcium salts seems to be explained by this slow equilibrium ad-justment.
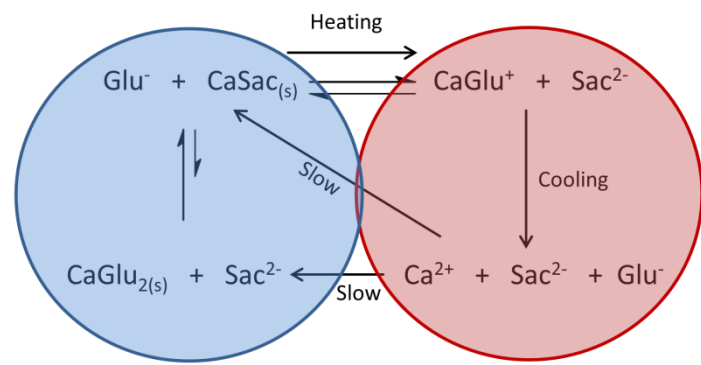

Figure 3. Scheme of stabilization effect of calcium D-saccharate on supersaturated solutions of calcium D-gluconate. The equilibrium and supersaturated conditions are represented in blue and red, respectively.

≪======≫
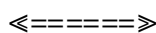
Environmentally friendly cleaning process based on spontaneous supersaturation

Scale deposits formed in evaporators for lactose production was characterized to be composed of mainly calcium citrate tetrahydrate with phosphate contaminations. The dissolution of 3.0 g scale by citric acid was investigated with different concentrations and volumes and showed to be effective, especially for concentrations of acid around 1.0 ml L^{-1} (for volumes from 25 to 100 mL). It was verified that the dissolution of scale by citric acid leads to spontaneous supersaturation in relation to calcium citrate, being the same overshooting mechanism described for dissolution of calcium citrate in excess of citrate. It was also verified that calcium citrate tetrahydrate slowly precipitates from these supersaturated solutions, with acceptable purity for further technical use. The inverse solubility of calcium citrate encourages use of cold water for flushing the process equipment. Mixed solutions of nitric and citric acids were also investigated and have showed synergistic effect for the dissolution of scale.
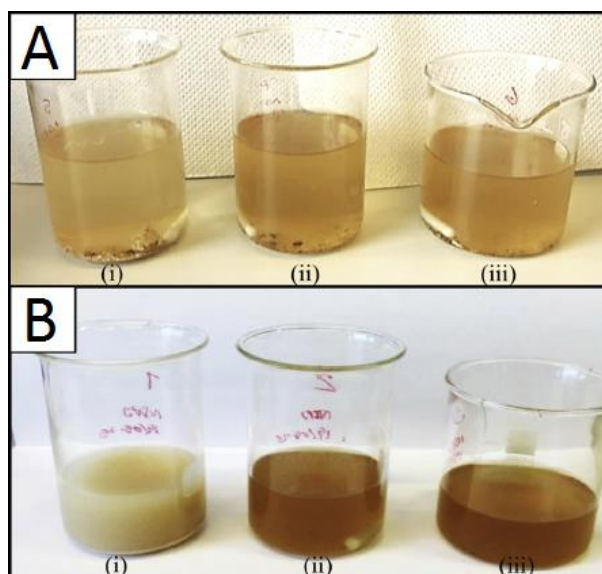

Figure 4. Suspensions prepared with 3.0 g of scale isolated from heating surface of an evaporator used to concentrate whey permeate from lactose production treated with: 100 mL (A) or 50 mL (B) of citric acid of concentration 0.1 mol L^{-1} (i), 0.5 mol L^{-1} (ii) or 1.0 mol L^{-1} (iii). The black material not dissolving is Maillard reaction products.

≪======≫

Spontaneous supersaturation of calcium hydroxycarboxylates

In relation to mixed solutions of calcium hydroxycarboxylates and citrate, citrate has been shown to assist the dissolution of calcium hydroxycarboxylates forming supersaturated solutions with respect to calcium citrate at constant temperature without heating. This spontaneous supersaturation depends on a combination of thermodynamic and kinetic effects, including stronger complex formation between calcium and citrate ions and a slow precipitation rate of calcium citrate. The dissolution of calcium hydroxycarboxylates by sodium citrate resulted in robust supersaturation with high degrees of supersaturation. For the dissolution of calcium L-lactate, a linear relationship between the degree of supersaturation and the concentration of added citrate was verified. The lag phase prior to the precipitation of calcium citrate has been shown to be shorter for higher degrees of supersaturation for calcium L-lactate and less dependent on the degree of supersaturation for calcium D-gluconate and calcium citrate. These findings seem to explain the positive effect of citrate in calcium absorption in humans.
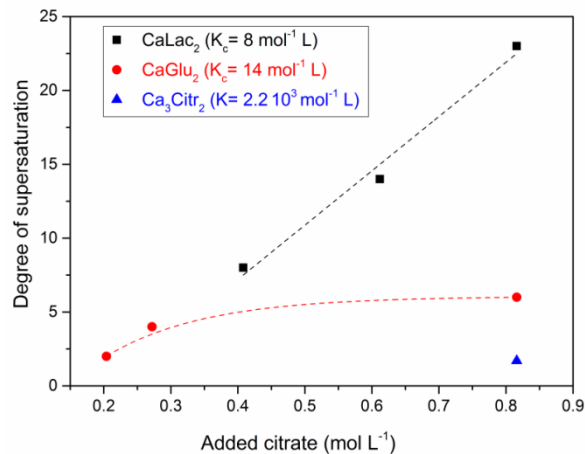
Figure 5. Degree of supersaturation of calcium citrate as function of added citrate in the dissolution of excess of calcium lactate, calcium gluconate and calcium citrate.

≪======≫
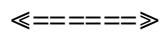
Solubilization of amorphous calcium phosphate in presence of citrate

In systems containing phosphate, citrate, and calcium ions, supersaturation with respect to calcium citrate was verified for acidic conditions. The dissolution of calcium hydrogenphosphate by hydrogencitrate may lead to solutions with a degree of supersaturation up to approximately 8. In a similar way, the acidification of suspensions containing amorphous calcium phosphate and citrate ions may form supersaturated solutions in relation to calcium citrate. It was also verified that depending on the resulting pH, the predominant species formed between calcium and citrate ions are different, but the crystallization rate of calcium citrate is the same for the same initial concentration of calcium at supersaturation, even if degrees of supersaturation are different for different pH. For more acidic conditions, it is suggested that calcium citrate tetrahydrate is formed from a solid state conversion of precipitated calcium hydrogencitrate, while for supersaturated solutions with higher pH this conversion may happen prior to the precipitation.
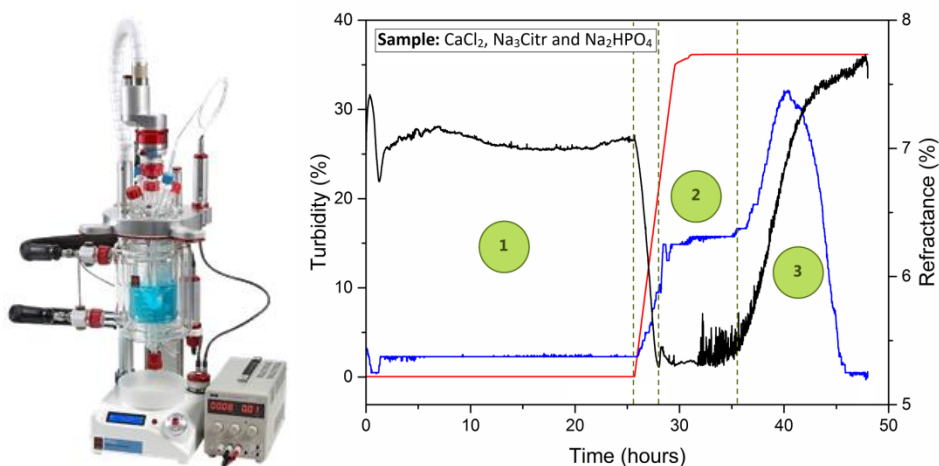

Figure 6. Atlas reactor equipped with a reaction vessel of 2.0 L, the equipment used for the experiments at Arla Food Ingredients. The plot shows the time evolution of turbidity (black), refraction index (blue) and the addition of HCl (red). 1: instant precipitation of amorphous calcium phosphate; 2: supersaturation of calcium citrate after acidification for 8 hours; 3: slow precipitation of calcium citrate.

≪======≫

DGL as a mobilizer of calcium phosphate

Calcium hydrogenphosphate dissolves freely in aqueous δ-gluconolactone (DGL)/gluconate forming supersaturated solutions in relation to calcium gluconate. These solutions can be supersaturated up to a factor of seven and the lag phase for precipitation of calcium gluconate is very long, up to 9 days, especially for undisturbed solutions and seems to be increased by the presence of calcium saccharate. A linear relationship between the critical concentrations of gluconate required to dissolve increasing amounts of calcium hydrogen phosphate was determined. The spontaneous supersaturation seems to be limited by the solubility product of calcium hydrogenphosphate, while the equilibrium concentration is controlled by the solubility product of calcium gluconate. Such dissolution overshooting in the presence of gluconate and other hydroxycarboxylates may not only increase calcium bioavailability, but may also be important during acidification of cheese milk by δ-gluconolactone. During curd formation initiated by δ-gluconolactone, calcium may be mobilized from binding to phosphate esters in caseins and increase the formation of protein network. Such cheese based on chemical acidification may also have higher bioavailability of calcium due to the presence of hydroxycarboxylates or their mixtures, especially gluconate, as gluconate from δ-gluconolactone may induce spontaneous supersaturations.
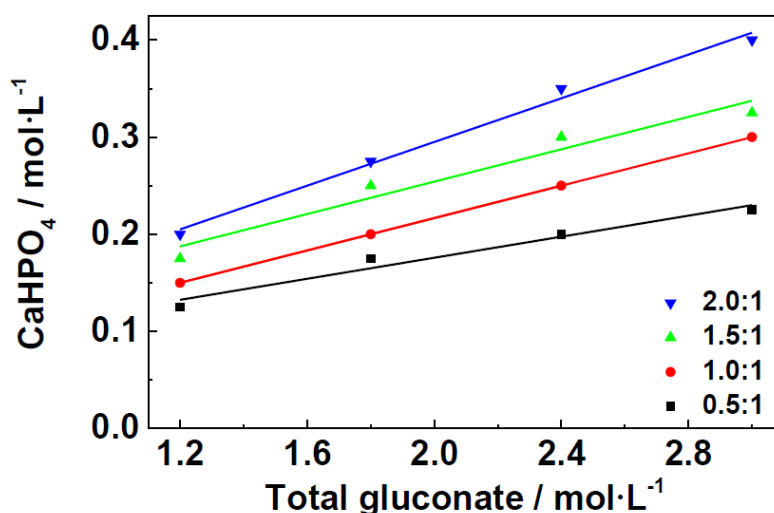

Figure 7. Critical combination of calcium hydrogenphosphate and total gluconate for which complete dissolution occur forming supersaturated solutions, the different colors represent different δ-gluconolactone / gluconate ratios. Below each line the solutions are supersaturated, above two-phase regions are found.

≪======≫

Calcium isocitrate: a new compound

Calcium isocitrate tetrahydrate was characterized and found to have lower solubility in water than calcium citrate tetrahydrate. The solubilities of both calcium salts decrease with increasing temperatures, but increase with pressure. It was observed that calcium isocitrate dissolves freely in aqueous sodium citrate forming spontaneously supersaturated solutions from which calcium citrate precipitation initiate after several hours. For similar conditions, calcium citrate dissolves in aqueous sodium isocitrate forming robust supersaturated solutions in relation to calcium isocitrate, from which no precipitation is observed for several months. Heating these solutions to 65 °C, however, initiates the precipitation. For calcium isocitrate in aqueous sodium isocitrate and for calcium citrate in aqueous sodium citrate, such isothermal supersaturations are less significant, but are induced by high hydrostatic pressure. The lag phase for precipitation of calcium citrate after pressure release is of a few hours, calcium isocitrate has an expressively longer lag phase of one week prior to precipitation. The extreme supersaturation robustness for calcium citrate dissolved in aqueous sodium isocitrate may be explained by the slow crystallization kinetics of calcium iso-

citrate probably in combination with an inhibiting effect of citrate on calcium isocitrate precipitation. Calcium citrate dissolved in aqueous isocitrate may form the basis for functional beverages with increased bioavailability of calcium, which could be based on blackberry as a natural source of isocitrate. The increased solubility of calcium citrate and calcium isocitrate for conditions of increased hydrostatic pressure may be a further invitation for the use of this non-thermal technique for mild processing.
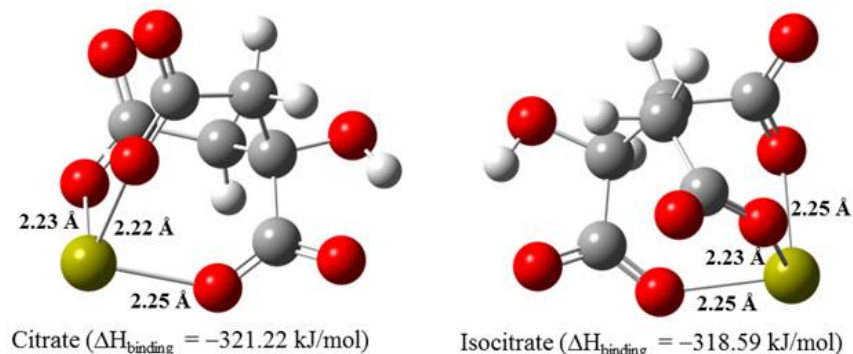

Figure 8. Optimized structure of calcium binding to citrate and isocitrate by density functional theory (DFT) calculation, confirming the stronger binding of calcium to citrate than to isocitrate as determined electrochemically.

≪======≫

Future perspectives

The robustness of the supersaturations studied in this project seems to be due to stronger calcium complex formation and slow free calcium adjustment, which seems to lower the driving force of precipitation. The supersaturation phenomena of calcium salts might have an important role in calcium nutrition and also in physiological process, like bone biomineralisation. The spontaneous supersaturations, especially the unique role of citrate, might be an inspiration for the formulation of novel fortified foods and beverages with perspectives of improved calcium bioavailability. δ-gluconolactone may even have an unrecognized role in improving calcium bioavailability from certain cheeses. Isocitrate, as is found in blackberry, should be studied further for the effect on supersaturation of calcium citrate.

11. Deviations

11.1 Scientific

Less attention has been payed to the importance of calcium binding by proteins for precipitation of calcium phosphate and calcium hydroxycarboxylates from whey. The effect was studied early in the project, but was found of less importance than originally believed. However, in a parallel study by Ning Tang, a Chinese PhD student collaborating with the MFF project, very interesting results concerting calcium binding to peptides were obtained and published in Journal of Agricultural and Food Chemistry (Tang, N.; Skibsted, L. "Calcium binding to amino acids and small glycine peptides in aqueous solution: toward peptide design for better calcium bioavailability". *Journal of Agricultural and Food Chemistry* (64), 2016, 4376-438). Also other aspects of the project became more demanding and promising for the overall goal of the projects. These aspects were related to the large supersaturation effects seen for combination of calcium hydroxycarboxylates including citrate/isocitrate combinations and of the robustness of supersatured solutions of calcium phosphate/citrate. The aspect of protein binding will be studied further in the continuing project, based on the results already published.

11.2 Financial

The project was supported originally by a 3-years PhD grant from CAPES to André C. Garcia, which was prolonged in six months.

11.3 Timetable

The project was originally scheduled with start in January 2013. The additional 50 % funding was, however, not available before late 2013 and the project was postponed with a start in January 2014. The project was prolonged to June 2018 within the original budget plus the additional funding from CAPES.

12. The relevance of the results, including relevance for the dairy industry

The principal of spontaneous isothermal supersaturation is new. It was first discovered for dissolution of calcium lactate in aqueous sodium gluconate (Vavrusova, M.; Skibsted, L. H. *Food and & Function* (5), 2014, 85) Lactic acid in combination with gluconic acid already find use as environmental friendly alternative to mineral acids for improvement of drilling through limestone (Rabie, A. I.; Saber, M. R.; El-Din, H. A. N. *SPE International Symposium on Oilfield Chemistry*, The Woodlands, Texas, US, 2015). Mobility of calcium phosphate by citrate has been studied in the current project and spontaneous supersaturation was shown during experiments in Arla Food Ingredients pilot plant to explain the solubilization of amorphous calcium phosphate from whey processing. This opens up for improving the calcium bioavailability from the whey mineral fraction in functional foods for prevention of osteoporosis. Stabilization of strongly supersaturated calcium phosphate/citrate solutions by hydroxycarboxylates, like saccharate and isocitrate, seems to hold the key for product formulation.

13. Communication and knowledge sharing about the project

Papers in international journals:

Vavrusova, M.; Skibsted, L. H. "Aqueous solubility of calcium citrate and interconversion between the tetrahydrate and the hexahydrate as a balance between endothermic dissolution and exothermic complex formation". *International Dairy Journal* (57), 2016, 20.

Garcia, A. C.; Vavrusova, M.; Skibsted, L. H. "Calcium D-saccharate: aqueous solubility, complex formation, and stabilization of supersaturation". *Journal of Agricultural and Food Chemistry* (64), 2016, 2352.

Vavrusova, M.; Johansen, N. P.; Garcia, A. C.; Skibsted, L. H. "Aqueous citric acid as a promising cleaning agent of whey evaporators". *International Dairy Journal* (69), 2017, 45.

Vavrusova, M.; Garcia, A. C.; Danielsen, B. P.; Skibsted, L. H. "Spontaneous supersaturation of calcium citrate from simultaneous isothermal dissolution of sodium citrate and sparingly soluble calcium hydroxycarboxylates in water". *RSC Advances* (7), 2017, 3078.

Vavrusova, M.; Danielsen, B. P.; Garcia, A. C.; Skibsted, L. H. "Codissolution of calcium hydrogenphosphate and sodium hydrogencitrate in water. Spontaneous supersaturation of calcium citrate increasing calcium bioavailability". *Journal of Food and Drug Analysis* (26), 2018, 330.

Garcia, A. C.; Vavrusova, M.; Skibsted, L. H. "Supersaturation of calcium citrate as a mechanism behind enhanced availability of calcium phosphates by presence of citrate". *Food Research International* (107), 2018, 195.

Submitted papers:

Cheng, H.; Skibsted, L. H. "Dissolution of calcium hydrogenphosphate in aqueous δ-gluconolactone, long-lasting supersaturation increasing calcium bioavailability", submitted to *International Dairy Journal*.

Cheng, H.; Garcia, A. C.; Tang, N.; Danielsen, B. P.; Skibsted, L. H. "Combinations of isocitrate and citrate enhance calcium salt solubility and supersaturation robustness. A perspective for functional beverages based on blackberry", to be submitted to *International Dairy Journal*.

Student theses:
André C. Garcia. "Supersaturation: A proposal for functional foods with improved calcium bioavailability", PhD defence on April 6th.

Other:
Garcia, A. C.; Vavrusova, M.; Danielsen, B. P.; Skibsted, L. H. "Spontaneous supersaturation of calcium hydroxycarboxylates during isothermal dissolution as a novel mechanism behind calcium bioavailability". Poster presented at 1st Food Chemistry Conference in Amsterdam, Oct-nov 2016.

14. Contribution to master and PhD education

The PhD project of André C. Garcia was within the frame of the project. His thesis will be defended on April 6th 2018.

André C. Garcia stayed at Arla Food Ingredients in Nr. Vium for two weeks (Sep 2016), where he conducted experiments, reported in the paper *Food Research International* (107), 2018, 195.

Martina Vavrusova spent a similar period in 2015 at Arla Food Ingredients in Nr. Vium.

15. New contacts/projects

The project has formed the basis for a new project supported by DDRF and by Danmark Innovationsfonden. This project "Supercalcium. Mineral from whey for customized foods" has started in January 2018 with professor Leif Skibsted as project leader. The support by Danmarks Innovationsfonden is part of a Danish/Brazilian project "Novel ageing-technologies and solutions to manufacture novel products for healthy ageing" with Professor Lilia Ahrné, from University of Copenhagen, as the Danish project leader and Associate Professor Daniel Cardoso, from University of São Paulo, São Carlos, as the Brazilian project leader.

16. Signature and date

The project is formally finalised when the project manager and DDRF-representative (e.g. steering committee leader) have signed this final report.

Date: _12/3 2018_ Signature, Project manager: _Leif Skibsted_____
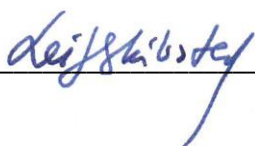
Date: **28 March 2018 Signature**, DDRF-representative: _____

Aqueous solubility of calcium citrate and interconversion between the tetrahydrate and the hexahydrate as a balance between endothermic dissolution and exothermic complex formation

CrossMark

Martina Vavrusova, Leif H. Skibsted[*]

Food Chemistry, Department of Food Science, Faculty of Science, University of Copenhagen, Rolighedsvej 30, DK-1958 Frederiksberg C, Denmark

ARTICLE INFO

ABSTRACT

Aqueous solubility of calcium citrate tetrahydrate was found to decrease with increasing temperature, while solubility of hexahydrate increased with a transition temperature at 51.6 °C. Excess citrate increased calcium citrate solubility but decreased the calcium ion activity of the saturated solution with an initial solubility overshooting to form supersaturated solutions indicating binding of calcium to citrate with an association constant of $3.6 \pm 0.1 \times 10^4$, $\Delta H^\circ = -5.07 \pm 0.04$ kJ mol^{-1}, $\Delta S^\circ = 70.3 \pm 0.3$ J mol^{-1} K^{-1} at 25 °C. Dissolution of the tetrahydrate and hexahydrate was found to have $\Delta H^\circ = 27 \pm 9$ kJ mol^{-1}, $\Delta S^\circ = -218 \pm 30$ J mol^{-1} K^{-1} and $\Delta H^\circ = 57 \pm 7$ kJ mol^{-1}, $\Delta S^\circ = -126 \pm 24$ J mol^{-1} K^{-1}, respectively, as determined from the temperature dependence of solubility corrected for complex formation. The exothermic complex formation results in inverse solubility only for the tetrahydrate with its moderate endothermic dissolution, which also precipitates at ambient temperature rather than the less soluble hexahydrate.

© 2016 Elsevier Ltd. All rights reserved.

1. Introduction

Citrate in milk is of importance for the high bioavailability of calcium from many dairy products. However, citrate may together with phosphate precipitate as calcium salts of low solubility under certain conditions used by dairy industry corrupting the quality of some dairy products related to whey and milk processing (Gao et al., 2010; Kubantseva, Hartel, & Swearingen, 2004; Pearce, Creamer, & Gilles, 1973; Rosmaninho & Melo, 2006; Vavrusova, Munk, & Skibsted, 2013). Knowledge of the solubility of calcium citrate in the presence of excess citrate seems accordingly important for optimising whey processing conditions and also for formulation and improvement of calcium supplements.

For the temperature interval of relevance for dairy processing, the tetrahydrate and the hexahydrate of calcium citrate are the solid compounds of intermediate relevance. Calcium from calcium citrate hydrates have a higher bioavailability than calcium from other calcium salts of similar low solubility indicating that complexation of

calcium by citrate may interfere with the precipitation reactions otherwise hampering calcium absorption from the intestines (Heaney, Recker, & Weaver, 1990; Mekmene & Gaucheron, 2011; Nicar & Pak, 1985; Pak & Avioli, 1988; Pathomrungsiyoungul, Grandison, & Lewis, 2010). In addition, precipitation of calcium salts of low solubility, mainly citrates and phosphates, contribute to fouling in particular in whey evaporators and often become the limiting factor for continuous dairy processing (Jeurnink & Brinkman, 1994; Jeurnink, Walstra, & deKruif, 1996). We have accordingly determined the solubility of the calcium citrate hydrates of relevance for whey processing for the temperature interval 0–100 °C. In addition, the complex constant for binding of calcium to citrate was quantified to characterise the dissolution and precipitation of calcium citrate and the thermodynamics of the transformation between the two hydrates under conditions relevant for dairy processing. Under some conditions of excess citrate, calcium citrate seems moreover spontaneously to form supersaturated solutions during dissolution, which could be important for an understanding of the higher bioavailability of dairy calcium. The present study also aims of providing a better understanding of factors determining solubility of calcium salts under conditions of dairy processing with the perspective of process optimisation and development of better cleaning procedures.

* Corresponding author. Tel.: +45 35 33 32 21.
  E-mail address: ls@life.ku.dk (L.H. Skibsted).

2. Methods and materials

2.1. Materials

Tricalcium dicitrate tetrahydrate (99%), ammonium purpurate 5,5-nitrilodibarbituric acid (murexid), and trisodium citrate dihydrate were all from Sigma Aldrich (Steinheim, Germany). Ethylenediaminetetraacetic acid disodium salt dihydrate (EDTA), calcium chloride dihydrate, and sodium hydroxide were from Merck (Darmstadt, Germany). All aqueous solutions were made from purified water from Milli-Q Plus (Millipore Corporation, Bedford, MA, USA).

2.2. EDTA titration

EDTA solution for titration with the concentration of 0.0100 mol L^{-1} was standardised against a 0.0100 mol L^{-1} aqueous solution of CaCl$_2$ made by weighing of dried calcium chloride dihydrate. 5.000 mL of sample was transferred to a titration flask and diluted with 15 mL of water. A total of 1.0 mL of 2.0 mol L^{-1} solution of NaOH was added to each sample to maintain basic pH, and 0.15 mL of 0.50% murexid solution was used as an indicator. Samples were titrated until initial pink colour changed to dark purple indicating the endpoint (Vogel, 1961).

2.3. Electrochemical measurement of calcium ion activity

A calcium ion activity was determined by a standard electrochemical method frequently used for rapid determination of ion activity (Mekmene & Gaucheron, 2011; Singh, Yeboah, Pambid, & Debayle, 1991; Williams-Jones & Seward, 1989). A calcium ion selective electrode ISE25Ca with a reference REF251 electrode from Radiometer (Copenhagen, Denmark) was calibrated using aqueous 1.00×10^{-4}, 1.00×10^{-3}, 1.00×10^{-2} mol L^{-1} CaCl$_2$ solutions prepared from a 1.000 mol L^{-1} CaCl$_2$ stock solution at 0, 10, 20, 25, 30, 40, or 50 °C. Calcium ion activity, a_{Ca}^{2+}, in the standard solutions was calculated based on the relationship between activity and concentration according to

$$a_{Ca^{2+}} = c_{Ca^{2+}} \times \gamma^{2+} \tag{1}$$

where γ^{2+} is the activity coefficient calculated from the Davies' equation as described previously (Vavrusova, Liang, & Skibsted, 2014)

$$\log \gamma^{2+} = -A_{DH}z^2 \left(\frac{\sqrt{I}}{1+\sqrt{I}} - 0.30I \right) \tag{2}$$

where A_{DH} is the Debye-Hückel constant with the numerical value of $A_{DH} = 0.491$, 0.498, 0.506, 0.510, 0.515, 0.525, or 0.536 at 0, 10, 20, 25, 30, 40, and 50 °C, respectively, and $z = 2$ for calcium ions (Davies, 1962). The calcium ion activity in the test solutions was calculated from a linear standard curve between electrode potential (mV) measured for the calibration solutions and $-\log a_{Ca}2+$ of the calibration solutions according to the Nernst equation at each temperature for experiments up to 50 °C, the temperature limit of the electrode. The validity of the activity measurements was confirmed at each temperature by a slope of the calibration plot in agreement with Nernst equation.

2.4. Solubility of tricalcium dicitrate in water

Saturated aqueous solutions of tricalcium dicitrate tetrahydrate were prepared by dissolution of the salt in water under constant stirring in closed flasks at temperature of 0, 10, 20, 25, 30, 40, 50, 70, and 100 °C in a thermostated chamber or water bath using excess of the salt. The samples were analysed after 2 h of equilibration with stirring at the respective temperature. Samples were filtered (589/3, Whatman, Dassel, Germany) prior to each analysis. Total calcium concentration was determined by EDTA titration and the calcium ion activity was determined by a calcium ion selective electrode ISE25Ca (section 2.3), for the saturated solutions of calcium salt at the investigated temperatures for experiments up to 50 °C. All solubility experiments were done in duplicates. Saturated aqueous solutions of tricalcium dicitrate hexahydrate were prepared by the same method using tricalcium dicitrate hexahydrate prepared by mixing calcium chloride at a concentration of 0.0300 mol L^{-1} with sodium citrate at a concentration of 0.0200 mol L^{-1} in water and stirred overnight at room temperature. Precipitate was collected by filtration and washed with water and ethanol prior to air-drying overnight. Water loss was determined by drying to constant weight, as described in the section 2.6, and the found value 18.8 ± 0.2% corresponds to the water content in the hexahydrate (18.0%) confirming that calcium citrate hexahydrate was formed. An aliquot of 0.500 g of the collected precipitate of calcium citrate hexahydrate was used for the solubility determination at 0, 10, 20, 25, 30, 40, 50, 70, and 100 °C. The calcium ion activity was measured electrochemically in the saturated aqueous solutions of calcium citrate hexahydrate for up to 50 °C.

2.5. Solubility determination of tricalcium dicitrate tetrahydrate in aqueous sodium citrate

Saturated solutions of tricalcium dicitrate tetrahydrate were prepared from 3.0 g in 100 mL of 0.00500 M, 0.0100 M, and 0.0200 M aqueous sodium citrate. Samples were under constant stirring at temperature of 10, 20, 25 and 30 °C in a thermostated chamber. Total calcium concentration and calcium ion activity were determined after 2, 24, 48, and 72 h of stirring at 10 °C by EDTA titration and electrochemically, respectively, after filtration. Equilibrium was found to be attained after 48 h of constant stirring at 10 °C. Therefore, total calcium concentration and the calcium ion activity were determined in the samples after 48 h for conditions of 10, 20, 25, and 30. All samples were prepared in duplicate.

2.6. Precipitates from saturated and supersaturated solutions of tricalcium dicitrate tetrahydrate

Saturated solutions of calcium citrate tetrahydrate in water were equilibrated at 0, 25, 50, 70, and 100 °C for 2 h under constant stirring. Precipitates were filtered and washed with ethanol and water, prior to air-drying overnight and in an oven at 105 °C until constant weight. A small amount of air-dried or oven-dried precipitate was dissolved in 100 mL of water and the total calcium was determined by EDTA titration. Water loss was calculated as a percentage difference between the weight of oven-dried and air-dried precipitate.

Saturated solution of tricalcium dicitrate tetrahydrate in water was equilibrated at 0 °C for 2 h under constant stirring. The solution was filtered at 0 °C and the filtrate allowed to equilibrate at 20 °C. The solution supersaturated with tricalcium dicitrate tetrahydrate at 20 °C was divided into three parts. The first part of supersaturated solution was seeded with a small amount of tricalcium dicitrate hexahydrate, the second solution was seeded with tricalcium dicitrate tetrahydrate, and the last solution was kept without any addition of calcium salts. All three solutions were thermostated at 20 °C for 2 d. The solutions were then filtered and the precipitates were washed with a small amount of ethanol and water, prior to air-drying overnight and in an oven at 105 °C until constant weight.

Water loss was calculated as a percentage difference between the weight of oven-dried and air-dried precipitate. Based on the percentage of water loss it is possible to distinguish between the two hydrates precipitated from supersaturated solutions under investigated conditions.

2.7. Differential scanning calorimetry

A DSC STAR^e System from Mettler Toledo (Schwerzenbach, Switzerland) based on the heat flux principle was used for differential scanning calorimetry of 14.26 mg of calcium citrate tetrahydrate and 7.05 mg of calcium citrate hexahydrate which were hermetically sealed in 40 μL aluminium DSC crucibles (Mettler Toledo, ME 27331). Calibration of heat flow and temperature was performed with indium ($T_m = 156.6$ °C, $\Delta H_{fus} = 28.5$ J g^{-1}) and zinc ($T_m = 419.5$ °C, $\Delta H_{fus} = 107.5$ J g^{-1}) as standards. The samples were scanned from 25.0 to 180.0 °C with a scanning rate 1 °C min^{-1} using an empty crucible as reference. The scanning of each hydrate took 2.5 h. Scanning at higher rates gave less resolution of the peaks and the thermograms are not reported.

3. Results and discussion

The solubility of calcium citrate tetrahydrate was found to decrease with increasing temperature, as seen from the solubility data presented in Table 1, and as reported by others (Boulet & Marier, 1960; Chatterjee & Dhar, 1924). The so-called inverse solubility of calcium citrate tetrahydrate is in contrast to what was found for the hexahydrate (Table 1), and for most other food related calcium salts (Kubantseva & Hartel, 2002; Vavrusova et al., 2014). The solubility of calcium citrate tetrahydrate continued to decrease throughout the investigated temperature interval and no solid state phase transformation was observed as it has been seen for some calcium salts during equilibration (Van Driessche et al., 2012). The solid phase of the equilibrated aqueous calcium citrate tetrahydrate solution was isolated after equilibration at 0, 25, 50, 70, and 100 °C, and the precipitates analysed for total calcium and water loss after air-drying and oven-drying to identify the solid phase. A calcium content of approximately 21%, which corresponds to content of calcium in calcium citrate with four waters, was found for the air-dried precipitates isolated at all the investigated temperatures. The precipitates were further dried in an oven at 105 °C until constant weight with a water loss of 11%, which corresponds to loss of approximately three and half water molecules (11.2%), in agreement with a determined calcium content of approximately 23% corresponding to the hemihydrate of calcium citrate (23.6%). The calcium citrate tetrahydrate had the same composition throughout the investigated temperature 0–100 °C interval when equilibrated from dissolution of calcium citrate tetrahydrate as also reported previously (Chatterjee & Dhar, 1924).

Calcium citrate precipitated at room temperature or below by mixing stoichiometric concentrations of calcium chloride with sodium citrate was expected to result in calcium citrate hexahydrate (Boulet & Marier, 1960; Chatterjee & Dhar, 1924). The precipitate formed at room temperature was confirmed by analysis to be calcium citrate hexahydrate, and was used for the solubility determination at 0, 10, 20, 25, 30, 40, 50, 70, and 100 °C by dissolution of the isolated salt. The solubility of calcium citrate hexahydrate was found to increase with temperature in contrast to calcium citrate tetrahydrate (Table 1). The solubility of the tetrahydrate and the hexahydrate is as shown in Fig. 1 the same at 51.6 °C. Calcium citrate hexahydrate is expected to transform into the tetrahydrate at this transition temperature. The calcium activity of the saturated solutions is seen to approach each other for the temperature around 30 °C but measurement of calcium ion activity is less precise for higher temperatures and not possible with the current method above 40–50 °C.

The calcium ion activity of the saturated solutions of calcium citrate tetrahydrate and of calcium citrate hexahydrate decreased with temperatures, as determined electrochemically (Table 1). The activities measured in the saturated solutions were based on activity standards calculating the activity from the calcium ion concentration using Davies equation (Davies, 1962). The calcium ion activity was found to decrease for the saturated calcium citrate tetrahydrate solutions with increasing temperature corresponding to the lower solubility of calcium citrate tetrahydrate at higher temperatures. Notably, the activity of calcium ion in the saturated
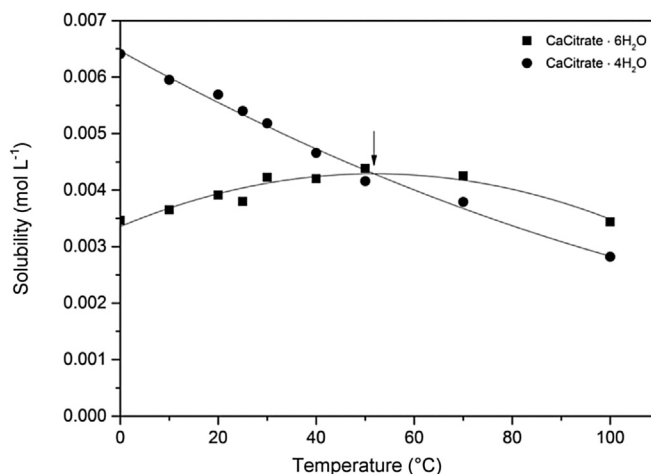

Fig. 1. Experimental solubilities of calcium citrate tetrahydrate (●; R^2 = 0.98) and calcium citrate hexahydrate (■; R^2 = 0.87) in water from 0 to 100 °C with full lines from fitting quadratic equations to experimental points. Transition temperature between the two hydrates was determined to be 51.6 °C from the point of intersection between the two curves.

Table 1
Solubilities of calcium citrate tetrahydrate and calcium citrate hexahydrate in water and calcium ion activity measured electrochemically in saturated solutions.

Temp. (°C)	Calcium citrate tetrahydrate		Calcium citrate hexahydrate	
	Solubility (mol L^{-1})	$a_{Ca}2+$	Solubility (mol L^{-1})	$a_{Ca}2+$
0	0.00641 ± 0.00004	0.0015 ± 0.0001	0.0035 ± 0.0001	0.00126 ± 0.00001
10	0.00595 ± 0.00004	0.0018 ± 0.0001	0.00365 ± 0.00004	0.00089 ± 0.00009
20	0.00569 ± 0.00004	0.00128 ± 0.00001	0.00391 ± 0.00004	0.00082 ± 0.00001
25	0.0054 ± 0.0001	0.00106 ± 0.00003	0.0038 ± 0.0001	0.00095 ± 0.00002
30	0.00518 ± 0.00004	0.00098 ± 0.00002	0.00423 ± 0.00004	0.00097 ± 0.00002
40	0.00466 ± 0.00004	0.00116 ± 0.00002	0.0042 ± 0.0001	0.00085 ± 0.00011
50	0.00416 ± 0.00004	0.0013 ± 0.0001	0.00438 ± 0.00004	0.00070 ± 0.00007
70	0.00379 ± 0.00004	–	0.00425 ± 0.0001	–
100	0.00282 ± 0.00004	–	0.00344 ± 0.00004	–
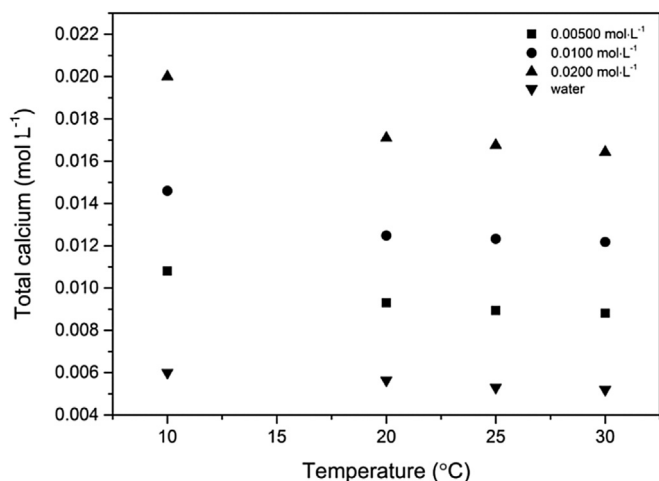
Fig. 2. Total calcium concentration in aqueous solutions of (■) 0.00500 mol L^{-1}, (●) 0.0100 mol L^{-1}, and (▲) 0.0200 mol L^{-1} sodium citrate dihydrate saturated with calcium citrate tetrahydrate after 48 h of equilibration (▼, water).

solution of the hexahydrate also decreased despite increasing solubility as for some other calcium hydroxycarboxylates, where the calcium ion activities of saturated solutions were found to decrease despite an increasing solubility of these salts with temperature as the result of endothermic binding of calcium to hydroxycarboxylates anions (Ghosh & Nair, 1970; Vavrusova et al., 2014).

Dissolution of calcium citrate tetrahydrate in the presence of excess of citrate was found to lead to increased solubility of the slightly soluble salt, an effect assigned to complex formation between citrate and calcium (Fig. 2). The opposite effect of decreased solubility was found for addition of sodium lactate to calcium lactate (Kubantseva et al., 2004; Vavrusova et al., 2013). Citrate binds stronger to calcium than lactate resulting in increased solubility of calcium citrate tetrahydrate in presence of excess of citrate ions. Notably, the dissolution equilibrium for calcium citrate tetrahydrate in the presence of excess citrate was established only after approximately 48 h, which is in contrast to a fast establishment of dissolution equilibrium in water for calcium citrate tetrahydrate (Fig. 3). A similar slow equilibration has also been observed for saturated solutions of calcium citrate in the presence of perchlorate (Ciavatta, De Tommaso, & Iuliano, 2001). Interestingly,
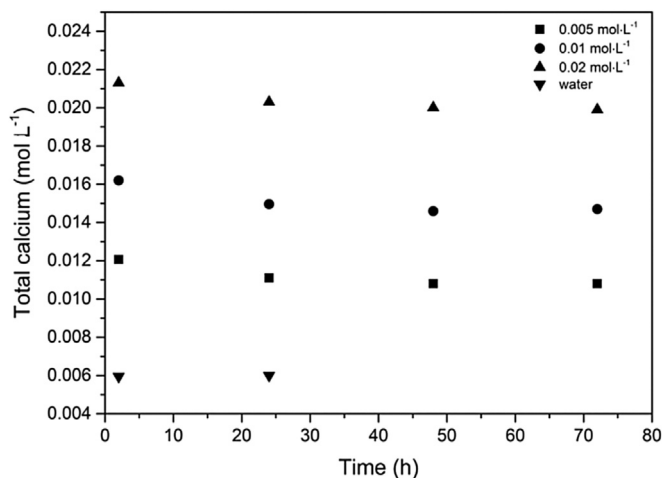
the solubility of saturated solutions of calcium citrate in an excess of citrate was higher by 6% after 2 h than at dissolution equilibrium, as may be seen from Fig. 3. Calcium ion activity decreased with increasing concentration of added citrate (Fig. 4), confirming complex formation. To quantify the binding of citrate to calcium and the lowering of calcium ion activity, the ion speciation in solutions needs to be considered. The dissolution of the calcium citrate is proposed as stepwise reactions as also seen for other calcium hydroxycarboxylates (Kubantseva & Hartel, 2002; Pearce et al., 1973; Vavrusova et al., 2014):

$$Ca_3Cit_2 \cdot 4H_2O \rightleftharpoons Ca^{2+} + 2CaCit^- + 4H_2O \tag{3}$$

$$CaCit^- \rightleftharpoons Ca^{2+} + Cit^{3-} \tag{4}$$
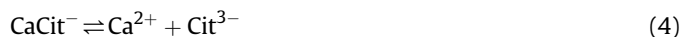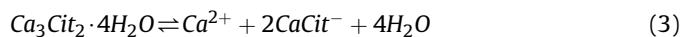
with a complete dissociation into Ca^{2+} and the 1:1 complex, $CaCit^-$, as shown in eq. (3). The 1:1 complex between Ca^{2+} and citrate, Cit^{3-}, will dissociate partly, see eq. (4). This thermodynamic model is in agreement with models previously suggested for similar conditions (Hastings, McLean, Eichelberger, Hall, & Da Costa, 1934). The thermodynamic association constant for the complex formation is defined as

$$K_a = \frac{a_{CaCit^-}}{a_{Ca^{2+}} a_{Cit^{3-}}} = \frac{[CaCit^-] \cdot \gamma^-}{[Ca^{2+}] \cdot \gamma^{2+} \cdot [Cit^{3-}] \cdot \gamma^{3-}} = K_c \cdot \frac{\gamma^-}{\gamma^{2+} \cdot \gamma^{3-}} \tag{5}$$

where γ^-, γ^{2+}, and γ^{3-} are activity coefficients for the 1:1 complex, calcium ion, and citrate ion, respectively. The concentration based association constant, K_c, is defined as

$$K_c = \frac{[CaCit^-]}{[Ca^{2+}][Cit^{3-}]} = K_a \cdot \frac{\gamma^{2+} \cdot \gamma^{3-}}{\gamma^-} \tag{6}$$

The so-called apparent constant or mixed constant, K_a', is defined for the complex formation based on calcium ion activity and the concentrations of the complex and citrate anion

$$K_a' = \frac{[CaCit^-]}{a_{Ca^{2+}}[Cit^{3-}]} \tag{7}$$

The association constants defined in eqs. (5)–(7) were calculated for the conditions of excess citrate at 10, 20, 25, and 30 °C


Fig. 3. Time course for dissolution of calcium citrate tetrahydrate in aqueous solutions of (■) 0.00500 mol L^{-1}, (●) 0.0100 mol L^{-1}, and (▲) 0.0200 mol L^{-1} sodium citrate dihydrate and in water at 10 °C under constant stirring (▼, water).
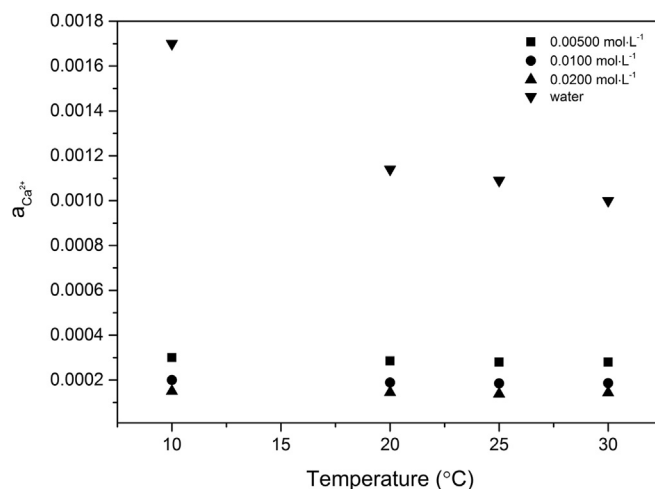
Fig. 4. Calcium ion activities, $a_{Ca^{2+}}$, in aqueous solutions of (■) 0.00500 mol L^{-1}, (●) 0.0100 mol L^{-1}, and (▲) 0.0200 mol L^{-1} sodium citrate dihydrate and in water after 24 h of equilibration (▼, water).

using an iterative calculation procedure. The initial and the final pH were close to neutral around 6.7. Initially, the ionic strength, I, was calculated assuming a complete dissociation of calcium citrate and including concentration of added sodium citrate (I = $5c_{Ca}^{2+}$ + 6y, where c_{Ca}^{2+} is total calcium ion concentration from calcium citrate, and y is the sodium citrate concentration). The simple assumption that the activity coefficient depends only on the charge of the ion was made as it is also for the Davies equation, which was used for the calculation of the activity coefficient for all ions present (Davies, 1962). The concentration of free citrate ligand follows from

$$\left[Cit^{3-}\right] = \left[Ca^{2+}\right] - \frac{c_{Ca^{2+}}}{3} + y = \frac{a_{Ca^{2+}}}{\gamma^{2+}} - \frac{c_{Ca^{2+}}}{3} + y \qquad (8)$$

and the concentration of the 1:1 calcium citrate complex and the free calcium ion concentration from

$$\left[CaCit^-\right] = c_{Ca^{2+}} - \left[Ca^{2+}\right] = c_{Ca^{2+}} - \frac{a_{Ca^{2+}}}{\gamma^{2+}} \qquad (9)$$

and

$$\left[Ca^{2+}\right] = a_{Ca^{2+}} \Big/ \gamma^{2+} \qquad (10)$$

A new estimate of ionic strength was made according to

$$I = \frac{1}{2}\left(4\left[Ca^{2+}\right] + \left[CaCit^-\right] + 9\left[Cit^{3-}\right] + 3y\right) \qquad (11)$$

and the calculations of concentrations of all species repeated. This iterative calculation procedure was repeated until the ionic strength was not influenced further, and the final values for the concentrations of the 1:1 calcium citrate complex, free citrate ions, and free calcium ions were calculated at 10, 20, 25, and 30 °C for all three added concentrations of sodium citrate. The final values for the three different types of association constants are presented in Table 2 for the four temperatures investigated. The high values of the thermodynamic association constants are in agreement with a strong ability of citrate ions to complex calcium as also reported previously (Meyer, 1974; Singh et al., 1991). The thermodynamic association constant showed little variation with the concentration of sodium citrate as is expected confirming the validity of the two

step dissolution of calcium citrate as described in eqs. (3) and (4). The moderate increase of K_a with increasing ionic strength reflects the limitations of Davies equation for the relative high ionic strength for the highly charged ions and the variation in the sodium ion concentration (Fig. 5). The concentration based and the apparent association constant both are only valid at the ionic strength at which they were determined, but may be of use for calculations of calcium speciation under conditions of constant ionic strength and temperature. The constant value obtained for the thermodynamic association constant for increasing concentrations of excess citrate relative to calcium at each of the four temperatures confirms the 1:1 composition of the complex. In addition, the attention should be paid to future investigations of calcium citrate solubility at low pH, conditions also relevant for fermented dairy products, together with significantly weaker calcium binding to protonated citrate (Meyer, 1974).

The values for the thermodynamic association constant determined by extrapolation to zero ionic strength by linear regression at each of the four temperatures were further used for the determination of the thermodynamic parameters for complex formation, ΔH^o_{ass} and ΔS^o_{ass}. The van't Hoff equation, as it is often used for this type of calculation, is linear only for temperature intervals where ΔH^o is independent of temperature. As shown in from Fig. 6, the present equilibrium data require a different approach for calculation of thermodynamic parameters. Non-linearity in the van't Hoff plot is related to the changes of the heat capacity, ΔC_p^o, for complex formation, leading to the variations in ΔH^o and ΔS^o with temperature. For ΔH^o and ΔS^o depending on temperature, the integrated versions of the relationship between ΔC_p^o, ΔH^o, and ΔS^o also known as Kirchoff's law results for a ΔC_p^o independent of temperature in

$$\Delta H^o = \Delta H_r^o + \Delta C_p^o(T - T_r) \qquad (12)$$

and

$$\Delta S^o = \Delta S_r^o + \Delta C_p^o \ln(T/T_r) \qquad (13)$$

where T_r is a reference temperature with ΔH_r^o and ΔS_r^o as numerical values at the reference temperature. The thermodynamic parameters related to complex formation without assuming constant

Table 2
Thermodynamic association constant, K_a, apparent (mixed) association constant, K'_a, and concentration based association constant, K_c, of the 1:1 calcium citrate complex in aqueous sodium citrate solutions saturated with calcium citrate tetrahydrate after 48 h of equilibration at 10, 20, 25, and 30 °C.

Temp. (°C)	Sodium citrate (mol L^{-1})								
	0.00500			0.0100			0.0200		
	$K_a \times 10^3$	$K_a' \times 10^3$	$K_c \times 10^3$ (mol^{-1} L)	$K_a \times 10^3$	$K_a' \times 10^3$	$K_c \times 10^3$ (mol^{-1} L)	$K_a \times 10^3$	$K_a' \times 10^3$	$K_c \times 10^3$ (mol^{-1} L)
10	54.8 ± 2.5	17.7 ± 0.8	10.0 ± 0.5	57.5 ± 4.6	13 ± 1	5.9 ± 0.5	66.3 ± 0.7	9.50 ± 0.06	3.60 ± 0.02
20	41.4 ± 1.5	12.7 ± 0.5	7.2 ± 0.3	48.95 ± 0.05	10.25 ± 0.01	4.69 ± 0.005	57.6 ± 1.3	7.9 ± 0.2	2.92 ± 0.07
25	39.4 ± 1.4	11.9 ± 0.5	6.6 ± 0.3	49.6 ± 0.8	10.2 ± 0.2	4.65 ± 0.08	59.8 ± 0.5	8.04 ± 0.07	2.95 ± 0.03
30	38.4 ± 0.9	11.5 ± 0.3	6.3 ± 0.2	48.9 ± 0.4	9.94 ± 0.07	4.48 ± 0.03	57.3 ± 0.9	7.5 ± 0.1	2.73 ± 0.04

Table 3
Thermodynamic solubility product, K_{sp}, and concentration solubility product, $K_{sp,c}$, of calcium citrate tetrahydrate and hexahydrate based on iterative calculations using aqueous solubilities of calcium citrate tetrahydrate and hexahydrate in water and thermodynamic association constant, K_a, of the 1:1 calcium citrate complex.

| Temp. (ºC)	Ca$_3$(Citr)$_2$·4H$_2$O		Ca$_3$(Citr)$_2$·6H$_2$O	
	K_{sp}	$K_{sp,c}$ (mol^5 L^{-5})	K_{sp}	$K_{sp,c}$ (mol^5 L^{-5})
0	2.15 ± 0.05 × 10^{-17}	2.6 ± 0.1 × 10^{-16}	2.4 ± 0.2 × 10^{-18}	1.6 ± 0.1 × 10^{-17}
10	5.1 ± 0.2 × 10^{-17}	6.2 ± 0.3 × 10^{-16}	8.8 ± 0.4 × 10^{-18}	6.7 ± 0.4 × 10^{-17}
20	7.9 ± 0.2 × 10^{-17}	9.9 ± 0.3 × 10^{-16}	2.06 ± 0.06 × 10^{-17}	1.79 ± 0.06 × 10^{-16}
25	7.6 ± 0.5 × 10^{-17}	9.3 ± 0.9 × 10^{-16}	2.1 ± 0.3 × 10^{-17}	1.8 ± 0.3 × 10^{-16}
30	6.4 ± 0.2 × 10^{-17}	7.7 ± 0.3 × 10^{-16}	3.1 ± 0.1 × 10^{-17}	3.0 ± 0.1 × 10^{-16}
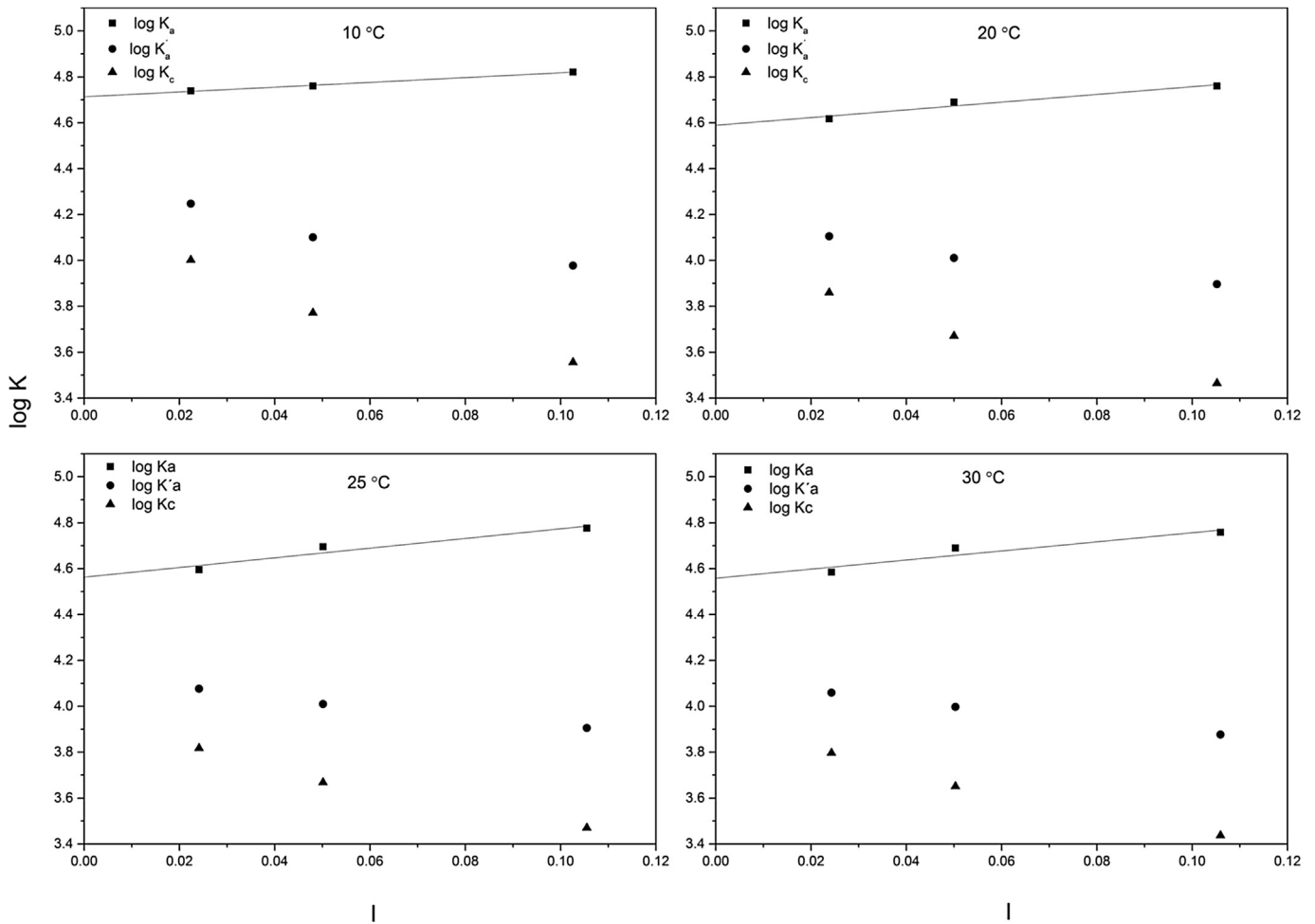
Fig. 5. Association constant for the 1:1 complex of calcium with citrate as a function of ionic strength in aqueous solution of sodium citrate saturated with calcium citrate tetrahydrate at 10, 20, 25, and 30 °C: ■, thermodynamic constant; K_a, ●, apparent (mixed) constant, K_a'; ▲, concentration constant, K_c. The thermodynamic association constant is extrapolated linearly to zero ionic strength to give the values of the K_a presented in Fig. 6.

ΔC_p^o may be calculated using a quadratic equation by polynomial fitting (Haidacher, Vailaya, & Horvath, 1996; Privalov & Makhatadze, 1990; Vailaya & Horvath, 1996)

$$\ln K_a = a + \frac{b}{T} + \frac{c}{T^2} \tag{14}$$

The parameters a, b, and c of eq. (14) were fitted to the experimental values and had the value a = 93.2 ± 0.3, b = −49.9 ± 0.2 × 10³ K, and c = 7.53 ± 0.03 × 10⁶ K², and were used to calculate the thermodynamic parameters

$$\Delta H_{ass}^o = -R\left(b + \frac{2c}{T}\right) \tag{15}$$

$$\Delta S_{ass}^o = -R\left(b + \frac{2c}{T}\right) \tag{16}$$

The thermodynamic parameters for formation of the calcium citrate complex are presented in Table 4. The complex formation is exothermic as $\Delta H_{ass}^o < 0$, which is in contrast to the endothermic complex formation for some other calcium hydroxycarboxylate complexes (Ghosh & Nair, 1970; Vavrusova et al., 2014). The change in enthalpy is negative, in contrast to a previous report of a thermoneutral complex formation (Singh et al., 1991). The small positive change in entropy may result from the greater number of

solvent molecules bound to the free calcium ions and free citrate ions compared with the undissociated forms of the complex and the increased number of free water by complexation.

From the solubility of the tetrahydrate and the hexahydrate of calcium citrate in water (Table 1), the solubility product of two hydrates were determined both as the thermodynamic solubility product, K_{sp}, and the solubility product based on concentrations, $K_{sp,c}$

$$K_{sp} = a_{Ca^{2+}}^3 \times a_{Citr^{3-}}^2 \tag{17}$$

$$K_{sp,c} = \left[Ca^{2+}\right]^3 \left[Cit^{3-}\right]^2 \tag{18}$$

$K_{sp,c}$ is only valid for the ionic strength of the saturated solution, while K_{sp} is of general validity at the actual temperature. The calculations depend on an iterative procedure initially assuming the activity coefficient of all ions to be one corresponding to zero ionic strength. Subsequently the thermodynamic association constant, K_a, determined for the investigated temperatures as presented in Fig. 6, were used for calculations of the equilibrium concentrations of free calcium ions by solving the quadratic equation resulting from eq. (5), using K_a at the actual temperature, and total calcium concentration as determined by titration. Concentrations of complex ions and citrate ions were then calculated. Based on the
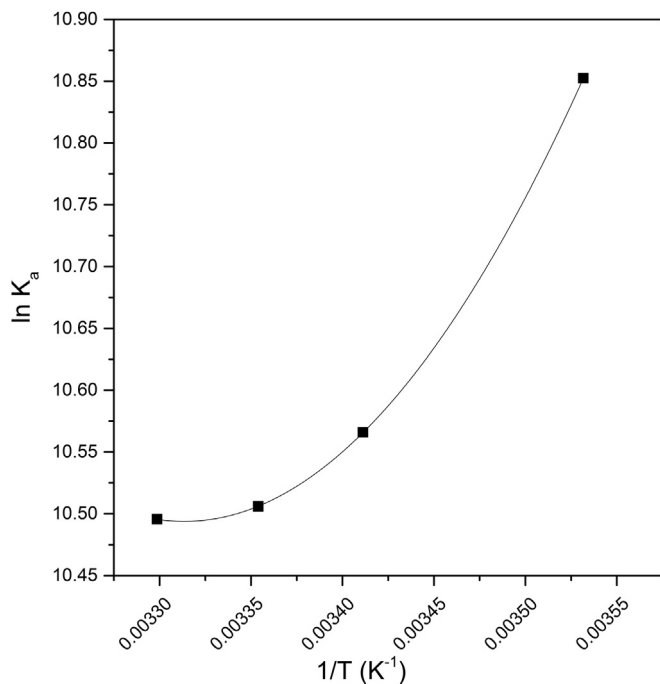
Fig. 6. Effects of temperature on the thermodynamic association constant, K_a, of the 1:1 complex of calcium with citrate as extrapolated to zero ionic strength as seen in Fig. 5 for each temperature. Full line is quadratic regression line according to eq. (14).

resulting distribution of ions, an adjusted ionic strength was calculated which allowed the calculation of activity coefficients of the ion species, which were used for correction of K_a to the concentration based constant, K_c, as seen from eq. (5). All the calculations were repeated until ionic strength did not change. The final values for $K_{sp,c}$ based on concentrations of calcium and citrate are presented in Table 3 together with values for K_{sp} based on the calcium activity and citrate activity as final values from the iterative calculations. The solubility product of both the tetrahydrate and the hexahydrate increases with temperature, most significantly for the hexahydrate. As seen from Fig. 7, the solubility may be described by the van't Hoff equation

$$\ln K_{sp} = -\frac{\Delta H^\circ}{RT} + \frac{\Delta S^\circ}{R} \tag{19}$$

from which values of ΔH° and ΔS° for dissolution of $Ca_3(Citr)_2 \cdot 4H_2O$ and $Ca_3(Citr)_2 \cdot 6H_2O$ were determined based on the thermodynamic solubility product, as presented in Table 4, by linear regression. Calculations based on the concentration based solubility product, $K_{sp,c}$, gave similar numerical values for ΔH° and ΔS°. As may be seen from Fig. 7, the solubility product has a common value at 54.9 °C as derived from temperature effect on the thermodynamic solubility product, and at 54.7 °C as derived from temperature effects on concentration based solubility product. These values are in fair agreement with the value of 51.6 °C determined as the point of intersection between the solubility curves for the two hydrates, as presented in Fig. 1. Other reactions such as

Table 4
Thermodynamic parameters for dissolution of calcium citrate tetrahydrate and hexahydrate in water and binding of calcium to citrate based on the thermodynamic solubility product, K_{sp}, and determined from the regression of Fig. 7 and from the thermodynamic association constant, K_a, as determined from the regression of Fig. 6, respectively.

Reaction	ΔH° (kJ mol^{-1})	ΔS° (J mol^{-1} K^{-1})
$Ca_3(Citr)_2 \cdot 4H_2O \rightarrow 3Ca^{2+} + 2Citr^{3-} + 4H_2O$	27 ± 9	-218 ± 30
$Ca_3(Citr)_2 \cdot 6H_2O \rightarrow 3Ca^{2+} + 2Citr^{3-} + 6H_2O$	57 ± 7	-126 ± 24
$Ca^{2+} + Citr^{3-} \rightarrow CaCitr^-$	-5.07 ± 0.04	70.3 ± 0.3
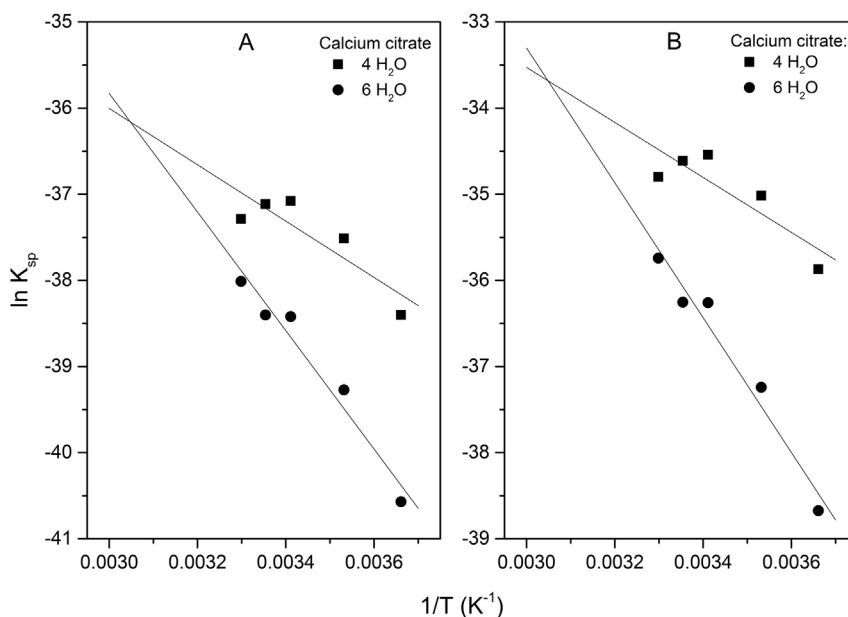
**Fig. 7.** Temperature effects on the solubility product of calcium citrate tetrahydrate (■) and calcium citrate hexahydrate (●) in water: A, thermodynamic solubility product, K_{sp}; B, concentration based solubility product, $K_{sp,c}$. Full lines are based on linear regression.
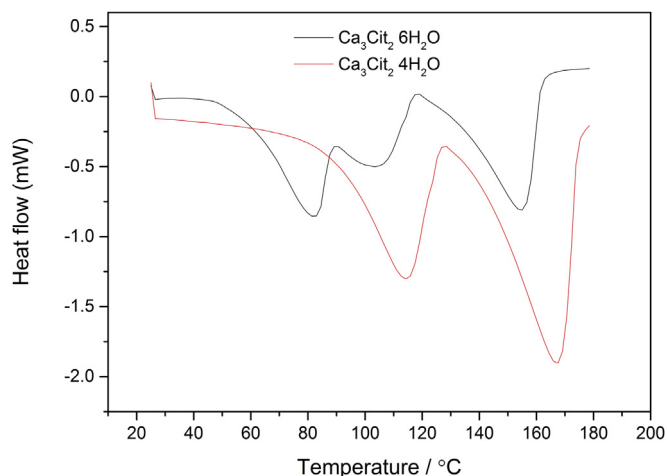
Fig. 8. Differential scanning calorimetry of calcium citrate hydrates. For calcium citrate tetrahydrate (predominantly the lower line) a total of 14.26 mg was heated and the integrated area from 54 to 102 °C was found to be 1239 mJ, corresponding to 49.5 kJ mol^{-1}. For calcium citrate hexahydrate (predominantly the upper line) a total of 7.05 mg was heated and the integrated area from 22 to 94 °C was found to be1682 mJ, corresponding to 145 kJ mol^{-1}. Scanning rate was 1.00 °C min^{-1}.


Fig. 9. Enthalpy of dissolution of calcium citrate hexahydrate, $\Delta H^{\circ}_{dissol}(6H_2O) = 57$ kJ mol^{-1}, from temperature dependence of solubility product of $Ca_3(Citr)_2 \cdot 6H_2O$, and enthalpy of dissolution of calcium citrate tetrahydrate, $\Delta H^{\circ}_{dissol}(4H_2O) = 27$ kJ mol^{-1}, from temperature dependence of solubility product of $Ca_3(Citr)_2 \cdot 4H_2O$. The difference between the two dissolution enthalpies correspond to the enthalpy of transformation between the two hydrates in dissolution equilibria in water $\Delta H_{transform}$ $(6, 4H_2O) = 57 - 27 = 30$ kJ mol^{-1}. Enthalpy of transformation was also obtained as the difference in the enthalpies for dehydration of the two hydrates as determined for the solids by DSC: $\Delta H_{transform}(6, 4H_2O) = \Delta H_{dehydr}(6H_2O) - \Delta H_{dehydr}(4H_2O) = 95.5$ kJ mol^{-1} which also includes heat of evaporation for water.

decarboxylation, isomerisation, or dehydration of citrate need only to be considered under more harsh conditions such as under high temperature evaporation and drying (Barbooti & Alsammerrai, 1986; Srivastava, Gunjikar, & Sinha, 1987).

The conversion of calcium citrate hexahydrate to the tetrahydrate was also studied using differential scanning calorimetry. Heating of solid of each of the two hydrates of calcium citrate from 0 to 170 °C gave evidence for one endothermic event for the tetrahydrate prior to degradation around 150 °C and for two partly overlapping endothermic events for the hexahydrate prior to degradation around 150 °C, respectively. The thermograms as seen in Fig. 8 show that the dehydration of the hexahydrate peaks at 80 °C and at 102 °C, while the dehydration of the tetrahydrate peaks at 108 °C. The difference in dehydration enthalpy for the tetrahydrate

$$Ca_3Cit_2 \cdot 4H_2O_{(s)} \rightarrow Ca_3Cit_{2(s)} + 4H_2O_{(l)} \qquad (20)$$

and of the hexahydrate

$$Ca_3Cit_2 \cdot 6H_2O_{(s)} \rightarrow Ca_3Cit_{2(s)} + 6H_2O_{(l)} \qquad (21)$$
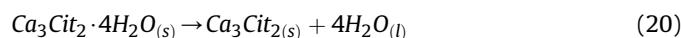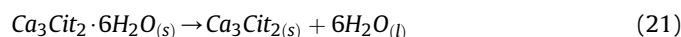
corresponding to the transformation of the hexahydrate to the tetrahydrate

$$Ca_3Cit_2 \cdot 6H_2O_{(s)} \rightarrow Ca_3Cit_2 \cdot 4H_2O_{(s)} + 2H_2O_{(l)} \qquad (22)$$
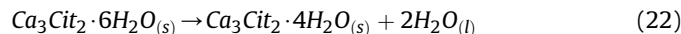
may be calculated as the difference

$$\Delta H_{transform}(6, 4H_2O) = \Delta H_{dehydr}(6H_2O) - \Delta H_{dehydr}(4H_2O) \qquad (23)$$

The values for $\Delta H_{dehydr}(4H_2O) = 49.5$ kJ mol^{-1} and $\Delta H_{dehydr}(6H_2O) = 145$ kJ mol^{-1} corresponding to the reaction of eqs. (20) and (21), respectively, were obtained by integration of the thermograms for each of the two hydrates, see Fig. 8. The heat of transformation of the hexahydrate to the tetrahydrate is accordingly found using eq. (23) to have the value $\Delta H_{transform}(6, 4H_2O) = 145 - 49.5 = 95.5$ kJ mol^{-1}. This value for $\Delta H_{transform}(6, 4H_2O)$ is valid for the solid state transformation and differs from the value of $+30$ kJ mol^{-1} derived from the temperature dependence of

the solubility of the two hydrates (Fig. 9). Evaporation of liquid water during temperature scan, see eqs. (21) and (22), contributes to the somewhat higher value for $\Delta H_{transform}$ obtained by DSC compared with the value obtained from the equilibrium studies. The temperature of transformation is also somewhat higher for the solid state transformation with a value around 80 °C as measured by the scanning calorimetry as compared with the transformation temperature of 51.6 °C obtained from the solubility studies. This is not surprising as DSC does not measure equilibrium dehydration as for the suspension in water of the hydrates, but will depend on heating rate, particle size, and nature of the crucible used for heating.

According to the solubility curve, as seen in Fig. 1, the hexahydrate is expected to precipitate below the transition temperature, i.e., 51.6 °C. A calcium citrate tetrahydrate solution saturated at 0 °C, when taken to ambient temperature and becoming supersaturated was, however, found to lead to precipitation of the tetrahydrate, both when seeded with the tetrahydrate and the hexahydrate. This observation may be understood according to Ostwald's rule of stages, according to which, a less stable phase often is formed prior to transformation to the thermodynamic stable form (Ostwald, 1899). Similar effects were observed for other salts important for dairy industry (Gao et al., 2010). This is clearly of relevance to evaporation processes of whey, where phosphates and citrates of calcium are possible precipitates also as double salts.

A related observation should draw some attention. During dissolution of calcium citrate tetrahydrate in aqueous sodium citrate, a solubility overshooting is observed, which does not take place for dissolution in water. Such spontaneous supersaturation for isothermal dissolution was previously demonstrated for dissolution of calcium lactate in sodium gluconate (Vavrusova & Skibsted, 2014). The present observation of an almost 10% dissolution overshooting may be of importance for making calcium supplements based on whey product more bioavailable and is now the subject of detailed studies.

4. Conclusion

Aqueous solubility of calcium citrate tetrahydrate was found to decrease with increasing temperature, while the solubility of calcium citrate hexahydrate increased. The transition temperature between the two hydrates was found to be 51.6 °C. Excess citrate

increased the solubility of calcium citrate, but decreased the calcium ion activity of the saturated solution with an initial solubility overshooting to result in supersaturated solutions indicating binding of calcium to citrate. So-called inverse solubility is the result of the exothermic complex formation, but only for the tetrahydrate with the moderate endothermic dissolution. The tetrahydrate was also found to precipitate at ambient temperature from moderate supersaturated solutions rather than the less soluble hexahydrate.

Acknowledgements

References

Barbooti, M. M., & Alsammerrai, D. A. (1986). Thermal decomposition of citric acid. *Thermochimica Acta, 98*, 119–126.

Boulet, M., & Marier, J. R. (1960). Solubility of tricalcium citrate in solutions of variable ionic strength and in milk ultrafiltrates. *Journal of Dairy Science, 43*, 155–164.

Chatterjee, K. P., & Dhar, N. R. (1924). Studies of sparingly soluble salts, readily obtained from hot solutions of reacting substances I. *Journal of Physical Chemistry, 28*, 1009–1028.

Ciavatta, L., De Tommaso, G., & Iuliano, M. (2001). The solubility of calcium citrate hydrate in sodium perchlorate solutions. *Analytical Letters, 34*, 1053–1062.

Davies, C. W. (1962). *Ion association*. London, UK: Butterworth & Co, Ltd.

Gao, R., van Halsema, F. E. D., Temminghoff, E. J. M., van Leeuwen, H. P., van Valenberg, H. J. F., Eisner, M. D., et al. (2010). Modelling ion composition in simulated milk ultrafiltrate (SMUF). I: influence of calcium phosphate precipitation. *Food Chemistry, 122*, 700–709.

Ghosh, R., & Nair, V. S. K. (1970). Studies of metal complexes in aqueous solution. 1. Calcium and copper lactates. *Journal of Inorganic and Nuclear Chemistry, 32*, 3025–3032.

Haidacher, D., Vailaya, A., & Horvath, C. (1996). Temperature effects in hydrophobic interaction chromatography. *Proceedings of the National Academy of Sciences of the United States of America, 93*, 2290–2295.

Hastings, A. B., McLean, F. C., Eichelberger, L., Hall, J. L., & Da Costa, E. (1934). The ionization of calcium, magnesium, and strontium citrates. *Journal of Biological Chemistry, 107*, 351–370.

Heaney, R. P., Recker, R. R., & Weaver, C. M. (1990). Absorbability of calcium sources – the limited role of solubility. *Calcified Tissue International, 46*, 300–304.

Jeurnink, T. J. M., & Brinkman, D. W. (1994). The cleaning of heat exchangers and evaporators after processing milk or whey. *International Dairy Journal, 4*, 347–368.

Jeurnink, T. J. M., Walstra, P., & deKruif, C. G. (1996). Mechanisms of fouling in dairy processing. *Netherlands Milk and Dairy Journal, 50*, 407–426.

Kubantseva, N., & Hartel, R. W. (2002). Solubility of calcium lactate in aqueous solution. *Food Reviews International, 18*, 135–149.

Kubantseva, N., Hartel, R. W., & Swearingen, P. A. (2004). Factors affecting solubility of calcium lactate in aqueous solutions. *Journal of Dairy Science, 87*, 863–867.

Mekmene, O., & Gaucheron, F. (2011). Determination of calcium-binding constants of caseins, phosphoserine, citrate and pyrophosphate: a modelling approach using free calcium measurement. *Food Chemistry, 127*, 676–682.

Meyer, J. L. (1974). Formation constants for interaction of citrate with calcium and magnesium-ions. *Analytical Biochemistry, 62*, 295–300.

Nicar, M. J., & Pak, C. Y. C. (1985). Calcium bioavailability from calcium-carbonate and calcium citrate. *Journal of Clinical Endocrinology and Metabolism, 61*, 391–393.

Ostwald, W. (1899). Studien über die Bildung und Umwandlung fester Körper. *Zeitschrift für Physikalische Chemie, 22*, 289–330.

Pak, C. Y. C., & Avioli, L. V. (1988). Factors affecting absorbability of calcium from calcium salts and food. *Calcified Tissue International, 43*, 55–60.

Pathomrungsiyounggul, P., Grandison, A. S., & Lewis, M. J. (2010). Effect of calcium carbonate, calcium citrate, tricalcium phosphate, calcium gluconate and calcium lactate on some physicochemical properties of soymilk. *International Journal of Food Science and Technology, 45*, 2234–2240.

Pearce, K. N., Creamer, L. K., & Gilles, J. (1973). Calcium lactate deposits on rindless Cheddar cheese. *New Zealand Journal of Dairy Science and Technology, 8*, 3–7.

Privalov, P. L., & Makhatadze, G. I. (1990). Heat-capacity of proteins. 2. Partial molar heat-capacity of the unfolded polypeptide-chain of proteins – protein unfolding effects. *Journal of Molecular Biology, 213*, 385–391.

Rosmaninho, R., & Melo, L. F. (2006). The effect of citrate on calcium phosphate deposition from simulated milk ultrafiltrate (SMUF) solution. *Journal of Food Engineering, 73*, 379–387.

Singh, R. P., Yeboah, Y. D., Pambid, E. R., & Debayle, P. (1991). Stability constant of the calcium citrate(3-) ion-pair complex. *Journal of Chemical and Engineering Data, 36*, 52–54.

Srivastava, A., Gunjikar, V. G., & Sinha, A. P. B. (1987). Thermoanalytical studies of zinc citrate, bismuth citrate and calcium citrate. *Thermochimica Acta, 117*, 201–217.

Vailaya, A., & Horvath, C. (1996). Retention thermodynamics in hydrophobic interaction chromatography. *Industrial and Engineering Chemistry Research, 35*, 2964–2981.

Van Driessche, A. E. S., Benning, L. G., Rodriguez-Blanco, J. D., Ossorio, M., Bots, P., & Garcia-Ruiz, J. M. (2012). The role and implications of bassanite as a stable precursor phase to gypsum precipitation. *Science, 336*, 69–72.

Vavrusova, M., Liang, R., & Skibsted, L. H. (2014). Thermodynamics of dissolution of calcium hydroxycarboxylates in water. *Journal of Agricultural and Food Chemistry, 62*, 5675–5681.

Vavrusova, M., Munk, M. B., & Skibsted, L. H. (2013). Aqueous solubility of calcium l-lactate, calcium d-gluconate, and calcium d-lactobionate: importance of complex formation for solubility increase by hydroxycarboxylate mixtures. *Journal of Agricultural and Food Chemistry, 61*, 8207–8214.

Vavrusova, M., & Skibsted, L. H. (2014). Spontaneous supersaturation of calcium d-gluconate during isothermal dissolution of calcium l-lactate in aqueous sodium d-gluconate. *Food and Function, 5*, 85–91.

Vogel, A. I. (1961). *A text-book of quantitative inorganic analysis including elementary instrumental analysis*. London, UK: Longman.

Williams-Jones, A. E., & Seward, T. M. (1989). The stability of calcium-chloride ion-pairs in aqueous-solutions at temperatures between 100 and 360 °C. *Geochimica et Cosmochimica Acta, 53*, 313–318.

Calcium D-Saccharate: Aqueous Solubility, Complex Formation, and Stabilization of Supersaturation

André C. Garcia,[†,‡] Martina Vavrusova,[†] and Leif H. Skibsted*,[†]

[†]Food Chemistry, Department of Food Science, University of Copenhagen, Rolighedsvej 30, DK-1958 Frederiksberg C, Denmark

[‡]Insituto Federal de Educação, Ciência e Tecnologia de São Paulo, Campus Capivari, Avenida Doutor Ênio Pires de Camargo, 2971, São João Batista, Capivari, São Paulo 13360-000, Brazil

ABSTRACT: Molar conductivity of saturated aqueous solutions of calcium D-saccharate, used as a stabilizer of beverages fortified with calcium D-gluconate, increases strongly upon dilution, indicating complex formation between calcium and D-saccharate ions, for which, at 25 °C, $K_{assoc} = 1032 \pm 80$, $\Delta H^{\circ}_{assoc} = -34 \pm 6$ kJ mol^{-1}, and $\Delta S^{\circ}_{assoc} = -55 \pm 9$ J mol^{-1} K^{-1}, were determined electrochemically. Calcium D-saccharate is sparingly soluble, with a solubility product, K_{sp}, of $(6.17 \pm 0.32) \times 10^{-7}$ at 25 °C, only moderately increasing with the temperature: $\Delta H^{\circ}_{sol} = 48 \pm 2$ kJ mol^{-1}, and $\Delta S^{\circ}_{assoc} = 42 \pm 7$ J mol^{-1} K^{-1}. Equilibria in supersaturated solutions of calcium D-saccharate seem only to adjust slowly, as seen from calcium activity measurements in calcium D-saccharate solutions made supersaturated by cooling. Solutions formed by isothermal dissolution of calcium D-gluconate in aqueous potassium D-saccharate becomes spontaneously supersaturated with both D-gluconate and D-saccharate calcium salts, from which only calcium D-saccharate slowly precipitates. Calcium D-saccharate is suggested to act as a stabilizer of supersaturated solutions of other calcium hydroxycarboxylates with endothermic complex formation through a heat-induced shift in calcium complex distribution with slow equilibration upon cooling.

KEYWORDS: calcium D-saccharate, calcium D-gluconate, calcium complexes, calcium salt solubility, spontaneous supersaturation

INTRODUCTION

Dairy products are one of the most important sources of calcium in the human diet as a result of the high bioavailability ensured by the calcium binding to caseins, proteins, peptides, and anions present in the serum phase of the milk, which prevents the precipitation of calcium salts during digestion.[1−4] An adequate calcium intake reduces the risk of chronic diseases, such as hypertension, osteoporosis, colon cancer, breast cancer, and kidney stones, among others.[5,6]

It is important to better understand calcium binding not only to components present in milk but also to those added to dairy products or formed during milk processing to optimize calcium bioavailability of dairy products and, consequently, improve dairy technology.[7,8] In this context, the development of calcium-fortified foods must consider the interaction of different components, such as mixtures of hydroxycarboxylates, which have shown to increase the solubility of sparingly soluble calcium salts, such as calcium lactate.[8−10]

Not only are dairy products fortified with calcium but also soy milk, which naturally presents an unsatisfactory calcium concentration for human nutrition.[11,12] It has been reported that calcium D-saccharate can be used to stabilize soy milk fortified with calcium D-gluconate;[13] however, there is a lack of information on the physical chemistry and thermodynamic properties of calcium D-saccharate. Calcium D-saccharate is also known to prevent precipitation of calcium D-gluconate from supersaturated aqueous solutions of calcium D-gluconate used for injection in calcium therapy, despite calcium D-saccharate being less soluble than calcium D-gluconate.[14] The aim of our work was to describe some basic chemical properties of calcium D-saccharate as well as investigate mixed solutions of D-saccharate and D-gluconate calcium salts to better understand

the mechanism behind the unusual supersaturation phenomena. Such knowledge may also help to understand why some calcium salts have better bioavailability than others, despite similar low solubility.

MATERIALS AND METHODS

Chemicals. Calcium D-saccharate tetrahydrate (98.5−102%), D-saccharic acid potassium salt (≥98%), calcium D-gluconate monohydrate (≥98%), sodium D-gluconate (97%), ammonium purpurate 5,5-nitrilodibarbituric acid (murexide indicator), and calcium chloride dihydrate (≥99%) were all from Sigma-Aldrich (Steinheim, Germany). Sodium chloride, sodium hydroxide, and ethylenediaminetetraacetic acid disodium salt dihydrate (EDTA) were all from Merck (Darmstadt, Germany). All aqueous solutions were made from purified water using a Milli-Q Plus system from Millipore Corp. (Bedford, MA).

EDTA Titration. Titrant solution of EDTA of concentration of 1.00×10^{-2} mol L^{-1} was standardized against 1.00×10^{-2} mol L^{-1} CaCl$_2$. A total of 1.000, 5.000, or 10.00 mL of the sample was transferred to an Erlenmeyer and diluted to 20 mL with water. A total of 1.0 mL of 2.0 mol L^{-1} of NaOH was added to the sample to maintain basic pH, and 0.20 mL of 0.50% murexide solution was used as an indicator. Samples were titrated until the initial pink color changed to dark purple, indicating the end point of the titration.

Ion Coupled Plasma Optical Emission Spectrometry (ICP−OES). A total of 100 μL of the samples were mixed with 750 μL of 70% of HNO$_3$ (SCP Science, Baie-d'Urfé, Quebec, Canada) and 375 μL of 15% H$_2$O$_2$ (Sigma-Adrich, Steinheim, Germany) and, hereafter, digested in a pressurized microwave oven (Ultrawave, Milestone, Inc.,
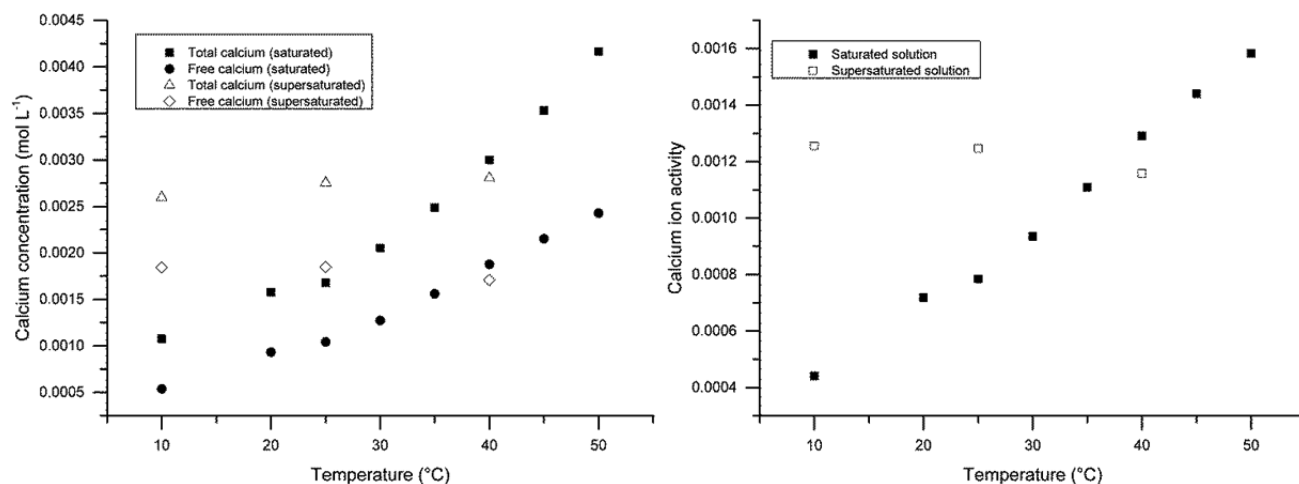
Figure 1. (A) Total calcium and free calcium concentrations and (B) calcium ion activity for saturated calcium D-saccharate solutions (filled points) and supersaturated (open points) at different temperatures.

Sorisole, Italy) for 10 min with a starting pressure of 40 bar and temperature of 240 °C. After digestion, the samples were diluted to 14 mL with Milli-Q water before measurement on ICP−OES (model 5100, Agilent Technologies, Santa Clara, CA) equipped with a Meinhard nebulizer and cyclonic spray chamber. For quantification, an external 10-point calibration standard P/N 4400-132565 and 104 P/N 4400-ICP-MSCS (CPI International, Amsterdam, Netherlands) were used. A National Institute of Standards and Technology (NIST) 1515 apple leaf certified reference material (NIST, Gaithersburg, MD) was analyzed together with the samples to evaluate the accuracy and precision of the analysis. For quantification of calcium, the monitored wavelength was 612.22 nm. The results were accepted when the limit of quantification (LOQ) was exceeded, the accuracy was within ±10%, and the coefficient of variation (CV, %) was lower than 2%.

Electrochemical Measurement of Free Calcium. Calcium ion activity was determined in the filtrate by a calcium ion selective electrode ISE25Ca with a reference REF 251 electrode (Radiometer, Copenhagen, Denmark). The electrode calibration was performed with calcium chloride standard solutions of 1.00×10^{-4}, 1.00×10^{-3}, and 1.00×10^{-2} mol L^{-1} prepared from a 1.00 mol L^{-1} stock solution. Calcium ion activity, $a_{Ca^{2+}}$, was determined in the samples from the linear relationship, derived from the Nernst equation, between electrode potential (mV) and the corresponding pCa ($= -\log a_{Ca^{2+}}$) of the calibration solutions as previously described.[15] The free calcium concentration, [Ca^{2+}], was calculated on the basis of iterative calculations between the relationship of activity and concentration, ionic strength, and Davies equation,[16] according to eqs 1, 2, and 3, respectively

$$a_{Ca^{2+}} = [Ca^{2+}]\gamma^{2\pm} \tag{1}$$

where $\gamma^{2\pm}$ corresponds to the activity coefficient of bivalent ions

$$I = \frac{1}{2}\sum_i c_i z_i^2 \tag{2}$$

where c_i corresponds to the concentration of the ions in solution and z_i corresponds to the charge

$$\log \gamma^{z\pm} = -A_{DH}z^2\left(\frac{\sqrt{I}}{I + \sqrt{I}} - 0.30I\right) \tag{3}$$

where A_{DH} is the Debye−Hückel constant[17] depending upon the temperature of the experiments. To determine the initial ionic strength in the beginning of the iterative calculations, the free calcium concentration was considered to be equal to calcium ion activity ([Ca^{2+}] = $a_{Ca^{2+}}$).

Conductivity Measurements of Calcium D-Saccharate Solutions. A saturated solution of calcium D-saccharate was prepared and

diluted to four different concentrations. The conductivity of these solutions was determined at 20 °C by a 4-pole conductivity cell, model CDC866T (Radiometer, Copenhagen, Denmark), calibrated with a 0.01 D potassium chloride standard solution (1408 μS cm^{-1}).

Dissolution and Solubility Determination. Aqueous saturated solutions of calcium D-saccharate tetrahydrate were prepared by adding 2.0 g of the salt to 100 mL of water. Samples were kept under constant stirring for 2 h at 10, 20, 25, 30, and 50 °C. After this period, the samples were filtered (589/3, Whatman, Dassel, Germany). The solubility, corresponding to the total calcium concentration, was determined by EDTA titration, and the free calcium ion concentration was determined with the calcium ion selective electrode.

Supersaturated Solutions. Supersaturated solutions of calcium D-saccharate were prepared by adding 200 mg of the salt to 200 mL of water (1.00 g L^{-1}). The samples were heated to 65 °C to attain the complete dissolution of the salt and then were slowly cooled.

Mixed Calcium D-Saccharate/Chloride Solutions. A stock solution of calcium D-saccharate was prepared with a concentration of 1.00×10^{-3} mol L^{-1}. After 2 h of stirring at 25 °C, calcium chloride was added at two different concentrations: 2.00×10^{-4} and 4.00×10^{-4} mol L^{-1}, and the samples were stirred at 25 °C for 2 h to equilibrate and then analyzed for total calcium and calcium ion activity.

Mixed Calcium D-Gluconate/D-Saccharate Solutions. A total of 2.0 g of calcium D-saccharate was added to 100 mL of solutions of sodium D-gluconate with different concentrations (1.00×10^{-3}, 2.00×10^{-3}, 4.00×10^{-3}, 1.00×10^{-2}, 5.00×10^{-2}, 1.00×10^{-1}, 5.00×10^{-1}, and 9.17×10^{-1} mol L^{-1}). The samples were under constant stirring for 2 h at 25 °C and filtered as described in the Dissolution and Solubility Determination section, and then the total calcium concentration and calcium ion activity were determined. To ensure that any changes in the total calcium concentration and calcium ion activity were attributed not only to changes in the ionic strength of the solutions, the same experiment was repeated using sodium chloride, instead of sodium D-gluconate. Experiments with "opposite" salt combination were also conducted, by adding 5.0 g of calcium D-gluconate to 50 mL of solutions of 9.60×10^{-2} mol L^{-1} potassium D-saccharate. To dissolve potassium D-saccharate (D-saccharic acid potassium salt), sodium hydroxide was added in the same concentration as the salt. Samples were under constant stirring for 2 h at 25 °C and filtered, and then the total calcium concentration and calcium ion activity were determined.

■ RESULTS AND DISCUSSION

The aqueous solubility of calcium D-saccharate increases with an increasing temperature. In the temperature interval investigated, from 10 to 50 °C, it was observed that the total calcium concentration, determined by EDTA titration,

increased more than 3.5 times, while the free calcium concentration, determined electrochemically as calcium ion activity (see Figure 1) and corrected to concentration, increased 4.5 times, as may be seen from Figure 1. The increasing solubility with the temperature is in agreement with the temperature effect on solubility of other calcium salts of organic acids previously reported in the literature[8,9,18−20] and shows that the overall dissolution of calcium D-saccharate (reactions of eqs 4 and 5) is an endothermic process.

The difference between the total calcium concentration and free calcium concentration indicates that the dissolution of calcium saccharate is a stepwise process.

$$CaSac_{(s)} \rightleftharpoons CaSac_{(aq)} \tag{4}$$

$$CaSac_{(aq)} \rightleftharpoons Ca^{2+} + Sac^{2-} \tag{5}$$

Dissolved calcium D-saccharate will only dissociate partly, and the solubility product of calcium saccharate needs to be corrected for the association between calcium and D-saccharate. For the dissociation reaction of calcium D-saccharate (eq 5), it was possible to determine the solubility product, K_{sp} (eq 6), and the association constant, K_{assoc} (eq 7), for the different temperatures, assuming that the activity coefficient is equal for the calcium ion and D-saccharate ion and that the activity coefficient is unity for the undissociated calcium saccharate ion pair

$$K_{sp} = a_{Ca^{2+}} a_{Sac^{2-}} = [Ca^{2+}]\Upsilon^{2\pm}[Sac^{2-}]\Upsilon^{2\pm} = (a_{Ca^{2+}})^2 \tag{6}$$

$$K_{assoc} = \frac{[CaSac]}{a_{Ca^{2+}} a_{Sac^{2-}}} = \frac{[CaSac]}{[Ca^{2+}]\Upsilon^{2\pm}[Sac^{2-}]\Upsilon^{2\pm}}$$
$$= \frac{C_{Ca^{2+}} - [Ca^{2+}]}{(a_{Ca^{2+}})^2} \tag{7}$$

in which $c_{Ca^{2+}}$ corresponds to the total calcium concentration, determined by EDTA titration, and $[Ca^{2+}]$ corresponds to the free calcium concentration, calculated from calcium ion activity ($a_{Ca^{2+}}$) and determined electrochemically using Davies equation for correction from activity to concentration (eqs 1 and 3). The results are summarized in Table 1.

The temperature dependence of the thermodynamic solubility product and the thermodynamic association constant further allows for the determination of $\Delta H°$ and $\Delta S°$ for dissolution and complex formation, respectively, using the van't Hoff equation. The deviation from linearity in the van't Hoff plot (Figure 2) was unexpected, considering the previously reported results for other calcium salts;[21] on the other hand, the temperature interval studied herein is broader. From Kirchoff's law, enthalpy and entropy changes are related to heat capacity changes ($\Delta C_p°$) according to[22−24]

$$\Delta H° = \Delta C_p°(T - T_H) \tag{8}$$

$$\Delta S° = \Delta C_p^0 \ln\left(\frac{T}{T_S}\right) \tag{9}$$

in which T_H and T_S are reference temperatures, defined according to convenience. The combination of eqs 8 and 9 with the van't Hoff equation leads to a quadratic equation, which allows for the evaluation of the nonlinear van't Hoff plot by polynomial fitting. Figure 2 exhibits the van't Hoff plots for calcium D-saccharate, with a linear fit for the solubility product

Table 1. Aqueous Solubility, Total Calcium ($c_{Ca^{2+}}$) and Free Calcium [Ca²⁺] Concentrations, Measured Calcium Ion Activity ($a_{Ca^{2+}}$), Ionic Strength, Activity Coefficient, Thermodynamic Solubility Product, and Association Constant for Saturated Solutions of Calcium D-Saccharate at Different Temperatures

temperature (°C)	solubility[a] (g/100 mL)	$c_{Ca^{2+}}$ (mol L⁻¹)	[Ca²⁺] (mol L⁻¹)	$a_{Ca^{2+}}$	I	$\gamma_{Ca^{2+}}$	K_{sp}	K_{assoc}
10	(2.67 ± 0.09) × 10⁻²	(1.08 ± 0.04) × 10⁻³	(0.54 ± 0.08) × 10⁻³	(4.40 ± 0.57) × 10⁻⁴	(2.15 ± 0.03) × 10⁻²	0.819 ± 0.011	(1.96 ± 0.51) × 10⁻⁷	2848 ± 956
20	(3.91 ± 0.13) × 10⁻²	(1.58 ± 0.05) × 10⁻³	(0.93 ± 0.02) × 10⁻³	(7.18 ± 0.15) × 10⁻⁴	(3.74 ± 0.01) × 10⁻²	0.769 ± 0.002	(5.15 ± 0.22) × 10⁻⁷	1248 ± 10
25	(4.17 ± 0.04) × 10⁻²	(1.68 ± 0.02) × 10⁻³	(1.04 ± 0.03) × 10⁻³	(7.84 ± 0.85) × 10⁻⁴	(4.17 ± 0.01) × 10⁻²	0.756 ± 0.003	(6.14 ± 0.13) × 10⁻⁷	1038 ± 107
30	(5.09 ± 0.09) × 10⁻²	(2.05 ± 0.04) × 10⁻³	(1.27 ± 0.01) × 10⁻³	(9.35 ± 0.09) × 10⁻⁴	(5.09 ± 0.06) × 10⁻²	0.734 ± 0.001	(8.74 ± 0.17) × 10⁻⁷	890 ± 7
35	(6.17 ± 0.09) × 10⁻²	(2.49 ± 0.04) × 10⁻³	(1.56 ± 0.03) × 10⁻³	(1.11 ± 0.02) × 10⁻³	(6.24 ± 0.01) × 10⁻²	0.711 ± 0.002	(1.23 ± 0.04) × 10⁻⁶	755 ± 74
40	(7.45 ± 0.13) × 10⁻²	(3.00 ± 0.05) × 10⁻³	(1.88 ± 0.02) × 10⁻³	(1.29 ± 0.01) × 10⁻³	(7.50 ± 0.07) × 10⁻²	0.688 ± 0.001	(1.67 ± 0.03) × 10⁻⁶	674 ± 11
45	(8.77 ± 0.04) × 10⁻²	(3.53 ± 0.02) × 10⁻³	(2.15 ± 0.02) × 10⁻³	(1.44 ± 0.01) × 10⁻³	(8.60 ± 0.08) × 10⁻²	0.669 ± 0.001	(2.07 ± 0.03) × 10⁻⁶	666 ± 12
50	(1.03 ± 0.01) × 10⁻¹	(4.16 ± 0.02) × 10⁻³	(2.43 ± 0.02) × 10⁻³	(1.58 ± 0.01) × 10⁻³	(9.71 ± 0.09) × 10⁻²	0.652 ± 0.001	(2.51 ± 0.04) × 10⁻⁶	693 ± 27

[a]Solubility expressed as calcium D-saccharate anhydrous.
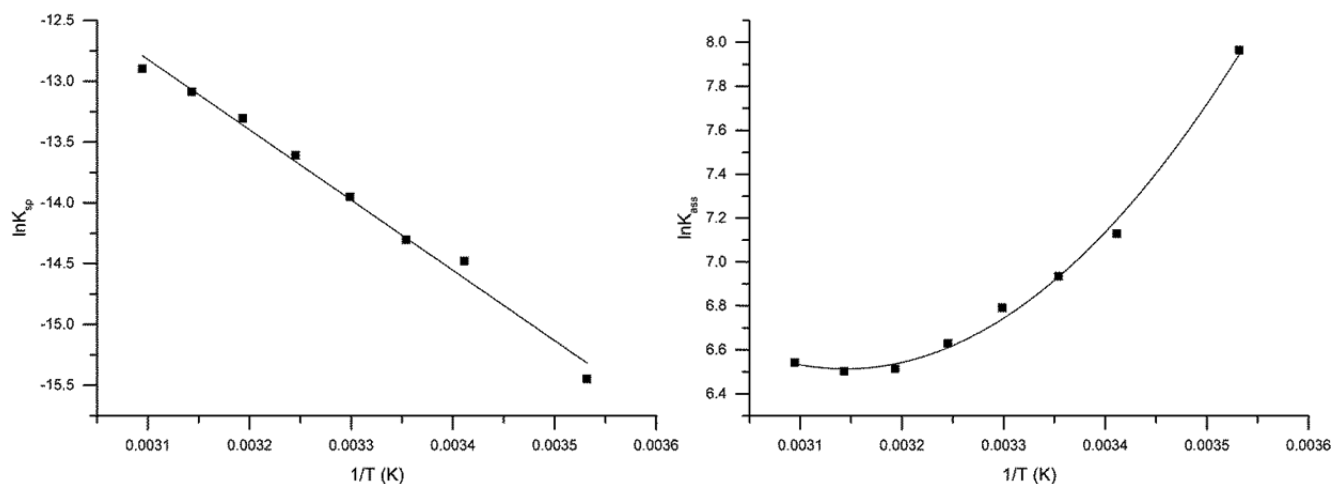
Figure 2. van't Hoff plots for calcium D-saccharate in water: (A) linear fit of the solubility product plot ($\ln K_{sp} = 5.09186 - 5778.426x$) and (B) polynomial fit of the association constant ($\ln K_{assoc} = 100.90915 - 60040.204x + 9547050x^2$).

Table 2. Added Calcium Chloride, Measured Calcium Ion Activity, Concentrations (mol L^{-1}) of Total Calcium, Free Calcium, D-Saccharate, and Calcium D-Saccharate Complex, Ionic Strength, and Thermodynamic Complex Constants for Calcium D-Saccharate in Solutions with Added Calcium Chloride

c_{CaCl_2}	$a_{Ca^{2+}}$	$c_{Ca^{2+}}$	$[Ca^{2+}]$	$[Sac^{2-}]$	$[CaSac]$	I	K_{assoc}
2.00×10^{-4}	$(6.18 \pm 0.03) \times 10^{-4}$	$(1.14 \pm 0.06) \times 10^{-3}$	7.98×10^{-4}	6.61×10^{-4}	3.41×10^{-4}	3.12×10^{-3}	1077
4.00×10^{-4}	$(7.45 \pm 0.04) \times 10^{-4}$	$(1.37 \pm 0.04) \times 10^{-3}$	9.80×10^{-4}	6.12×10^{-4}	3.87×10^{-4}	3.59×10^{-3}	1118

Table 3. Calcium D-Saccharate Concentration in mol L^{-1}, Molar Conductivity, Λ/c_{CaSac}, Degree of Dissociation, Dissociation Constant, Onsager Correction Factor, and Thermodynamic Association Constant as Calculated from Conductivity

c_{CaSac}	$\sqrt{c_{CaSac}}$ (mol L^{-1})	Λ/c_{CaSac} [a]	α_{dis}	K'_{dis}	correction factor	$\log K_{dis}$	K_{assoc}
3.16×10^{-4}	1.78×10^{-2}	190	0.82	1.18×10^{-3}	0.093	-3.02	1049
6.32×10^{-4}	2.51×10^{-2}	170	0.74	1.33×10^{-3}	0.120	-3.00	991
9.48×10^{-4}	3.08×10^{-2}	156	0.68	1.37×10^{-3}	0.150	-3.01	1031
1.26×10^{-3}	3.56×10^{-2}	145	0.63	1.35×10^{-3}	0.160	-3.03	1071
1.58×10^{-4}	3.97×10^{-2}	138	0.60	1.42×10^{-3}	0.180	-3.03	1066

[a]Experimental conductivity, Λ, multiplied by 1000 and divided by the calcium D-saccharate concentration.

and a polynomial fit for the association constant, with both constants based on activity.

From the Kirchoff relations, the parameters a, b, and c from the quadratic equation of the polynomial fit (Figure 2) can be used to determine enthalpy and entropy of the complex formation according to

$$\Delta H° = -R\left(b + \frac{2c}{T}\right) \tag{10}$$

$$\Delta S° = R\left(a - \frac{c}{T^2}\right) \tag{11}$$

The values at 25 °C using the regression parameters given in Figure 2 were calculated from eqs 10 and 11 and yield $\Delta H°_{assoc}$ = -34 ± 6 kJ mol^{-1}, $\Delta S°_{assoc}$ = -55 ± 9 J mol^{-1} K^{-1}, and K_{assoc} = 1032 ± 80. From the thermodynamic parameters determined from experimental data, the complex formation is concluded to be an exothermic process.

From the van't Hoff plot for the solubility product (Figure 2), the enthalpy and entropy of dissolution were calculated: $\Delta H°_{sp}$ = 48 ± 2 kJ mol^{-1}, $\Delta S°_{sp}$ = 42 ± 7 J mol^{-1} K^{-1}, and K_{sp} = $(6.17 \pm 0.32) \times 10^{-7}$, at 25 °C. Calcium D-saccharate dissolution is an endothermic process.

To confirm the stoichiometry of the complex formed between calcium and D-saccharate, calcium chloride was added at different concentrations to a solution of calcium D-saccharate (1.00×10^{-3} mol L^{-1}) in such a way that the total calcium concentration would not result in precipitation of calcium D-saccharate. Calcium ion activity was then determined electrochemically for these solutions. To determine the concentrations of free calcium ion $[Ca^{2+}]$, D-saccharate ion $[Sac^{2-}]$, and calcium D-saccharate complex $[CaSac]$, iterative calculations were used in a way similar to that described in the Materials and Methods. Table 2 summarizes the results of these experiments and calculation.

The thermodynamic association constant of calcium D-saccharate at 25 °C in the presence of calcium chloride (Table 2) was found to be in agreement with the results obtained for the solutions of calcium D-saccharate (Table 1), which confirms the 1:1 stoichiometry assumed in the calculations.

Conductivity of electrolytes is sensitive to incomplete dissociation of electrolytes. The conductivity, Λ, determined at 20 °C for saturated solution of calcium D-saccharate (1.58×10^{-3} mol L^{-1}) and lower concentrations are shown in Table 3 as the molar conductivity, Λ/c_{CaSac}. The conductivity of calcium D-saccharate is expected to depend linearly upon the square root of the concentration, but, as observed for other 2:2

electrolytes,[25,26] some curvature is observed in the plot of Figure 3 for higher concentrations, indicating deviation from
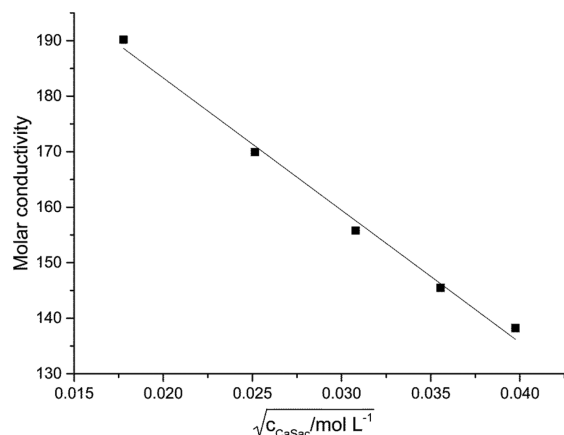

Figure 3. Molar conductivity versus square root of calcium D-saccharate concentration at 20 °C. From the linear regression, Λ/c_{CaSac} = 230.95686 − 2383.6547x, the molar conductivity at infinity dilution is determined to be Λ^∞ = 231.

ideality in addition to effects from ion association. From the limiting equivalent conductivity of calcium D-saccharate obtained by extrapolation of the curve to infinity dilution, Λ^∞ = 231, the degree of dissociation, α_{dis}, of the salt can be calculated according to

$$\alpha_{dis} = \frac{\Lambda}{c_{CaSac}\Lambda^\infty} \tag{12}$$

as presented in Table 3 for each concentration. The dissociation constant, K'_{dis}, for calcium D-saccharate may be further calculated using

$$K'_{dis} = \frac{[Ca^{2+}][Sac^{2-}]}{[CaSac]} = \frac{c_{CaSac}\alpha_{dis}c_{CaSac}\alpha_{dis}}{c_{CaSac}(1 - \alpha_{dis})} = \frac{c_{CaSac}\alpha_{dis}^2}{(1 - \alpha_{dis})} \tag{13}$$

in which c_{CaSac} corresponds to the total concentration of calcium D-saccharate in the solutions.

The dissociation constant (K'_{dis}) obtained from conductivity, however, needs further correction to obtain the thermodynamic dissociation constant, K_{dis}, by

$$\log K_{dis} = \log\left(\frac{c_{CaSac}\alpha_{dis}^2}{(1 - \alpha_{dis})}\right) - 5.76\sqrt{(c_{CaSac}\alpha_{dis})} \tag{14}$$

in which, according to the Onsager theory for electrolyte conductivity in diluted solution, the second term of eq 14 is a correction from non-ideality for a 2:2 electrolyte at finite concentrations.[25]

With the Onsager correction, the dissociation constant is fairly constant for all concentrations of calcium D-saccharate up to saturation. The average association constant ($K_{assoc} = K_{dis}^{-1}$) obtained from conductivity measurements is 1042 ± 32, which is comparable to the values determined electrochemically for 20 °C.

Calcium D-saccharate was found to form supersaturated solutions characterized by a significant lag phase for initiation of precipitation and with a rather slow rate of precipitation when initiated. To investigate the supersaturation phenomenon, supersaturated calcium D-saccharate solutions were prepared by dissolving 200 mg of calcium D-saccharate in 200 mL of water at 65 °C resulting in a total calcium concentration of 3.0×10^{-3} mol L^{-1}, followed by cooling to 25 °C. The total calcium concentration in the solution remained constant for at least 4 days, when undisturbed as determined by EDTA titration, $(3.02 ± 0.03) \times 10^{-3}$ mol L^{-1}. The calcium ion activity of the supersaturated solution also stayed constant during this period at 25 °C, $(1.28 ± 0.07) \times 10^{-3}$, confirming the absence of precipitation.

A supersaturated solution of calcium D-saccharate, prepared as previously described, showed the same total calcium concentration and calcium ion activity upon cooling from 40 to 25 to 10 °C after 2 h of equilibration at the lower temperatures, as seen in Figure 1 as the open points. The constant total calcium concentration confirms the lack of precipitation, while the constant calcium ion activity suggests that the association between calcium and D-saccharate is not adjusted in supersaturated solutions. The association process is highly exothermic, and a significant decrease of calcium ion
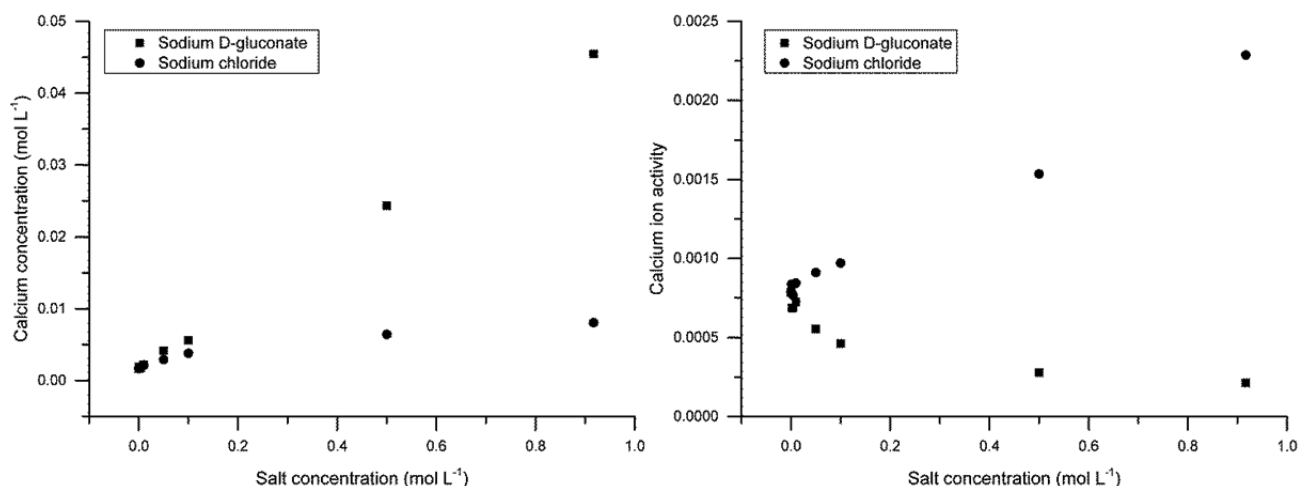

Figure 4. (A) Total calcium concentration in saturated solutions of calcium D-saccharate in the presence of increasing concentrations of sodium D-gluconate and sodium chloride. The two highest total calcium concentrations were quantified through ICP−OES, otherwise by EDTA titration. (B) Calcium ion activity in saturated solutions of calcium D-saccharate in the presence of increasing concentrations of sodium D-gluconate and sodium chloride. All experiments were performed at 25 °C.

activity was expected at lower temperatures as a result of a more significant complex formation at a lower temperature.

Calcium D-saccharate is known to prevent precipitation of calcium D-gluconate from highly supersaturated calcium D-gluconate solutions effectively during long-term storage of such mixed solutions.[14] D-Gluconate forms a calcium complex like D-saccharate but with a lower affinity and notably in an endothermic process,[21] in contrast to saccharate, with ΔH_{assoc}° = 34 and −34 kJ mol^{-1} for D-gluconate and D-saccharate, respectively. The effect of D-gluconate on calcium D-saccharate solubility was investigated in sodium D-gluconate solutions of increasing concentration in comparison to the effect of sodium chloride to separate the effects from increasing ionic strength and complex formation by D-gluconate. The increasing solubility of calcium D-saccharate and the decreasing calcium ion activity in the presence of D-gluconate (Figure 4) confirm the complex formation between calcium and D-gluconate.[27]

In the presence of sodium chloride, both calcium ion activity and solubility of calcium D-saccharate increased but the thermodynamic association constant and the thermodynamic solubility product remained constant, except for concentrations of sodium chloride above 0.10 mol L^{-1}, where the Davies equation is no longer valid (see Table 4).

Table 4. Ionic Strength, Solubility Product, and Association Constant of Saturated Solutions of Calcium D-Saccharate in the Presence of an Increasing Concentration of Sodium Chloride (in mol L^{-1})

c_{NaCl}	I	K_{sp}	K_{assoc}
1.00×10^{-3}	5.60×10^{-3}	6.99×10^{-7}	909
2.00×10^{-3}	6.72×10^{-3}	6.96×10^{-7}	972
4.00×10^{-3}	8.50×10^{-3}	5.87×10^{-7}	1319
1.00×10^{-2}	1.56×10^{-2}	7.10×10^{-7}	1063
5.00×10^{-2}	5.84×10^{-2}	8.30×10^{-7}	992
1.00×10^{-1}	1.11×10^{-1}	9.41×10^{-7}	1250
5.00×10^{-1}	5.21×10^{-1}	(2.35×10^{-6})	(491)
9.17×10^{-1}	9.42×10^{-1}	(5.23×10^{-6})	(368)

In the presence of sodium D-gluconate, calcium ion activity decreased, while the solubility of calcium D-saccharate increased more significantly than in the presence of sodium chloride at the same concentration. The calcium activity and free calcium concentration, calculated from the measured calcium ion activity, are decreasing in the presence of sodium D-gluconate as a result of the formation of the complex between the calcium ion and the D-gluconate anion in addition to the complex formation between the calcium ion and the D-saccharate anion, which shifts the equilibria toward more dissolution of calcium D-saccharate. Combining the equilibrium of calcium D-saccharate (eq 5), with K_{assoc}^{Sac} = 1032, and calcium D-gluconate (eq 15), the distribution of the different species in solution was calculated using the following equations, valid at 25 °C:

$$Ca^{2+} + Glu^{-} \rightleftharpoons CaGlu^{+} \qquad K_{assoc}^{Glu} = 70 \tag{15}$$
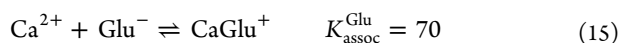
$$K_{assoc}^{Glu} = \frac{[CaGlu^{+}]\Upsilon^{\pm}}{[Ca^{2+}]\Upsilon^{2\pm}[Glu^{-}]\Upsilon^{\pm}} = \frac{[CaGlu^{+}]}{[Ca^{2+}]\Upsilon^{2\pm}[Glu^{-}]} \tag{16}$$

$$CaSac + Glu^{-} \rightleftharpoons CaGlu^{+} + Sac^{2-} \tag{17}$$
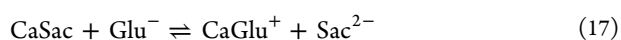
$$K = \frac{K_{assoc}^{Glu}}{K_{assoc}^{Sac}} \qquad \frac{[CaGlu^{+}][Sac^{2-}]\Upsilon^{2\pm}}{[CaSac][Glu^{-}]} = 6.74 \times 10^{-3} \tag{18}$$

$$[CaGlu^{+}] + [CaSac] = c_{Ca^{2+}} - [Ca^{2+}] \tag{19}$$

$$[Sac^{2-}] = c_{Ca^{2+}} - [CaSac] \tag{20}$$

$$[Glu^{-}] = c_{NaGlu}^{0} - [CaGlu^{+}] \tag{21}$$

where c_{NaGlu}^{0} is the initial concentration of sodium gluconate, $c_{Ca^{2+}}$ is the total calcium concentration determined by EDTA titration (or ICP−OES) as the solubility of calcium D-saccharate, and $[Ca^{2+}]$ is the free calcium ion concentration. Equations 18−21 contain the information necessary to calculate the free concentrations of the calcium D-gluconate complex ($[CaGlu^{+}]$), the calcium D-saccharate complex ($[CaSac]$), the D-gluconate ion ($[Glu^{-}]$), and the D-saccharate ion ($[Sac^{2-}]$), as the four unknowns of these equations. The calculations were performed by iteration until a stable value for ionic strength was achieved. The results are summarized in Table 5.

The ionic products of calcium D-saccharate (Q_{CaSac}) were quite constant and fairly close to the solubility product, except for the solutions with the highest concentrations of sodium D-gluconate (5.00×10^{-1} and 9.17×10^{-1} mol L^{-1}; see Table 5). Such deviations are expected for solutions with high concentrations of electrolytes, outside the validity of the Debye−Hückel limiting law theory,[16] and, notably, were also observed for the solubility products and association constants of calcium D-saccharate determined in the presence of high concentrations of sodium chloride (Table 4). On the other hand, the ionic products of calcium D-gluconate (Q_{CaGlu_2}) were lower than the experimental solubility product, except for the solutions with the highest concentrations of sodium D-gluconate. Accordingly, the solutions were saturated with calcium D-saccharate but undersaturated with calcium D-gluconate. Siegrist[14] attributes the stability of this kind of mixed solution to the formation of a double complex between calcium, D-saccharate, and D-gluconate, but from the experiments at moderate ionic strength, there is no evidence to support the formation of such complexes; on the contrary, by the iterative calculations, we were able to explain the distribution of these species in solution in agreement with the solubility products of calcium D-saccharate.

To further investigate the influence of the two hydroxycarboxylates on the precipitation equilibria of the solutions with both anions present, experiments with the "opposite" salts, calcium D-gluconate and potassium D-saccharate, were performed. The total calcium concentration and calcium ion activity were analyzed in a saturated solution of calcium D-gluconate at 25 °C and found equal to $(9.57 \pm 0.04) \times 10^{-2}$ mol L^{-1} and $(8.36 \pm 0.26) \times 10^{-3}$, respectively, in agreement with reported values.[8,20] These results were used as reference for the mixed salt experiments.

A spontaneous supersaturation phenomenon was observed for calcium D-gluconate in the presence of potassium D-saccharate solution. After 2 h of stirring, the samples were filtered (system A in Table 6) and analyzed for calcium ion activity and total calcium concentration. Calcium ion activity was lower in relation to saturated solution of calcium D-gluconate, but the total calcium concentration was higher. At 2 h after filtration, a solid started to precipitate in the filtrate, indicating that the solution was metastable. The samples were

Table 5. Concentrations (in mol L^{-1}) of Total Calcium, Free Calcium Ion, Calcium D-Gluconate Complex, Calcium D-Saccharate Complex, D-Gluconate Ion, and D-Saccharate Ion, Together with Measured Calcium Ion Activity, Ionic Strength, and Ionic Products, Q_{CaSac} and Q_{CaGlu_2}, Based on Activity in Saturated Solutions of Calcium D-Saccharate in Aqueous Solutions of Increasing Concentrations of Sodium D-Gluconate at 25 °C after Filtration[a]

c_{NaGlu}^0	$c_{Ca^{2+}}$	$a_{Ca^{2+}}$	I	$[Ca^{2+}]$	$[CaGlu^+]$	$[Sac^{2-}]$	$[CaSac]$	$[Glu^-]$	Q_{CaSac}^b	$Q_{CaGlu_2}^c$
1.00×10^{-3}	$(1.89 \pm 0.19) \times 10^{-3}$	$(7.96 \pm 0.13) \times 10^{-4}$	5.45×10^{-3}	1.09×10^{-3}	4.31×10^{-5}	1.13×10^{-3}	7.57×10^{-4}	9.57×10^{-4}	6.58×10^{-7}	6.23×10^{-10}
2.00×10^{-3}	$(1.66 \pm 0.04) \times 10^{-3}$	$(6.85 \pm 0.04) \times 10^{-4}$	5.96×10^{-3}	9.52×10^{-4}	7.90×10^{-5}	1.03×10^{-3}	6.28×10^{-4}	1.92×10^{-3}	5.09×10^{-7}	2.15×10^{-9}
4.00×10^{-3}	$(1.78 \pm 0.02) \times 10^{-3}$	$(6.88 \pm 0.15) \times 10^{-4}$	8.31×10^{-3}	1.01×10^{-3}	1.43×10^{-4}	1.15×10^{-3}	6.31×10^{-4}	3.86×10^{-3}	5.40×10^{-7}	8.46×10^{-9}
1.00×10^{-2}	$(2.18 \pm 0.04) \times 10^{-3}$	$(7.25 \pm 0.04) \times 10^{-4}$	1.63×10^{-2}	1.20×10^{-3}	7.20×10^{-4}	1.92×10^{-3}	2.25×10^{-3}	9.28×10^{-3}	8.39×10^{-7}	4.84×10^{-8}
5.00×10^{-2}	$(4.17 \pm 0.09) \times 10^{-3}$	$(5.54 \pm 0.06) \times 10^{-4}$	5.82×10^{-2}	1.27×10^{-3}	1.55×10^{-3}	2.83×10^{-3}	1.34×10^{-3}	4.84×10^{-2}	6.82×10^{-7}	8.58×10^{-7}
1.00×10^{-1}	$(5.62 \pm 0.04) \times 10^{-3}$	$(4.61 \pm 0.09) \times 10^{-4}$	1.10×10^{-1}	1.27×10^{-3}	2.70×10^{-3}	3.97×10^{-3}	1.65×10^{-3}	9.73×10^{-2}	6.63×10^{-7}	2.63×10^{-6}
5.00×10^{-1}	$(2.43 \pm 0.01) \times 10^{-2}$	$(2.78 \pm 0.02) \times 10^{-4}$	5.35×10^{-1}	9.52×10^{-4}	1.55×10^{-2}	1.65×10^{-2}	7.85×10^{-3}	4.84×10^{-1}	1.34×10^{-6}	3.53×10^{-5}
9.17×10^{-1}	$(4.55 \pm 0.01) \times 10^{-2}$	$(2.13 \pm 0.03) \times 10^{-4}$	9.79×10^{-1}	5.54×10^{-4}	2.98×10^{-2}	3.03×10^{-2}	1.51×10^{-2}	8.87×10^{-1}	2.48×10^{-6}	1.04×10^{-4}

[a]K_{sp} values based on activities are $(6.17 \pm 0.32) \times 10^{-7}$ for calcium D-saccharate and $(1.71 \pm 0.11) \times 10^{-6}$ for calcium D-gluconate, as found for simple aqueous solutions. [b]Ionic product of calcium D-saccharate based on activity $(a_{Ca^{2+}} a_{Sac^{2-}})$. [c]Ionic product of calcium D-gluconate base on activity $[a_{Ca^{2+}}(a_{Glu^-})^2]$.

Table 6. Concentrations (in mol L^{-1}) of Total Calcium, Free Calcium Ion, Calcium D-Gluconate Complex, Calcium D-Saccharate Complex, D-Gluconate Ion, and D-Saccharate Ion, Together with Measured Calcium Ion Activity, Ionic Strength, and Ionic Products, Q_{CaSac} and Q_{CaGlu_2}, Based on Activity in Saturated Solutions of Calcium D-Gluconate in Aqueous Solution of 9.60×10^{-2} mol L^{-1} of Potassium D-Saccharate at 25 °C[a]

system	$c_{Ca^{2+}}$	$a_{Ca^{2+}}$	I	$[Ca^{2+}]$	$[CaGlu^+]$	$[Sac^{2-}]$	$[CaSac]$	$[Glu^-]$	Q_{CaSac}^b	$Q_{CaGlu_2}^c$
A	$(1.10 \pm 0.01) \times 10^{-1}$	$(2.34 \pm 0.05) \times 10^{-3}$	4.32×10^{-1}	8.20×10^{-3}	3.26×10^{-2}	2.68×10^{-2}	6.92×10^{-2}	1.87×10^{-1}	1.79×10^{-5}	4.39×10^{-5}
B	$(4.81 \pm 0.03) \times 10^{-2}$	$(1.43 \pm 0.06) \times 10^{-3}$	3.92×10^{-1}	5.02×10^{-3}	1.58×10^{-2}	6.79×10^{-3}	2.73×10^{-2}	2.04×10^{-1}	2.77×10^{-6}	3.18×10^{-5}

[a]System A is a metastable solution, and system B refers to the solutions after equilibration. K_{sp} values based on activities are $(6.17 \pm 0.32) \times 10^{-7}$ for calcium D-saccharate and $(1.71 \pm 0.11) \times 10^{-6}$ for calcium D-gluconate, as found for simple aqueous solutions. [b]Ionic product of calcium D-saccharate based on activity $(a_{Ca^{2+}} a_{Sac^{2-}})$. [c]Ionic product of calcium D-gluconate based on activity $[a_{Ca^{2+}}(a_{Glu^-})^2]$.

left overnight stirring at 25 °C and then filtrated. The filtrate solution (system B in Table 6) exhibited a lower calcium ion activity and lower total calcium concentration in relation to both saturated calcium D-gluconate solution and the super-saturated solution (system A). The solids of this last filtration were dried, isolated, and characterized by the relative percentage of calcium by EDTA titration and found to have the value of 13.9 ± 0.1%. Calcium D-saccharate tetrahydrate contains 12.5% of calcium, while calcium D-gluconate monohydrate presents 8.9%. This indicates that the precipitates collected from this supersaturated solution of both hydroxycarboxylates are a hydrate of calcium D-saccharate.

To evaluate these mixed systems in a more systematic way, iterative calculations were performed to verify the distribution of the different species in solution using

$$[Sac^{2-}] = c_{KHSac}^{0} - [CaSac] \qquad (22)$$

$$[Sac^{2-}] = c_{KHSac}^{0} - [CaSac] - (c_{Ca^{2+}}^{super} - c_{Ca^{2+}}) \qquad (23)$$

$$[Glu^{-}] = 2c_{Ca^{2+}}^{super} - [CaGlu^{+}] \qquad (24)$$

where c_{KHSac}^{0} is the initial concentration of potassium D-saccharate, $c_{Ca^{2+}}^{super}$ is the total calcium concentration in the supersaturate solution, and $c_{Ca^{2+}}$ is the total calcium concentration after the equilibration period.

Two considerations had to be performed to make the iterative calculations possible. First, during the first 2 h after the addition of calcium D-gluconate to the solution of potassium D-saccharate, no form of D-saccharate has precipitated. Second, the difference in the total calcium concentration from supersaturation approaching equilibrium (system A to system B in Table 6) was attributed to the precipitation of calcium D-saccharate.

For the supersaturated solution (system A from Table 6), eqs 18, 19, 22, and 24 were used, and for the solution after equilibration (system B from Table 6), eqs 18, 19, 23, and 24 were used, taking into account the precipitation of calcium D-saccharate. Table 6 summarizes the results of the iterative calculations, performed until a stable value of the ionic strength was achieved.

The iterative calculations confirmed the supersaturation in system A indicated by continuous dissolution of calcium D-gluconate. The ionic products for both calcium D-saccharate and calcium D-gluconate are higher than the solubility product of the respective salts (29 times for calcium D-saccharate and 25 times for calcium D-gluconate), indicating that the solution is supersaturated in relation to both calcium salts. A similar behavior is reported for calcium L-lactate in the presence of sodium D-gluconate,[28] where the addition of an anion that forms a less soluble salt leads to a spontaneous supersaturation of the solution before the precipitation. After the precipitation of calcium D-saccharate (system B), the solution reaches a similar speciation as observed for the mixed solutions of calcium D-saccharate and sodium D-gluconate with a comparable ionic strength (results reported in Table 5).

The D-saccharate ion has been found to form a significantly stronger complex with the calcium ion than L-lactate, D-gluconate, and D-lacobionate,[21] all hydroxycarboxylates used for food fortification with calcium. D-Saccharate binding to calcium is exothermic in contrast to L-lactate, D-gluconate, and D-lactobionate, for which the binding is endothermic and the complex formation is entropy-driven (see Table 7). The calcium D-saccharate complex seems to be stabilized through

Table 7. Thermodynamic Association Constants for 1:1 Calcium Hydroxycarboxylate Complexes in Water and Thermodynamic Parameters of Complex Formation at 25 °C

hydroxycarboxylate	K_{assoc}	ΔH_{assoc}° (kJ mol^{-1})	ΔS_{assoc}° (J mol^{-1} K^{-1})
L-lactate[21]	49	31	135
D-gluconate[21]	88	34	150
D-lactobionate[21]	140	29	137
D-saccharate	1032	−34	−55

ring formation, as also seen by the negative entropy of association. Adjustment of calcium ion activity in supersaturated solutions of calcium D-saccharate was found slow, and this may hold the key to an understanding of spontaneous supersaturation of both calcium D-gluconate and calcium D-saccharate, when solid calcium D-gluconate is dissolved in aqueous solutions of potassium D-saccharate. During dissolution, the complex formation between D-saccharate and calcium assists the solubilization; however, the dissociation of the calcium D-saccharate complex formed during dissolution is slow in the supersaturated solution formed, resulting in supersaturation in calcium D-gluconate as well. The stabilization effect of calcium D-saccharate on supersaturated solutions of calcium D-gluconate seen after heating of the solution may also be understood based on the significant temperature effect on the distribution between calcium D-saccharate and calcium D-gluconate complex upon heating (see Figure 5).
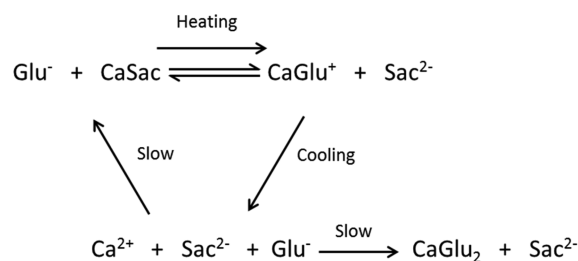

Figure 5. Scheme of the stabilization effect of calcium D-saccharate on supersaturated solutions of calcium D-gluconate.

Many dairy products are supersaturated with calcium salts, which may improve the bioavailability of calcium but, on the other hand, may result in unwanted precipitation of calcium salts during processing and storage. These phenomena seem often overlooked and barely understood. The results of the present study explain, at least partly, the mechanism behind such supersaturation and outline possible procedures based on natural ingredients and heating profiles for prevention of precipitation, corrupting quality, and decreasing bioavailability of mineral nutrients. At the same time, this understanding could facilitate the design of novel food products with increased calcium bioavailability.

■ AUTHOR INFORMATION

Corresponding Author
*Telephone: +45-3533-3322. E-mail: ls@food.ku.dk.

Notes

The authors declare no competing financial interest.

■ REFERENCES

(1) Gaucheron, F. The minerals of milk. *Reprod., Nutr., Dev.* **2005**, *45*, 473−483.

(2) Hansen, C.; Werner, E.; Erbes, H. J.; Larrat, V.; Kaltwasser, J. P. Intestinal calcium absorption from different calcium preparations: influence of anion and solubility. *Osteoporosis Int.* **1996**, *6*, 386−393.

(3) Holt, C. An equilibrium thermodynamic model of the sequestration of calcium phosphate by casein micelles and its application to the calculation of the partition of salts in milk. *Eur. Biophys. J.* **2004**, *33*, 421−434.

(4) Kitts, D. D.; Yuan, Y. V. Caseinophosphopeptides and calcium biovailability. *Trends Food Sci. Technol.* **1992**, *3*, 31−35.

(5) Nicklas, T. A. Calcium intake trends and health consequences from childhood through adulthood. *J. Am. Coll. Nutr.* **2003**, *22*, 340−356.

(6) Miller, G. D.; Jarvis, J. K.; McBean, L. D. The importance of meeting calcium needs with foods. *J. Am. Coll. Nutr.* **2001**, *20*, 168S−185S.

(7) Vavrusova, M.; Skibsted, L. H. Calcium binding to dipeptides of aspartate and glutamate in comparison with orthophosphoserine. *J. Agric. Food Chem.* **2013**, *61*, 5380−5384.

(8) Vavrusova, M.; Munk, M. B.; Skibsted, L. H. Aqueous solubility of calcium L-lactate, calcium D-gluconate, and calcium D-lactobionate: importance of complex formation for solubility increase by hydroxycarboxylate mixtures. *J. Agric. Food Chem.* **2013**, *61*, 8207−8214.

(9) Kubantseva, N.; Hartel, R. W.; Swearingen, P. A. Factors affecting solubility of calcium lactate in aqueous solutions. *J. Dairy Sci.* **2004**, *87*, 863−867.

(10) Phadungath, C.; Metzger, L. E. Effect of sodium gluconate on the solubility of calcium lactate. *J. Dairy Sci.* **2011**, *94*, 4843−4849.

(11) Zhao, Y. D.; Martin, B. R.; Weaver, C. M. Calcium bioavailability of calcium carbonate fortified soymilk is equivalent to cow's milk in young women. *J. Nutr.* **2005**, *135*, 2379−2382.

(12) Márquez, A. L.; Salvatore, G. N.; Otero, R. G.; Wagner, J. R.; Palazolo, G. G. Impact of freeze-thaw treatment on the stability of calcium-fortified soy beverages. *LWT-Food Sci. Technol.* **2015**, *62*, 474−481.

(13) Rasyid, F.; Hansen, P. M. T. Stabilization of soy milk fortified with calcium gluconate. *Food Hydrocolloids* **1991**, *4*, 415−422.

(14) Siegrist, H. Kalziumglukonat-injektionslösungen mit zuasatz von kalziumlaevulinat bzw. kalzium-D-saccharat. *Pharm. Acta Helv.* **1949**, *24*, 430−441.

(15) Vavrusova, M.; Raitio, R.; Orlien, V.; Skibsted, L. H. Calcium hydroxy palmitate: possible precursor phase in calcium precipitation by palmitate. *Food Chem.* **2013**, *138*, 2415−2420.

(16) Davies, C. W. *Ion Association*; Butterworths: Washington, D.C., 1962.

(17) Manov, G. G.; Bates, R. G.; Hamer, W. J.; Acree, S. F. Values of the constants in the Debye—Hückel equation for activity coefficients. *J. Am. Chem. Soc.* **1943**, *65*, 1765−1767.

(18) Cao, X.; Lee, H.-J.; Yun, H.; Koo, Y.-M. Solubilities of calcium and zinc lactate in water and water-ethanol mixture. *Korean J. Chem. Eng.* **2001**, *18*, 133−135.

(19) Mishelevich, A.; Apelblat, A. Solubilities of magnesium-L-ascorbate, calcium-L-ascorbate, magnesium-L-glutamate, magnesium-D-gluconate, calcium-D-gluconate, calcium-D-heptagluconate, L-aspartic acid, and 3-nitrobenzoic acid in water. *J. Chem. Thermodyn.* **2008**, *40*, 897−900.

(20) Van Loon, L. R.; Glaus, M. A.; Vercammen, K. Solubility products of calcium isosaccharinate and calcium gluconate. *Acta Chem. Scand.* **1999**, *53*, 235−240.

(21) Vavrusova, M.; Liang, R.; Skibsted, L. H. Thermodynamics of dissolution of calcium hydroxycarboxylates in water. *J. Agric. Food Chem.* **2014**, *62*, 5675−5681.

(22) Galaon, T.; David, V. Deviation from van't Hoff dependence in RP-LC induced by tautomeric interconversion observed for four compounds. *J. Sep. Sci.* **2011**, *34*, 1423−1428.

(23) Vailaya, A. Fundamentals of reversed phase chromatography: thermodynamic and exothermodynamic treatment. *J. Liq. Chromatogr. Relat. Technol.* **2005**, *28*, 965−1054.

(24) Vailaya, A.; Horváth, C. Retention thermodynamics in hydrophobic interaction chromatography. *Ind. Eng. Chem. Res.* **1996**, *35*, 2964−2981.

(25) Dunsmore, H. S.; James, J. C. The electrolytic dissociation of magnesium sulphate and lanthanum ferricyanide in mixed solvents. *J. Chem. Soc.* **1951**, 2925−2930.

(26) Money, R. W.; Davies, C. W. The extent of dissociation of salts in water. Part IV.: bi-bivalent salts. *Trans. Faraday Soc.* **1932**, *28*, 609−614.

(27) Skibsted, L. H.; Kilde, G. Dissociation constant of calcium gluconate. Calculations from hydrogen ion and calcium ion activities. *Dan. Tidsskr. Farm.* **1972**, *46*, 41−46.

(28) Vavrusova, M.; Skibsted, L. H. Spontaneous supersaturation of calcium D-gluconate during isothermal dissolution of calcium L-lactate in aqueous sodium D-gluconate. *Food Funct.* **2014**, *5*, 85−91.

Short communication

Aqueous citric acid as a promising cleaning agent of whey evaporators

Martina Vavrusova [a], Nikolaj P. Johansen [a], André C. Garcia [a, b], Leif H. Skibsted [a, *]

[a] Department of Food Science, University of Copenhagen, Rolighedsvej 30, DK-1958, Frederiksberg C, Denmark
[b] Instituto Federal de Educação, Ciência e Tecnologia de São Paulo, Campus Capivari, Avenida Doutor Ênio Pires de Camargo, 2971, São João Batista, CEP: 13360-000, Capivari, SP, Brazil

A R T I C L E   I N F O

A B S T R A C T

Scale in evaporators for lactose production was identified as mainly calcium citrate tetrahydrate with phosphate contaminations. Dissolution of 3.00 g of scale in aqueous solutions of 0.100, 0.500, and 1.00 mol L^{-1} citric acid with final volumes of 100, 50, and 25 mL was investigated. The highest concentration of citric acid was the most effective for all the investigated volumes. From the citric acid solutions, spontaneously supersaturated in calcium citrate tetrahydrate during scale dissolution in the smaller volumes for all citric acid concentrations, calcium citrate tetrahydrate slowly precipitated in acceptable purity for technical use. Dissolution efficiency of aqueous solutions of 0.200 mol L^{-1} nitric acid combined with 0.100, 0.500, and 1.00 mol L^{-1} citric acid with final volumes of 100, 50, and 25 mL showed synergistic effect especially for the higher concentrations and lower volumes of two acids.

© 2017 Elsevier Ltd. All rights reserved.

1. Introduction

Whey is a valuable dairy by-product from cheese production from which whey proteins are isolated for use as highly nutritive food ingredients (Marshall, 2004). Lactose may be crystallised from whey permeate during further processing, including reduction of volume by evaporation. During the evaporation process mineral salts precipitate and accumulate on heating surfaces. Deposition of scale on heating surfaces is known as fouling. The main components of the whey deposit are calcium salts, especially calcium citrate tetrahydrate precipitating from the concentrated whey (Jeurnink & Brinkman, 1994; Jeurnink, Walstra, & deKruif, 1996). Calcium salts such as calcium citrate tetrahydrate and some calcium phosphates have decreasing solubility with increasing temperature, known as reverse solubility and further contributing to mineral deposition during evaporation of whey at higher temperatures (Vavrusova & Skibsted, 2016). Deposition of mineral salts during concentration of whey permeate has a negative impact on operation costs and may also compromise the final product quality of lactose. Therefore, the evaporators need regular cleaning with removal of the scale, and since the scale mainly consists of calcium salts cleaning with acid is often preferred (Jeurnink & Brinkman, 1994). Cleaning procedures should whenever possible be based on biodegradable, noncorrosive and nontoxic agents.

Based on our recent finding of solubility overshooting, which describes increased solubility of calcium citrate tetrahydrate when dissolving solid calcium citrate tetrahydrate in aqueous sodium citrate at ambient conditions, we have explored the possibility of replacing the acids such as nitric acid normally used for cleaning the whey evaporators during lactose concentration with citric acid (Vavrusova & Skibsted, 2016; Vavrusova, Garcia, Danielsen, & Skibsted, 2017). The efficiency of citric acid was further compared with aqueous nitric acid as is often used for evaporator cleaning. Furthermore, the effect of combining citric acid and nitric acid was also investigated to improve cleaning.

2. Methods and materials

2.1. Materials

Calcium citrate tetrahydrate, calcium hydrogen phosphate dihydrate, citric acid, nitric acid, and hydroxyapatite were all from Sigma Aldrich (Steinheim, Germany). Scale was collected from heating surfaces of evaporators used to concentrate whey permeate during lactose production and was kindly provided by Arla Foods Ingredients (Nr. Vium, Denmark).

* Corresponding author. Tel.: +45 35 33 32 21.
  E-mail address: ls@food.ku.dk (L.H. Skibsted).

2.2. Dissolution of scale in citric acid

Aqueous citric acid with a concentration of 0.100 mol L^{-1}, 0.500 mol L^{-1}, and 1.00 mol L^{-1} in a final volume of 100 mL, 50 mL, and 25 mL was added to 3.00 g of scale samples. Samples were stirred on magnetic stirrer for 1 h at ambient temperature.

For dissolution of scale after stepwise addition of citric acid, aliquots of 5—10 mL of aqueous citric acid with a concentration of 0.100 mol L^{-1}, 0.500 mol L^{-1}, and 1.00 mol L^{-1} were added with intervals of 10 min to 3.00 g of scale samples to a final volume of 100 mL. The samples were stirred on magnetic stirrer for 24 h at ambient temperature, following the addition of aqueous citric acid.

2.3. Dissolution of scale in citric acid combined with nitric acid

Aqueous citric acid with a concentration of 0.100 mol L^{-1}, 0.500 mol L^{-1}, and 1.00 mol L^{-1} combined with 0.200 mol L^{-1} nitric acid with final volumes of 100 mL, 50 mL, and 25 mL were added to 3.00 g of scale samples. Aqueous nitric acid of 0.200 mol L^{-1} with final volumes of 100 mL, 50 mL, and 25 mL added to 3.00 g of scale samples was used as a control. Samples were stirred on magnetic stirrer for 1 h at ambient temperature.

2.4. Infrared spectra

Fourier transform infrared (FT-IR) spectra of scale samples and precipitates, collected after reaction of 3.00 g of scale with 0.100 mol L^{-1} citric acid in 25 mL of aqueous citric acid solution after overnight stirring at ambient temperature, were recorded on a FT-IR spectrometer (Bomem MB100, ABB, Quebec, Canada) equipped with an attenuated total reflection (ATR) attachment. All spectra were obtained by accumulation of 64 scans, with resolution of 4 cm^{-1}, in the spectral region 500—4000 cm^{-1}. The scale was freeze dried and finely ground prior to FT-IR analysis. Calcium citrate tetrahydrate, calcium hydrogen phosphate dihydrate, and hydroxyapatite were used as standards for comparing with the scale sample.

2.5. Inductive coupled plasma-optical emission spectroscopy analysis of scale

Calcium, potassium, magnesium, sodium, and phosphate content were determined in the solutions from dissolution of 3.0 g of scale in 0.100 mol L^{-1}, 0.500 mol L^{-1}, and 1.00 mol L^{-1} in 100 mL of aqueous citric acid solution after overnight stirring by inductive coupled plasma-optical emission spectroscopy (ICP-OES) using an ICP-OES (Model 5100, Agilent Technologies, California) equipped with a Meinhard nebuliser and cyclonic spray chamber. For quantification of calcium, potassium, magnesium, sodium, and phosphorus the wavelengths were 318.1, 766.5, 279.6, 589.6, and 213.6 nm. The samples were initially dried and homogenised followed by complete digestion in a microwave oven.

3. Results and discussion

Complete dissolution of 3.00 g of scale, collected from heating surfaces of whey permeate evaporators, was achieved by adding 100 mL of citric acid with concentrations of 0.500 or 1.00 mol L^{-1}. Samples dissolved completely under such conditions resulting in clear solutions, which were suitable for analysis of elements. Addition of 100 mL of 0.100 mol L^{-1} citric acid resulted in partial dissolution as some white deposit of scale was still present (Fig. 1A). The treatment resulted in fractionation of the scale as a small amount of brown material did not dissolve under any conditions (Fig. 1A). The brown material not soluble in aqueous citric acid is

most likely a mixture of degraded organic material formed from Maillard reaction products and a proper identification would require more detailed studies. Quantification of elements present in the clear scale suspensions showed that the deposit consisted of mainly calcium salts (Table 1). Infrared spectroscopy of the solid scale material indicates that calcium citrate tetrahydrate is the major component of the scale being formed during processing of concentrated whey permeates (Fig. 2). However, the content of phosphorus determined by element analysis using ICP indicates that together with calcium citrate tetrahydrate some form of calcium phosphate is present in the scale as also indicated by infrared spectroscopy of the scale material (Fig. 2). This observation is in agreement with previous findings as precipitation of calcium citrate tetrahydrate from concentrated whey is often seen, but other calcium salts such as different types of calcium phosphates were also previously identified in scale material (Daufin et al., 1987; Jeurnink & Brinkman, 1994) or in simulated milk ultrafiltrate (Rosmaninho & Melo, 2006).

For low citric acid concentration and low volume of this cleaning liquid the white material did not dissolve completely (Fig. 1C and D). To obtain a complete dissolution of the white material of the scale, a ratio between citric acid and calcium citrate tetrahydrate of 5 or higher was found to be necessary (Fig. 1). This calculation was based on the assumption that the scale only consisted of calcium citrate tetrahydrate. The exact concentration and type of calcium phosphate was not confirmed in this study and therefore was not included in calculations for Fig. 1.

When the cleaning liquid was added stepwise in small volumes, the scale material did not dissolve even when kept for 24 h under constant stirring (Fig. 1B). Furthermore, stepwise addition resulted in an unexpected precipitation of a white material.

Complete dissolution by the required volume of cleaning liquid with a citric acid concentration above the critical concentration was calculated to depend on a spontaneous supersaturation as was previously observed for dissolution of calcium citrate in aqueous sodium citrate but not in water (Vavrusova & Skibsted, 2016):

$$Ca_3Cit_2 + Cit^{3-} \rightarrow 3\ CaCit^- \tag{1}$$

The supersaturated solutions obtained by dissolution of the scale were found to be sensitive to precipitation as seeded by non-dissolved calcium citrate tetrahydrate for the conditions of 0.100, 0.500, and 1.00 mol L^{-1} citric acid with final volume of 25 mL. Complete dissolution of calcium citrate tetrahydrate from the scale was only obtained by initial addition of the 1.00 mol L^{-1} citric acid after 1 h of stirring under these conditions (Fig. 3A). However, upon longer standing, precipitation occurred even for use of cleaning solution with the high concentration of citric acid (Fig. 3B). The white precipitate was identified by infrared spectroscopy to be calcium citrate tetrahydrate without phosphate contamination (Fig. 4). This precipitate may have potential in use as calcium citrate tetrahydrate of technical quality but further detailed investigation is needed.

For use of aqueous citric acid solutions for cleaning of evaporators fouled with scale mainly composed of calcium citrate tetrahydrate, it is accordingly recommended to try to flush initially with the full volume as seen in Fig. 1, as a stepwise use of the same volume of solution will result in secondary precipitation of calcium citrate tetrahydrate. Further, the effluent solution may be collected and left for precipitation, as calcium citrate tetrahydrate of a reasonable purity will precipitate upon standing at ambient temperature, as is shown in Fig. 4. It is also highly recommended to try to use cold water, or even ice-cold water, for flushing evaporators during cleaning in place (CIP) trials rather than using warm water as many calcium salts may precipitate when using warm water due

to the so-called inverse solubility, as previously described (Chatterjee & Dhar, 1924; Vavrusova & Skibsted, 2016). The brown material not soluble in the aqueous citric acid is released during dissolution from calcium salt matrix and may most likely easily be flushed away by water.

Aqueous nitric acid has been commonly used for cleaning of evaporators. Mixtures of citric acid and nitric acid were found to result in more efficient dissolution than nitric acid alone. Based on dissolution experiments with aqueous 0.200 mol L^{-1} nitric acid, which is commonly used, a critical volume was identified. For 3.0 g of scale, 100 mL of 0.200 mol L^{-1} nitric acid either alone or combined with 0.100, 0.500, and 1.00 mol L^{-1} citric acid is required for complete dissolution (Fig. 5A). However, for 50 and 25 mL of cleaning solution consisting of a minimum concentration of 0.500 mol L^{-1} citric acid combined with 0.200 mol L^{-1} nitric acid is required for complete dissolution of the white scale material (Fig. 5B and C). The synergistic effect of nitric acid combined with

Table 1
Composition of elements (mmol kg^{-1}) in dissolved fraction of the scale, which resulted from dissolution of 3.0 g of scale in 100 mL of aqueous citric acid (CA) with increasing concentration.[a]

Added CA (mol L^{-1})	Composition (mmol kg^{-1})				
	Ca	K	Mg	Na	P
0.100	66	0.15	5.19	0.65	22
0.500	96	0.14	5.59	0.70	23
1.00	98	0.14	5.76	0.80	24

[a] See also Fig. 1A.

citric acid was found to be especially effective for lower volumes of cleaning solution (Fig. 5B and C).

In conclusion, the use of citric acid as a cleaning agent for dairy processing equipment, fouled mainly with calcium citrate tetrahydrate, showed promising perspectives and should gain broader
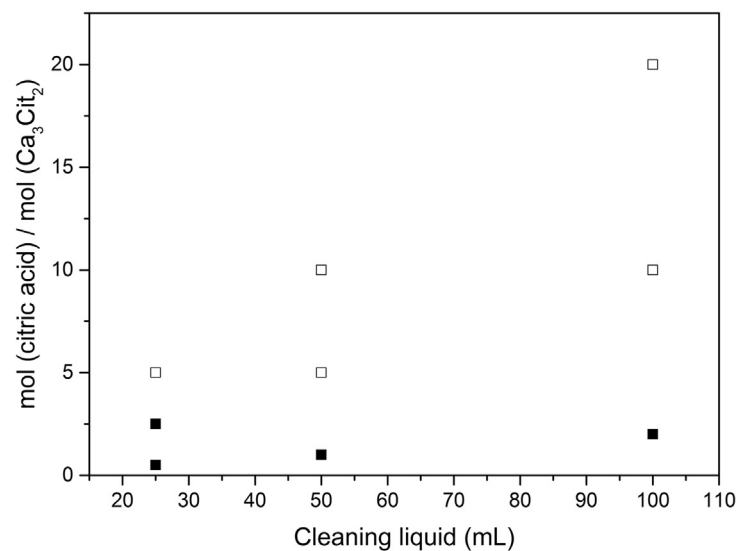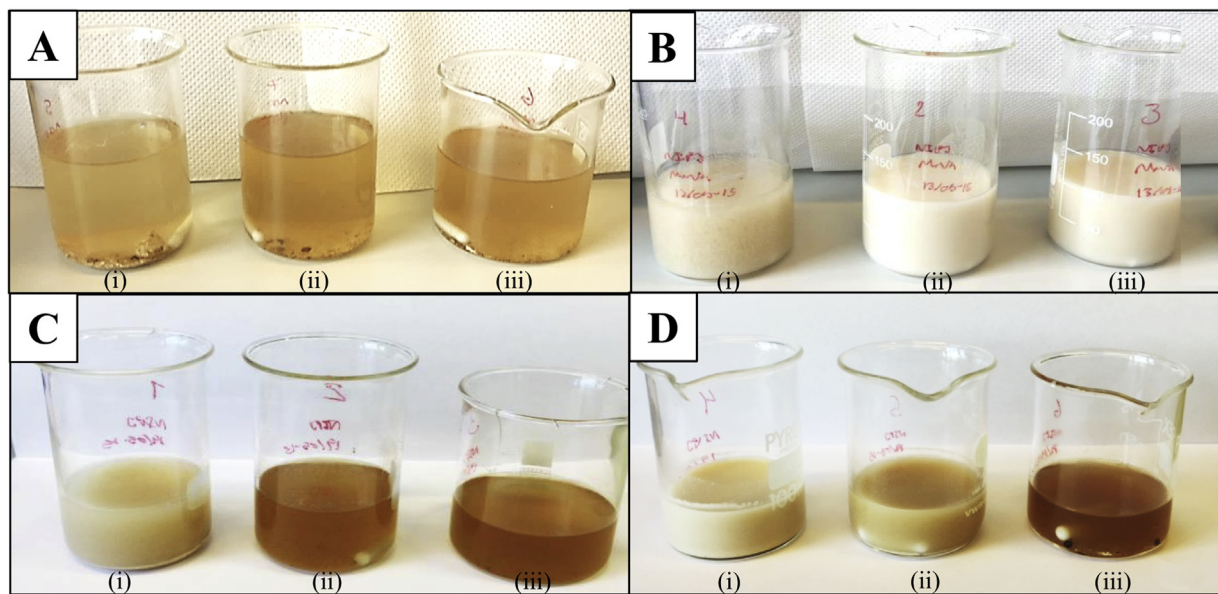

Fig. 1. Scale suspensions prepared from the scale isolated from heating surface of an evaporator used to concentrate whey permeate during lactose production treated with a cleaning liquid with (i) 0.100 mol L^{-1}, (ii) 0.500 mol L^{-1}, and (iii) 1.00 mol L^{-1} citric acid with a final volume of (A) 100 mL, (C) 50 mL and (D) 25 mL after 1 h of stirring for 3.00 g of scale sample at ambient temperature. Filled squares in diagram indicate that scale was only partly dissolved, while open squares indicated that scale dissolved by the cleaning liquid. Panel B shows the scale suspensions after stepwise addition (5–10 mL with intervals of 10 min) of (i) 0.100 mol L^{-1}, (ii) 0.500 mol L^{-1}, and (iii) 1.00 mol L^{-1} citric acid with the final volume of 100 mL after 24 h of stirring for 3.00 g of scale sample at ambient temperature.
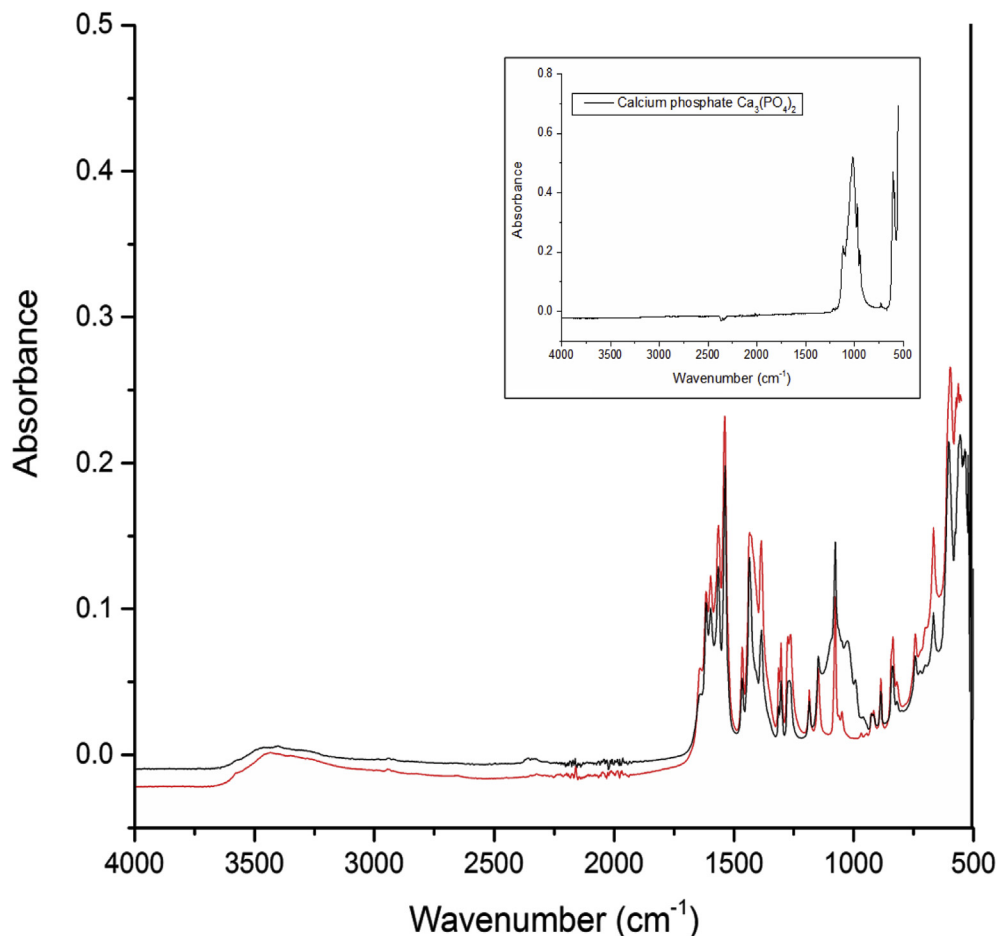
Fig. 2. FT-IR spectra of scale (black line) isolated from heating surface of an evaporator used to concentrate whey permeate during lactose production overlapped with the spectra of calcium citrate tetrahydrate (red line). The spectrum of calcium phosphate is shown as an insert for the spectral region with largest spectral deviation between scale material and calcium citrate. (For interpretation of the references to colour in this figure legend, the reader is referred to the web version of this article).
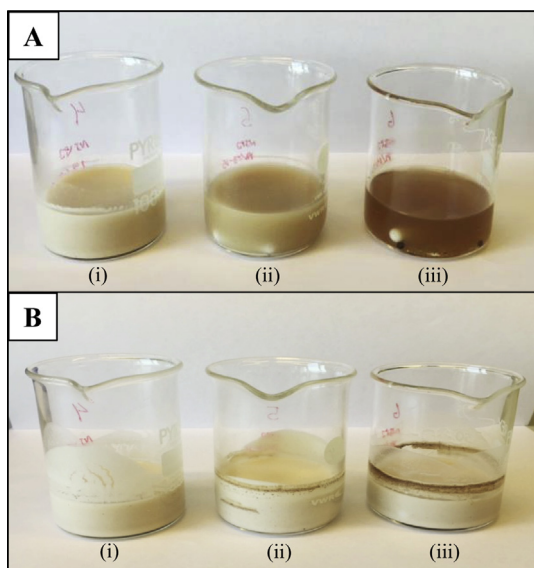
Fig. 3. Scale suspensions prepared from the scale isolated from heating surface of an evaporator used to concentrate whey permeate during lactose production treated with a cleaning liquid with (i) 0.100 mol L^{-1}, (ii) 0.500 mol L^{-1}, and (iii) 1.00 mol L^{-1} citric acid with a final volume of 25 mL after (A) 1 h and (B) 24 h stirring for 3.00 g of scale sample at ambient temperature.

attention. However, there is a clear need for more comprehensive experimental work on a bigger scale such as CIP trials. Other factors such as combining citric acid with other inorganic acids/compounds, and changes in temperature and pH should also be considered. Interestingly, the ability of the weak citric acid to
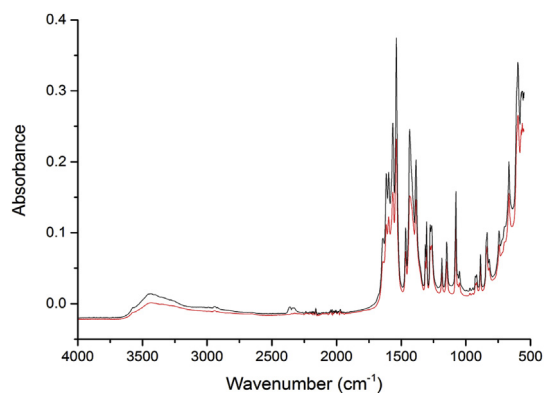
Fig. 4. Precipitate (black line) from solution of dissolved scale after reaction with 0.100 mol L^{-1} citric acid with the final volume of 25 mL after overnight stirring for 3.00 g of scale sample at ambient temperature overlapped with spectrum of calcium citrate tetrahydrate (red line). (For interpretation of the references to colour in this figure legend, the reader is referred to the web version of this article).
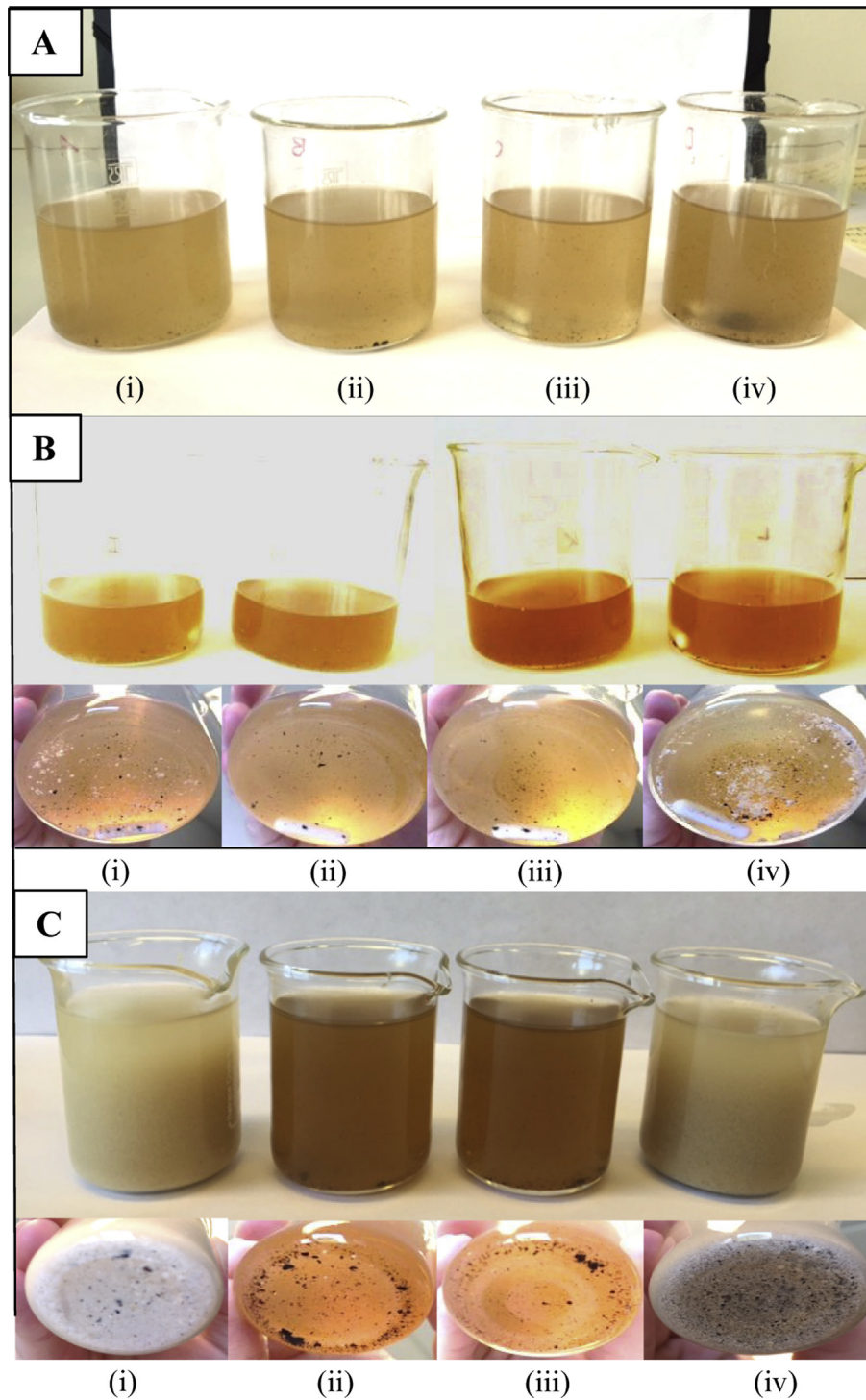
Fig. 5. Scale suspensions prepared from the scale isolated from heating surface of an evaporator used to concentrate whey permeate during lactose production treated with 0.200 mol L^{-1} nitric acid combined with (i) 0.100 mol L^{-1}, (ii) 0.500 mol L^{-1}, and (iii) 1.00 mol L^{-1} citric acid dissolution compared with (iv) 0.200 mol L^{-1} nitric acid alone with a final volume of (A) 100 mL, (B) 50 mL and (C) 25 mL after approximately 1 h of stirring for each 3.00 g of scale sample at ambient temperature.

dissolve the calcium salt of the same acid seems like a paradox and a surprising result of this work. Such increased solubility, also described in our previous studies as solubility overshooting, depends on a combination of two main factors such as enhanced rate of dissolution of calcium salt due to complex formation of calcium ions with excess added citrate even at low pH, and more importantly, a very slow rate for calcium citrate tetrahydrate precipitation (Vavrusova et al., 2017). The pH of all the scale samples was not

adjusted and was low after addition of aqueous citric acid and aqueous nitric acid or their combinations. Low pH contributes to dissolution of calcium salts of low solubility. Notably, the effect of solubility overshooting is for gluconate/lactate combinations now finding use in the oil industry to dissolve underground calcium minerals in order to increased yield of crude oil (Rabie, Saber, & Nasr El-Din, 2015). Combinations of different hydroxycarboxylates and even hydroxycarboxylates with inorganic acids as in the

present study, have resulted in unexpected effects such as increased solubility of calcium salts of low solubility, which may trigger further studies on a larger scale to improve cleaning strategies in dairy industry.

Acknowledgements

References

Chatterjee, K. P., & Dhar, N. R. (1924). Studies of sparingly soluble salts, readily obtained from hot solutions of reacting substances I. *Journal of Physical Chemistry, 28*, 1009—1028.

Daufin, G., Labbe, J. P., Quemerais, A., Brule, G., Michel, F., Roignant, M., et al. (1987). Fouling of a heat-exchange surface by whey, milk and model fluids — an analytical study. *Lait, 67*, 339—364.

Jeurnink, T. J. M., & Brinkman, D. W. (1994). The cleaning of heat exchangers and evaporators after processing milk or whey. *International Dairy Journal, 4*, 347—368.

Jeurnink, T. J. M., Walstra, P., & deKruif, C. G. (1996). Mechanisms of fouling in dairy processing. *Netherlands Milk and Dairy Journal, 50*, 407—426.

Marshall, K. (2004). Therapeutic applications of whey protein. *Alternative Medicine Reviews, 9*, 136—156.

Rabie, A. I., Saber, M. R., & Nasr El-Din, H. A. (2015). A new environmentally friendly acidizing fluids for HP/HT matrix acidizing treatments with enhanced product solubility. *Society of Petroleum Engineers*, 1—33.

Rosmaninho, R., & Melo, L. F. (2006). The effect of citrate on calcium phosphate deposition from simulated milk ultrafiltrate (SMUF) solution. *Journal of Food Engineering, 73*, 379—387.

Vavrusova, M., Garcia, A. C., Danielsen, B. P., & Skibsted, L. H. (2017). Spontaneous supersaturation of calcium citrate from simultaneous isothermal dissolution of sodium citrate and sparingly soluble calcium hydroxycarboxylates in water. *RSC Advances, 7*, 3078—3088.

Vavrusova, M., & Skibsted, L. H. (2016). Aqueous solubility of calcium citrate and interconversion between the tetrahydrate and the hexahydrate as a balance between endothermic dissolution and exothermic complex formation. *International Dairy Journal, 57*, 20—28.

Spontaneous supersaturation of calcium citrate from simultaneous isothermal dissolution of sodium citrate and sparingly soluble calcium hydroxycarboxylates in water

Martina Vavrusova,[a] André C. Garcia,[ab] Bente P. Danielsen[a] and Leif H. Skibsted*[a]

Strongly supersaturated homogeneous calcium citrate solutions are formed spontaneously when solid sodium citrate and solid calcium hydroxycarboxylates are dissolved simultaneously in water or when solid sodium citrate is dissolved in an already saturated aqueous solution of the calcium hydroxycarboxylate at ambient conditions. Maximal supersaturation of calcium citrate was found to decrease for an increasing value of the stability constant for calcium binding: L-lactate < D-gluconate < citrate, indicating citrate assisted dissolution through competitive complex formation as a thermodynamic factor controlling spontaneous supersaturation for up to a factor of more than twenty. Time elapsing prior to initiation of precipitation of calcium citrate was found to be shorter for a higher degree of supersaturation and lasted between hours and days. During subsequent precipitation equilibrium solubility of calcium citrate was approached with a simultaneous increase in water activity. Both thermodynamic and kinetic factors are suggested to be important for the spontaneous supersaturation, which seems to explain the paradoxal but well-stablished high bioavailability of calcium from the sparingly soluble calcium citrate and the high mobility of calcium in the presence of citrate during biomineralization.

Introduction

Citrate as a vehicle for calcium ions has been demonstrated to increase the bioavailability of calcium from food or from supplements under various conditions despite the low solubility of calcium citrate.[1,2] Milk and other dairy products, known as important calcium sources in human nutrition, have a significant content of citrate.[3]

Calcium citrate as a calcium source with an equilibrium release of 5 mM calcium to an aqueous environment also enhances bone regeneration by bone morphogenetic proteins by affecting osteoblast differentiation and proliferation.[4] A high production of citrate by osteoblasts was also identified as important for bone formation and an optimal structure of apatite nanocrystals for improved bone resistance to fracture.[5] A more specific role of citrate in apatite crystallization has now also been recognized during bone mineralization.[6–8]

A common factor for these observations from experimental human nutrition and from medical treatment of osteoporosis may be related to the solubility overshooting phenomena

recently observed for dissolution of calcium citrate tetrahydrate in aqueous solutions of sodium citrate but not in pure water.[9] Notably, the initial solubility of calcium citrate in aqueous sodium citrate was higher by approximately 10% than the equilibrium solubility established after 48 hours of isothermal equilibration of solutions with solid calcium citrate in the temperature interval from 0 to 100 °C.[9] Similarly spontaneous supersaturation of calcium D-gluconate in water by up to a factor of seven was observed by isothermal continuing dissolution of calcium L-lactate in an already saturated aqueous calcium L-lactate solution after addition of solid sodium D-gluconate.[10] Notably, both calcium L-lactate and calcium D-gluconate find widespread use for calcium fortification of food and beverages.[11,12]

Non-equilibrium conditions may also explain the increased bioavailability of calcium from mixtures of citric acid and calcium hydroxide compared to calcium citrate found in human intervention studies.[1] Likewise, a suspension of calcium citrate in aqueous potassium citrate had superior calcium bioavailability compared to tablet formulation of calcium citrate for patients after Roux-en-Y gastric bypass operations.[13]

The mechanism behind spontaneous formation of supersaturated aqueous solutions of sparingly soluble calcium hydroxycarboxylates under isothermal condition accordingly deserves more attention not only in relation to improvement of

[a]Department of Food Science, University of Copenhagen, Rolighedsvej 30, DK-1958 Frederiksberg C, Denmark. E-mail: ls@food.ku.dk

[b]Instituto Federal de Educação, Ciência e Tecnologia de São Paulo, Campus Capivari. Avenida Doutor Ênio Pires de Camargo, 2971 – São João Batista, CEP: 13360-000, Capivari, SP, Brazil

bioavailability of calcium from foods and supplements but also in relation to biomineralization and mineral mobility in calcified tissue. Most mammalian biofluids are supersaturated with respect to calcium hydroxyapatite but calcium phosphate deposition in various tissues is strictly controlled by specific crystallization inhibitors.[14] The dissolution process resulting in spontaneous supersaturation under isothermal conditions is less understood. We now report the results of investigations, which points towards a special role of citrate and possibly other hydroxycarboxylates in mineral mobility involving spontaneous isothermal supersaturation.

Experimental

Materials

Tricalcium dicitrate tetrahydrate, calcium L-lactate pentahydrate, calcium D-gluconate monohydrate, ammonium purpurate 5,5-nitrilodibarbituric acid (murexid), and trisodium citrate dihydrate were all from Sigma Aldrich (Steinheim, Germany). Purity of all calcium salts was of analytical grade. Ethylenediaminetetraacetic acid disodium salt dihydrate (EDTA), calcium chloride dihydrate, and sodium hydroxide were from Merck (Darmstadt, Germany). All aqueous solutions were made from purified water from Milli-Q Plus (Millipore Corporation, Bedford, MA).

Total calcium determination

Standardization of 0.0100 mol L^{-1} and 0.0500 mol L^{-1} solution of EDTA used for titration was obtained against a 0.0100 mol L^{-1} aqueous solution of CaCl$_2$ prepared by weighing of calcium chloride dihydrate. An aliquot of the 1.000 mL of sample was transferred to a titration flask and subsequently diluted with 25 mL of water. To maintain basic pH, 0.50 mL of 2.0 mol L^{-1} solution of NaOH was added to each sample, and 0.20 mL of 0.50% murexid solution was used as an indicator.

Electrochemical measurement of calcium ion activity

Calcium ion activity, $a_{Ca^{2+}}$, was measured using a calcium ion selective electrode ISE25Ca with a reference REF251 electrode from Radiometer (Copenhagen, Denmark). The calibration of the electrode was obtained using aqueous 1.00 × 10^{-4}, 1.00 × 10^{-3}, 1.00 × 10^{-2} mol L^{-1} CaCl$_2$ standard solutions prepared from a 1.000 mol L^{-1} CaCl$_2$ stock solution at 25 °C. Calcium ion activity, $a_{Ca^{2+}}$, in the standard solutions was calculated from the relationship between activity and calcium concentration, $c_{Ca^{2+}}$, according to

$$a_{Ca^{2+}} = c_{Ca^{2+}} \gamma^{2+} \tag{1}$$

where γ^{2+} is the activity coefficient calculated from the Davies' equation as described previously[15]

$$\log \gamma^{2+} = -A_{DH} z^2 \left(\frac{\sqrt{I}}{1 + \sqrt{I}} - 0.30I \right) \tag{2}$$

where A_{DH} is the Debye–Hückel constant with the numerical value of $A_{DH} = 0.510$ at 25 °C, I is the ionic strength, and z is the

charge of the ion, *i.e.*, 2 for calcium ions.[16] The calcium ion activity in the test solutions was calculated from a linear standard curve between electrode potential (mV) measured for the calibration solutions and $-\log a_{Ca^{2+}}$ of the calibration solutions according to the Nernst equation at 25 °C.

Water activity

Water activity, a_w, was determined using an Aqua lab CX-2 (Aqua lab, Pullman, WA, USA) at 25.0 ± 0.2 °C. The water activity was determined as the mean of measurements for two separate solutions. For measurement under conditions of supersaturation, solutions were prepared by mixing 16.00 g and 20.00 g of solid calcium L-lactate with 12.00 g and 24.00 g of solid sodium citrate, respectively, and 16.00 g of solid calcium D-gluconate with 24.00 g of solid sodium citrate, dissolved in 100 mL of water. Water activity was measured in the transparent solutions and after 96 h in the solution with precipitate, which was filtered off prior to measurement.

Dissolution experiments

1. Solid sodium citrate in saturated aqueous calcium L-lactate. (a) Saturated solutions of calcium L-lactate were prepared by adding 12.00 g (0.0389 mol) to 100 mL of water and equilibrating for two hours under constant stirring at 25 °C. The saturated solution contained 10.5 g (0.340 M) of calcium L-lactate in equilibrium with a precipitate of 1.5 g (0.0049 mol) of calcium L-lactate. Aliquots of 13.00 g (0.0442 mol) or 6.00 g (0.0204 M) of solid sodium citrate were added to the saturated calcium L-lactate solutions. Supersaturated homogeneous solutions appeared within approximately 10 minutes of moderate stirring at 25 °C. The homogeneous solutions were analysed for total calcium concentration and after 2, 24, 48, and 72 hours under constant stirring during which period precipitation occurred, and calcium ion activity was determined.

(b) Saturated solutions of calcium L-lactate were prepared by adding 16.00 g (0.0519 mol) to 100 mL of water and equilibrating for two hours under constant stirring at 25 °C. The saturated solution contained 10.5 g (0.340 M) of calcium L-lactate in equilibrium with a precipitate of 5.5 g (0.0178 mol). Aliquots of 12.00 g (0.0408 mol), or 24.00 g (0.0816 mol) of solid sodium citrate were added to the saturated calcium L-lactate solutions. Supersaturated homogeneous solutions appeared within approximately 12 minutes of moderate stirring at 25 °C for the conditions of 12.00 g and 24.00 g added solid sodium citrate. The homogeneous solutions were analysed for total calcium concentration and after 2, 24, 48, and 72 hours under constant stirring during which period precipitation occurred, and calcium ion activity was determined.

2. Solid sodium citrate in saturated aqueous calcium D-gluconate. (a) Saturated solutions of calcium D-gluconate were prepared by adding 5.00 g (0.0111 mol) to 100 mL of water and equilibrating for two hours under constant stirring at 25 °C. The saturated solution contained 4.3 g (0.096 M) of calcium D-gluconate in equilibrium with a precipitate of 0.70 g (0.0015 mol) of calcium D-gluconate. Aliquots of 13.00 g (0.0442 mol) or 6.00 g (0.0204 mol) of solid sodium citrate were added to the

saturated calcium D-gluconate solutions. Supersaturated homogeneous solutions appeared within approximately 10 minutes of moderate stirring at 25 °C. The homogeneous solutions were analysed for total calcium concentration and after 2, 24, 48, and 72 hours under constant stirring during which period precipitation occurred, and calcium ion activity was determined.

(b) Saturated solution of calcium D-gluconate was prepared by adding 6.50 g (0.0145 mol) to 100 mL of water and equilibrating for two hours under constant stirring at 25 °C. The saturated solution contained 4.3 g (0.096 M) of calcium D-gluconate in equilibrium with a precipitate of 2.2 g (0.0049 mol). An aliquot of 12.00 g (0.0408 mol) of solid sodium citrate was added to the saturated calcium D-gluconate solution. Supersaturated homogeneous solutions appeared within approximately 30 minutes of moderate stirring at 25 °C. The homogeneous solution was analysed for total calcium concentration and after 2, 24, 48, and 72 hours under constant stirring during which period precipitation occurred, and calcium ion activity was determined.

3. Solid calcium L-lactate and solid sodium citrate. To 16.00 g (0.0519 mol) of solid calcium L-lactate and 12.00 g (0.0408 mol) of solid sodium citrate was added 100 mL of water. A supersaturated homogeneous solution appeared within approximately 30 minutes of moderate stirring at 25 °C. The homogeneous solution was analysed for total calcium concentration and after 2, 24, 48, and 72 hours under constant stirring during which period precipitation occurred, and calcium ion activity was determined.

4. Solid calcium D-gluconate and solid sodium citrate. To 6.50 g (0.0145 mol) of solid calcium D-gluconate and 12.00 g (0.0408 mol) of solid sodium citrate was added 100 mL of water. A supersaturated homogeneous solution appeared within approximately 30 minutes of moderate stirring at 25 °C. The homogeneous solution was analysed for total calcium concentration and after 2, 24, 48, and 72 hours under constant stirring during which period precipitation occurred, and calcium ion activity was determined.

5. Solid sodium citrate in saturated aqueous calcium citrate. Saturated solution of calcium citrate was prepared by adding 2.00 g (0.0035 mol) to 100 mL of water and equilibrating for two hours under constant stirring at 25 °C. The saturated solution contained 0.100 g (0.00175 M) of calcium citrate in equilibrium with a precipitate of 1.9 g (0.0033 mol) of calcium citrate. Aliquot of 24.00 g (0.0816 mol) of solid sodium citrate was added to the saturated calcium citrate solution. A supersaturated homogeneous solution appeared within approximately 45 minutes of moderate stirring at 25 °C. The homogeneous solution was analysed for total calcium concentration and after 2, 24, 48, 72, 96, and 168 hours under constant stirring during which period precipitation occurred, and calcium ion activity was determined.

6. Minimum sodium citrate to dissolve calcium L-lactate. Various combinations of calcium L-lactate and sodium citrate have been investigated in order to find the minimum sodium citrate concentration required to dissolve a specified amount of calcium L-lactate to form maximal supersaturation. The

following combinations of sodium citrate and calcium L-lactate were found to result in maximal supersaturation: 16.00 g (0.0519 mol), 18.00 g (0.0584 mol), or 20.00 g (0.0649 mol) of solid calcium L-lactate combined with 12.00 g (0.0408 mol), 18.00 g (0.0612 mol), and 24.00 g (0.0816 mol) of solid sodium citrate, respectively, when for each of these combinations of calcium L-lactate and sodium citrate, 100 mL of water was added. The solutions were stored under moderate stirring at 25 °C for a period of 72 hours and analysed for total dissolved calcium and calcium ion activity was determined. During the period of 72 hours all solutions were inspected visually and it was noted when solutions temporally became clear and again unclear and time was noted for initiation of precipitation.

7. Minimum sodium citrate to dissolve calcium D-gluconate. Various combinations of calcium D-gluconate and sodium citrate have been investigated in order to find the minimum sodium citrate concentration required to dissolve a specified amount of calcium D-gluconate to form maximal supersaturation. The following combinations of sodium citrate and calcium D-gluconate have been found to result in maximal supersaturation: 6.50 g (0.0145 mol), 8.00 g (0.0178 mol), or 16.00 g (0.0357 mol) of solid calcium D-gluconate combined with 6.00 g (0.0204 mol), 8.00 g (0.0272 mol), and 24.00 g (0.0816 mol) of solid sodium citrate, respectively, when for each of these combinations of calcium D-gluconate and sodium citrate, 100 mL of water was added. The solutions were stored under moderate stirring at 25 °C for a period of 72 hours and analysed for total dissolved calcium and calcium ion activity was determined. During the period of 72 hours all solutions were inspected visually and it was noted when solutions temporally became clear and again unclear and time was noted for initiation of precipitation.

Association constant and solubility product of calcium citrate in aqueous solution of unity ionic strength

Association constant for calcium and citrate, and solubility product for calcium citrate, corrected for complex formation, were determined for a saturated solution of calcium citrate in aqueous solution with unity ionic strength, prepared by saturation of 3.0 g in 100 mL of water with ionic strength adjusted to 1.0 with KCl. The solution was stored under moderate stirring at 25.0 °C for a period of 48 hours and analysed for total calcium and calcium ion activity was determined. The sample was prepared in duplicate.

Calculation of the association constant and the solubility product of calcium citrate at ionic strength 1.0 at 25 °C was based on electrochemically determined calcium ion activity converted to calcium ion concentration, $[Ca^{2+}]$, by eqn (1). The complex concentration, $[CaCitr^-]$, was calculated according to

$$[CaCitr^-] = c_{Ca^{2+}} - [Ca^{2+}] \qquad (3)$$

where $c_{Ca^{2+}}$ is total calcium concentration, determined by EDTA titration and $[Citr^{3-}]$, the free citrate concentration was calculated according to

$$[Citr^{3-}] = c_{Citr^{3-}} - [CaCitr^-] \qquad (4)$$

where $c_{Citr^{3-}}$ is total citrate concentration. The association constant, K_c, based on concentration defined as

$$K_c = \frac{[CaCitr^-]}{[Ca^{2+}][Citr^{3-}]} \qquad (5)$$

was calculated using the iterative procedure already described[9] resulting in a value of $(2.2 \pm 0.3) \times 10^3$ M^{-1}, which is in good agreement with the value of $(2.95 \pm 0.03) \times 10^3$ M^{-1} found for aqueous 0.020 M sodium citrate at 25 °C.[9]

The solubility product, K_{sp}, for calcium citrate at ionic strength 1.0 at 25 °C corrected for complex formation was calculated according to

$$K_{sp} = [Ca^{2+}]^3[Citr^{3-}]^2 \qquad (6)$$

resulting in a value of $(7 \pm 2) \times 10^{-14}$ M^5.

Precipitate from supersaturated solutions of calcium citrate

Precipitates were collected by filtration from equilibrated solutions for all conditions and washed with water and ethanol prior to air-drying overnight and in an oven at 105 °C until constant weight. Water loss was calculated as the percentage difference between the weight of air dried and oven-dried precipitate.

Infrared spectra

Infrared spectra Fourier Transform Infrared (FT-IR) – Attenuated Total Reflection (ATR) Spectroscopy FT-IR of the precipitates collected from equilibrated mixed solutions were recorded with a FT-IR spectrometer (Bomem MB100, ABB, Quebec, Canada) equipped with an ATR attachment. All the spectra were obtained by accumulation of 64 scans, with resolution of 4 cm^{-1}, at 500–4000 cm^{-1}.

Results and discussion

Supersaturated aqueous solutions were found to be formed within a few minutes by dissolution of excess calcium L-lactate or of excess calcium D-gluconate in already saturated aqueous solutions by addition of solid sodium citrate to each of the two saturated solutions at a constant temperature of 25 °C. Similarly, for a saturated solution of calcium citrate in water at 25 °C, addition of solid sodium citrate resulted in continuing dissolution of calcium citrate. A significant supersaturation was evident in each case, since a precipitate identified by infrared spectroscopy as calcium citrate was formed subsequently in the solution with lag phase ranging from 30 min to 2 days for L-lactate and D-gluconate solutions. For solid calcium citrate, a similar spontaneous supersaturation has previously been reported for isothermal dissolution in aqueous solutions of sodium citrate.[9] The supersaturation of calcium citrate was studied with respect to calcium speciation for a moderate supersaturation of approximately 15% and also for approximately 50% supersaturation in two series of experiments, both series including calcium L-lactate and calcium D-gluconate. For all three hydroxycarboxylates, i.e. L-lactate, D-gluconate, and citrate, the maximal supersaturation obtained by dissolution of

the solid calcium salts mixed with solid sodium citrate was determined in separate experiments.

In a saturated solution of calcium L-lactate three ionic species are dominating according to the dissolution established as a two-step process

$$CaLact_2 \rightarrow CaLact^+ + Lact^- \qquad (7)$$

$$CaLact^+ \rightleftharpoons Ca^{2+} + Lact^- \qquad (8)$$

where Lact$^-$ is the lactate ion and CaLact$^+$ is the 1 : 1 complex between calcium and lactate. The addition of sodium citrate will lower the concentration of calcium ions due to a stronger complex formation by citrate:

$$Ca^{2+} + Citr^{3-} \rightleftharpoons CaCitr^- \qquad (9)$$

in effect increasing the solubility of calcium lactate. Citr^{3-} is the citrate ion and CaCitr$^-$ is the 1 : 1 complex. Notably, the dissolution of excess calcium L-lactate in saturated aqueous solution by an increasing concentration of citrate from dissolving sodium citrate will result in supersaturation with respect to calcium citrate either as the hexahydrate or tetrahydrate depending on temperature:[9,17]

$$3Ca^{2+} + 2Citr^{3-} \rightleftharpoons Ca_3Citr_2(s) \qquad (10)$$

No immediate precipitation of any of the calcium citrate hydrates was observed from these solutions supersaturated in calcium citrate. However, precipitate was formed with a lag phase ranging for up to 2 hours depending on the degree of supersaturation. The speciation of calcium in these supersaturated solutions depends on the chemical equilibria of eqn (8) and (9). Since citrate has a thermodynamic association constant of 3.6×10^4 at 25 °C for binding calcium compared to 49 for lactate, citrate can be assumed to control the free calcium ion concentration. The thermodynamic association constants are valid for ion activities as they were determined by extrapolation to zero ionic strength.[9,15] For the supersaturated solutions with ionic strength higher than unity concentration based association constants will have to replace the activity based association constants for quantitative calculations. The use of equilibrium constants determined for 1.0 M KCl or NaCl seems an acceptable approximation, since ionic strength in most of the supersaturated and the equilibrated solutions are close to unity. For the solutions with ionic strength higher than unity the same constants were used as it has been shown that calcium salts like calcium nitrate and calcium chloride have activity coefficients rather constant with values around 0.33 in the concentration range between 0.7 to 2.0 (molal scale) corresponding to the ionic strength interval of relevance for the supersaturated calcium hydroxycarboxylate solutions.[18,19] The association constant determined at ionic strength 1.0 for calcium citrate, $K_{aCaCitr} = (2.2 \pm 0.3) \times 10^3$ M^{-1} in the present study and in 1.0 M NaCl for calcium lactate, $K_{aCaLact} = 8 \pm 2$ M^{-1},[9,20] both based on concentrations, were accordingly used for the calculation of calcium speciation in the supersaturated solutions:

$$Ca^{2+} + Citr^{3-} \rightleftharpoons CaCitr^- \qquad (11)$$

corresponding to the equilibrium constant

$$K_{aCaCitr} = \frac{[CaCitr^-]}{[Ca^{2+}][Citr^{3-}]} = \frac{c_{Ca^{2+}} - [Ca^{2+}]}{[Ca^{2+}](c_{Citr^{3-}} - [CaCitr^-])} \qquad (12)$$

in which $c_{Ca^{2+}}$ is the total calcium ion concentration and $c_{Citr^{3-}}$ is the total citrate concentration originating from added citrate. Total calcium ion concentration as determined by EDTA titration and shown in Tables 1, 2 and 5 is thus equal to the final calcium concentration in the supersaturated solutions.

For the ligand exchange reaction

$$Citr^{3-} + CaLact^+ \rightleftharpoons CaCitr^- + Lact^- \qquad (13)$$

the ligand equilibrium constant is defined as

$$\frac{[CaCitr^-][Lact^-]}{[CaLact^+][Citr^{3-}]} = \frac{K_{aCaCitr}}{K_{aCaLact}} \qquad (14)$$

This equation together with three mass balance equations

$$[CaCitr^-] + [CaLact^+] = c_{Ca^{2+}} - [Ca^{2+}] \qquad (15)$$

$$[Lact^-] = 2c_{Ca^{2+}} - [CaLact^+] \qquad (16)$$

$$[Citr^{3-}] = c_{Citr^{3-}} - [CaCitr^-] \qquad (17)$$

and the equation for electroneutrality

$$[Na^+] + [CaLact^+] + 2[Ca^{2+}] = [CaCitr^-] + 3[Citr^{3-}] + [Lact^-] \qquad (18)$$

contains five unknowns. The five unknowns, $[Ca^{2+}]$, $[CaLact^+]$, $[CaCitr^-]$, $[Lact^-]$, and $[Citr^{3-}]$ were determined for each experiment from the five eqn (14)–(18) by an iterative procedure starting with an initial estimate of $[Ca^{2+}]$ similar to the calculations preformed for the calcium saccharate/gluconate equilibria.[21] The equilibrium concentrations for the supersaturated, homogeneous solutions not taking the precipitation equilibria into account, are presented in Table 1. The ionic products, Q, for each of the two salts

$$Q_{CaLact} = [Ca^{2+}][Lact^-]^2 \qquad (19)$$

$$Q_{CaCitr} = [Ca^{2+}]^3[Citr^{3-}]^2 \qquad (20)$$

calculated for each solutions are included in Table 1 together with ionic strength calculated from

$$I = 1/2(2^2[Ca^{2+}] + [Na^+] + [CaLact^+] + [CaCitr^-] \\ + [Lact^-] + 3^2[Citr^{3-}]) \qquad (21)$$

Similar calculations were done for the supersaturated solutions emerging from continuing dissolution of calcium D-gluconate in already saturated aqueous solutions of calcium D-gluconate or by simultaneous dissolution of calcium

Table 1 Supersaturated aqueous solutions of calcium citrate as formed at 25 °C by dissolution of calcium L-lactate in an already saturated solution of calcium L-lactate by addition of solid sodium citrate (sat/solid), or by simultaneous dissolution of solid calcium L-lactate and solid sodium citrate in water (solid/solid)

	Total Ca²⁺ in supersat. solution/M	Total lactate/M	Total citrate/M	Calcium ion activity	Free [Ca]²⁺/M	[CaLact⁺]/M	[CaCitr⁻]/M	[Lact⁻]/M	[Citr³⁻]/M	I	$Q_{CaLact} = [Ca^{2+}][Lact^-]^2$	$Q_{CaCitr} = [Ca^{2+}]^3[Citr^-]^2$
Sat/solid	0.366 ± 0.002	0.778	0.442	$(1.2 \pm 0.1) \times 10^{-3}$	$(2.1 \pm 0.1) \times 10^{-3}$	$(1.05 \pm 0.03) \times 10^{-2}$	0.354 ± 0.001	0.722 ± 0.003	$(8.8 \pm 0.1) \times 10^{-2}$	1.608 ± 0.004	$(1.11 \pm 0.04) \times 10^{-3}$	$(7.6 \pm 0.4) \times 10^{-11}$
Sat/solid	0.379 ± 0.001	0.778	0.204	$(3.92 \pm 0.03) \times 10^{-3}$	$(2.89 \pm 0.03) \times 10^{-2}$	0.149 ± 0.001	0.201 ± 0.001	0.609 ± 0.002	$(3.00 \pm 0.01) \times 10^{-3}$	0.857 ± 0.002	$(1.07 \pm 0.02) \times 10^{-2}$	$(2.17 \pm 0.05) \times 10^{-10}$
Sat/solid	0.50 ± 0.01	1.038	0.408	$(2.3 \pm 0.2) \times 10^{-3}$	$(1.0 \pm 0.1) \times 10^{-2}$	$(9 \pm 1) \times 10^{-2}$	0.394 ± 0.001	0.90 ± 0.01	$(1.4 \pm 0.1) \times 10^{-2}$	1.39 ± 0.01	$(8 \pm 1) \times 10^{-3}$	$(2.0 \pm 0.3) \times 10^{-10}$
Sat/solid	0.467 ± 0.001	1.038	0.816	$(6.4 \pm 0.1) \times 10^{-4}$	$(6.09 \pm 0.04) \times 10^{-4}$	$(4.43 \pm 0.04) \times 10^{-3}$	0.462 ± 0.001	0.930 ± 0.003	0.354 ± 0.001	3.516 ± 0.004	$(5.3 \pm 0.1) \times 10^{-4}$	$(2.84 \pm 0.04) \times 10^{-11}$
Solid/ solid	0.491 ± 0.001	1.038	0.408	$(2.32 \pm 0.04) \times 10^{-3}$	$(9.5 \pm 0.1) \times 10^{-3}$	$(8.77 \pm 0.05) \times 10^{-2}$	0.3934 ± 0.0001	0.893 ± 0.001	$(1.46 \pm 0.01) \times 10^{-2}$	1.384 ± 0.001	$(7.5 \pm 0.1) \times 10^{-3}$	$(1.81 \pm 0.3) \times 10^{-10}$

D-gluconate and sodium citrate in water see Table 2, using $K_{aCaGl} = 14 \pm 3$ M^{-1} as determined in 1.0 M NaCl.[20]

It should be evident from Table 1, by a comparison of the values of Q_{CaCitr} with the solubility product, $K_{spCaCitr} = (7 \pm 2) \times 10^{-14}$ M^5, determined for unity ionic strength, that all solutions are strongly supersaturated in calcium citrate. The solutions are to a varying degree saturated with calcium L-lactate as seen by a comparison of Q_{CaLact} with $K_{spCaLact} = (5.8 \pm 0.2) \times 10^{-3}$ M^3 valid for unity ionic strength.[20]

The robustness of supersaturated solutions of the calcium salts, important for biomineralization dynamics, was quantified by the length of the lag phase prior to initiation of precipitation. For the most robust solutions precipitation occurred within 24 or 48 hours, while for the less robust solutions, the precipitation occurred following 30 min of storage. All the supersaturated solutions showed precipitation after some time and in each case the precipitate isolated from the solution was identified as calcium citrate by infrared spectroscopy. The calcium content in solution was followed by EDTA titration and when constant, the iterative calculations were repeated for the equilibrium conditions with the adjusted calcium concentration and corrected citrate concentration. Citrate concentration, $c_{citr^{3-}}^{cr}$, was corrected for the part of the total citrate precipitated as calcium citrate

$$c_{Citr^{3-}}^{cr} = c_{Citr^{3-}} - c_{Citr^{3-}}^{pr} = c_{Citr^{3-}} - 2/3\left(c_{Ca^{2+}} - c_{Ca^{2+}}^{eq}\right) \tag{22}$$

$c_{citr^{3-}}^{pr}$ is precipitated citrate and $c_{Ca^{2+}}^{eq}$ is total calcium in the equilibrated solution determined by EDTA titration. All equilibrium concentrations of the calcium L-lactate sodium citrate solutions with precipitation of calcium citrate are shown in Table 3, and for the calcium D-gluconate sodium citrate solutions in Table 4.

The supersaturation of the calcium L-lactate sodium citrate solutions was confirmed in all cases since precipitation of calcium citrate was found to be initiated in a few hours. The ionic product Q_{CaCitr} as defined in eqn (20) should accordingly be compared with the solubility product, which is not known for the actual high ionic strengths conditions. The value $K_{sp} = 7 \times 10^{-14}$ M^5 for calcium citrate determined for unity ionic strength at 25 °C in the present study will probably be higher than the solubility product valid in these solutions with insignificant water for hydration of ions. A similar conclusion is reached for the equilibrium calcium D-gluconate sodium citrate solution. For both calcium L-lactate and calcium D-gluconate solutions supersaturated through dissolution of sodium citrate, precipitation of calcium citrate will lower the ionic product Q_{CaCitr}, which for both the L-lactate and D-gluconate solution becomes comparable with the solubility product for calcium citrates as may be seen from Tables 3 and 4, respectively. It should also be noted, that the ionic product of calcium L-lactate is less than the solubility product, which is ~1×10^{-3} M^{-3} for the equilibrated solutions, see Table 3. From Table 4 it may further be seen, that the ionic product also is lower than the solubility product for calcium D-gluconate, which is 5×10^{-5} M^{-3}. The solutions with calcium citrate precipitation are accordingly not supersaturated with calcium L-lactate or with calcium D-gluconate. Presence of

Table 2 Supersaturated aqueous solutions of calcium citrate as formed at 25 °C by dissolution of calcium D-gluconate in an already saturated solution by addition of solid sodium citrate (sat/solid), or by simultaneous dissolution of solid calcium D-gluconate and solid sodium citrate in water (solid/solid)

	Total Ca^{2+} in supersat. solution/M	Total gluconate/M	Total citrate/M	Calcium ion activity	Free [Ca]$^{2+}$/M	[CaGl$^+$]/M	[CaCitr$^-$]/M	[Gl$^-$]/M	[Citr^{3-}]/M	I	$Q_{CaGl} = [Ca^{2+}][Gl^-]^2$	$Q_{CaCitr} = [Ca^{2+}]^3[Citr^-]^2$
Sat/solid	0.102 ± 0.001	0.223	0.442	$(7.1 \pm 0.2) \times 10^{-5}$	$(1.37 \pm 0.01) \times 10^{-4}$	$(3.9 \pm 0.1) \times 10^{-4}$	0.102 ± 0.001	0.204 ± 0.001	0.340 ± 0.001	2.347 ± 0.002	$(5.7 \pm 0.1) \times 10^{-6}$	$(3.0 \pm 0.1) \times 10^{-13}$
Sat/solid	0.107 ± 0.001	0.223	0.204	$(2.33 \pm 0.02) \times 10^{-4}$	$(5.0 \pm 0.1) \times 10^{-4}$	$(1.4 \pm 0.1) \times 10^{-3}$	0.105 ± 0.001	0.213 ± 0.003	$(9.9 \pm 0.1) \times 10^{-2}$	0.912 ± 0.004	$(2.3 \pm 0.1) \times 10^{-5}$	$(1.2 \pm 0.1) \times 10^{-12}$
Sat/solid	0.144 ± 0.002	0.290	0.408	$(1.12 \pm 0.02) \times 10^{-4}$	$(2.5 \pm 0.1) \times 10^{-4}$	$(9.8 \pm 0.4) \times 10^{-4}$	0.142 ± 0.002	0.286 ± 0.004	0.266 ± 0.004	2.02 ± 0.01	$(2.0 \pm 0.1) \times 10^{-5}$	$(1.07 \pm 0.06) \times 10^{-12}$
Solid/solid	0.140 ± 0.001	0.290	0.408	$(1.030 \pm 0.003) \times 10^{-4}$	$(2.4 \pm 0.1) \times 10^{-4}$	$(9.23 \pm 0.01) \times 10^{-4}$	0.139 ± 0.001	0.279 ± 0.001	0.269 ± 0.001	2.03 ± 0.01	$(1.85 \pm 0.01) \times 10^{-5}$	$(9.77 \pm 0.01) \times 10^{-13}$

Table 3 Equilibrated aqueous solutions of calcium citrate as formed at 25 °C by dissolution of calcium L-lactate in an already saturated solution by addition of solid sodium citrate (sat/solid) or by simultaneous dissolution of solid calcium L-lactate and solid sodium citrate in water (solid/solid)

	Total Ca²⁺ in equilib./M	Total lactate/M	Total citrate/M	Correc. citrate/M	Calcium ion activity	Free [Ca²⁺]/M	[CaLact⁺]/M	[CaCitr⁻]/M	[Lact⁻]/M	[Citr³⁻]/M	I	$Q_{CaLact} = [Ca^{2+}][Lact^-]^2$	$Q_{CaCitr} = [Ca^{2+}]^3[Citr^{3-}]^2$
Sat/solid	$(2.81 \pm 0.01) \times 10^{-2}$	0.778	0.442	0.217 ± 0.001	$(1.27 \pm 0.02) \times 10^{-4}$	$(6.8 \pm 0.1) \times 10^{-5}$	$(3.0 \pm 0.1) \times 10^{-5}$	$(2.80 \pm 0.01) \times 10^{-2}$	$(5.62 \pm 0.01) \times 10^{-2}$	0.189 ± 0.001	1.56 ± 0.01	$(2.14 \pm 0.01) \times 10^{-7}$	$(1.1 \pm 0.1) \times 10^{-14}$
Sat/solid	0.121 ± 0.001	0.778	0.204	0.168 ± 0.002	$(1.84 \pm 0.02) \times 10^{-3}$	$(1.13 \pm 0.03) \times 10^{-3}$	$(2.0 \pm 0.1) \times 10^{-3}$	0.118 ± 0.001	0.239 ± 0.002	$(5.1 \pm 0.1) \times 10^{-2}$	0.715 ± 0.002	$(6.4 \pm 0.3) \times 10^{-5}$	$(3.6 \pm 0.2) \times 10^{-12}$
Sat/solid	$(6.81 \pm 0.04) \times 10^{-2}$	1.038	0.408	0.123 ± 0.005	$(5.3 \pm 0.3) \times 10^{-4}$	$(5.6 \pm 0.1) \times 10^{-4}$	$(5.9 \pm 0.1) \times 10^{-4}$	$(6.70 \pm 0.04) \times 10^{-2}$	0.136 ± 0.001	$(5.60 \pm 0.04) \times 10^{-2}$	0.967 ± 0.001	$(1.02 \pm 0.03) \times 10^{-5}$	$(5.4 \pm 0.1) \times 10^{-13}$
Sat/solid	$(2.8 \pm 0.4) \times 10^{-2}$	1.038	0.816	0.523 ± 0.003	$(2.6 \pm 0.5) \times 10^{-5}$	$(2.6 \pm 0.5) \times 10^{-5}$	$(1.1 \pm 0.4) \times 10^{-5}$	$(2.8 \pm 0.5) \times 10^{-2}$	$(6 \pm 1) \times 10^{-2}$	0.495 ± 0.005	3.49 ± 0.02	$(8 \pm 5) \times 10^{-8}$	$(4 \pm 2) \times 10^{-15}$
Solid/solid	$(6.87 \pm 0.04) \times 10^{-2}$	1.038	0.408	0.127 ± 0.001	$(5.4 \pm 0.1) \times 10^{-4}$	$(5.3 \pm 0.1) \times 10^{-4}$	$(5.7 \pm 0.1) \times 10^{-4}$	$(6.76 \pm 0.04) \times 10^{-2}$	0.137 ± 0.001	$(5.94 \pm 0.04) \times 10^{-2}$	0.983 ± 0.001	$(9.9 \pm 0.3) \times 10^{-6}$	$(5.2 \pm 0.1) \times 10^{-13}$

Table 4 Equilibrated aqueous solutions of calcium citrate as formed at 25 °C by dissolution of calcium D-gluconate in an already saturated solution by addition of solid sodium citrate (sat/solid) or by simultaneous dissolution of solid calcium D-gluconate and sodium citrate in water (solid/solid)

	Total Ca²⁺ in equilib./M	Total gluconate/M	Total citrate/M	Correc. citrate/M	Calcium ion activity	Free [Ca]²⁺/M	[CaGl⁺]/M	[CaCitr⁻]/M	[Gl⁻]/M	[Citr³⁻]/M	I	$Q_{CaGl} = [Ca^{2+}][Gl^-]^2$	$Q_{CaCitr} = [Ca^{2+}]^3[Citr^{3-}]^2$
Sat/solid	$(4.68 \pm 0.01) \times 10^{-2}$	0.223	0.442	0.405 ± 0.001	$(2.43 \pm 0.03) \times 10^{-5}$	$(6.0 \pm 0.1) \times 10^{-5}$	$(7.8 \pm 0.4) \times 10^{-5}$	$(4.7 \pm 0.1) \times 10^{-2}$	$(9.4 \pm 0.2) \times 10^{-2}$	0.358 ± 0.001	2.346 ± 0.003	$(5.2 \pm 0.4) \times 10^{-7}$	$(2.7 \pm 0.2) \times 10^{-14}$
Sat/solid	$(4.7 \pm 0.2) \times 10^{-2}$	0.223	0.204	0.164 ± 0.001	$(8.303 \pm 0.001) \times 10^{-5}$	$(1.8 \pm 0.1) \times 10^{-4}$	$(2.4 \pm 0.2) \times 10^{-4}$	$(4.7 \pm 0.2) \times 10^{-2}$	$(9.4 \pm 0.4) \times 10^{-2}$	0.117 ± 0.002	0.904 ± 0.005	$(1.6 \pm 0.2) \times 10^{-6}$	$(9 \pm 1) \times 10^{-14}$
Sat/solid	$(5.67 \pm 0.04) \times 10^{-2}$	0.290	0.408	0.350 ± 0.001	$(3.38 \pm 0.03) \times 10^{-5}$	$(8.8 \pm 0.1) \times 10^{-5}$	$(1.40 \pm 0.02) \times 10^{-4}$	$(5.65 \pm 0.04) \times 10^{-2}$	0.113 ± 0.001	0.2935 ± 0.0004	2.018 ± 0.001	$(1.13 \pm 0.03) \times 10^{-6}$	$(5.9 \pm 0.1) \times 10^{-14}$
Solid/solid	$(5.27 \pm 0.04) \times 10^{-2}$	0.290	0.408	0.3498 ± 0.0003	$(2.9 \pm 0.1) \times 10^{-5}$	$(8.1 \pm 0.1) \times 10^{-5}$	$(1.19 \pm 0.02) \times 10^{-4}$	$(5.25 \pm 0.04) \times 10^{-2}$	0.105 ± 0.001	0.2973 ± 0.0004	2.029 ± 0.001	$(9.0 \pm 0.2) \times 10^{-7}$	$(4.7 \pm 0.1) \times 10^{-14}$

Table 5 Supersaturated aqueous solutions of calcium citrate at 25 °C as formed by dissolution of calcium citrate in an already saturated solution of calcium citrate by addition of solid sodium citrate, and equilibrated solutions after subsequent precipitation of calcium citrate

	Total Ca^{2+} in solution/M	Total citrate/M	Citrate added/M	Calcium ion activity	$[Ca^{2+}]$/M	$[CaCit^-]$/M	$[Citr^{3-}]$/M	I	$Q = [Ca^{2+}]^3[Citr^{3-}]^2$
Calcium citrate supersaturated	0.086 ± 0.001	0.8730 ± 0.0005	0.816	$(2.15 \pm 0.02) \times 10^{-5}$	$(4.96 \pm 0.04) \times 10^{-5}$	$(8.5 \pm 0.1) \times 10^{-2}$	0.7875 ± 0.0002	4.811 ± 0.001	$(7.5 \pm 0.2) \times 10^{-14}$
Calcium citrate equilibrium	0.052 ± 0.001	0.828 ± 0.001	0.816	$(1.08 \pm 0.02) \times 10^{-5}$	$(3.0 \pm 0.1) \times 10^{-5}$	$(5.1 \pm 0.1) \times 10^{-2}$	0.7762 ± 0.0001	4.743 ± 0.001	$(1.7 \pm 0.1) \times 10^{-14}$

other hydrates or polymorph forms prior to equilibrium could also be established.[22] However, for calcium citrate, the other hydrate of relevance is calcium citrate hexahydrate, which has a lower not higher solubility.[9]

For a saturated solution of calcium citrate in water, addition of sodium citrate results in a continuing dissolution of calcium citrate. This somewhat surprising observation is, however, in agreement with previous findings[9] and is in parallel to the observations for calcium L-lactate and calcium D-gluconate. The stoichiometry of citrate assisted dissolution

$$Ca_3Citr_2(s) \rightarrow 2CaCitr^- + Ca^{2+} \quad (23)$$

$$Ca^{2+} + Citr^{3-} \rightleftharpoons CaCitr^- \quad (24)$$

$$Ca_3Citr_2(s) + Citr^{3-} \rightleftharpoons 3CaCitr^- \quad (25)$$
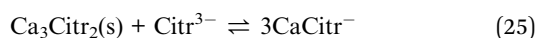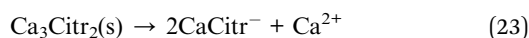
helps to identify the critical step for the supersaturation. The free calcium ion concentration needs now to be calculated according to the equilibrium

$$\underset{c_{Ca^{2+}} - [Ca^{2+}]}{CaCitr^-} \rightleftharpoons \underset{[Ca^{2+}]}{Ca^{2+}} + \underset{[Ca^{2+}] - 1/3c_{Ca^{2+}} + c_{Citr^{3-}}}{Citr^{3-}} \quad (26)$$

where again $c_{Citr^{3-}}$ is added sodium citrate concentration. For the equilibrium constant

$$K_{aCaCitr} = \frac{c_{Ca^{2+}} - [Ca^{2+}]}{[Ca^{2+}]([Ca^{2+}] - 1/3c_{Ca^{2+}} + c_{Citr^{3-}})} \quad (27)$$

with $c_{Ca^{2+}}$ as the total calcium ion concentration, the free calcium $[Ca^{2+}]$ ion concentration was calculated from the resulting quadratic equation

$$K_a[Ca^{2+}]^2 + [Ca^{2+}](1 - 1/3c_{Ca^{2+}}K_a + K_ac_{Citr^{3-}}) - c_{Ca^{2+}} = 0 \quad (28)$$

From the mass balance equations

$$[CaCitr^-] = c_{Ca^{2+}} - [Ca^{2+}] \quad (29)$$

$$[Citr^{3-}] = c_{Citr^{3-}} - [CaCitr^-] = 2/3c_{Ca^{2+}} + c_{Citr^{3-}} - [CaCitr^-] \quad (30)$$

the two other equilibrium concentrations, $[CaCitr^-]$, and $[Citr^{3-}]$, were now calculated from eqn (29) and (30), followed by calculation of the ionic product Q_{CaCitr} from eqn (20). The calculations were identical for the supersaturated solutions and the equilibrated solutions with reprecipitated calcium citrate except for the corrected total calcium concentration determined

by titration. The ionic product is clearly larger than the solubility product showing that the homogeneous solutions formed after addition of sodium citrate is becoming supersaturated with respect to calcium citrate. After reprecipitation, the ionic product is comparable to the solubility product previously determined, see Table 5, and the solution accordingly saturated.

Citrate has been found to dissolve excess of the calcium L-lactate, calcium D-gluconate, and calcium citrate in already saturated solutions of these calcium hydroxycarboxylates forming strongly supersaturated solutions in calcium citrate. From the supersaturated solutions, calcium citrate precipitates reaching solubility equilibrium, see Fig. 1. The precipitation results in an over-all increase in water activity, see Fig. 2. The increase in water activity may be explained simply by the less dissolved ion concentration for water binding. The calcium citrate supersaturation depends on two factors: (i) the relative strength of complex binding between citrate as ligand assisting the dissolution and the other hydroxycarboxylate ligand, and (ii) the initiation of precipitation of calcium citrate. This balance was investigated by a determination of the minimum amount of sodium citrate required for dissolution of a fixed amount of calcium L-lactate or calcium D-gluconate. Under specified conditions described in Experimental section, the degree of
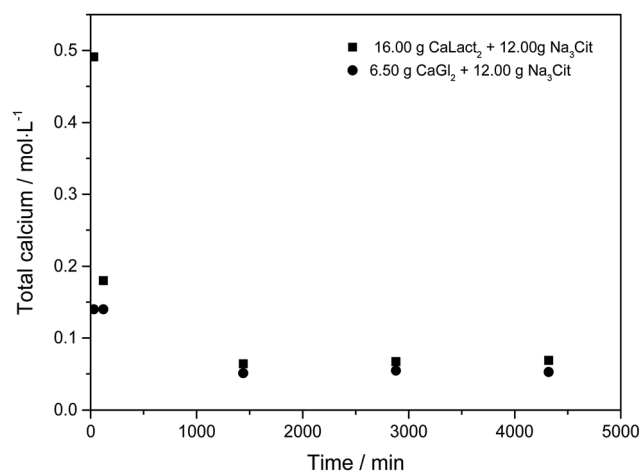

Fig. 1 Calcium concentration in 100 mL of water during dissolution of 16.00 g of solid calcium L-lactate mixed with 12.00 g of sodium citrate, and of 6.50 g of calcium D-gluconate mixed with 12.00 g of sodium citrate under constant stirring at 25 °C, followed by precipitation of calcium citrate.
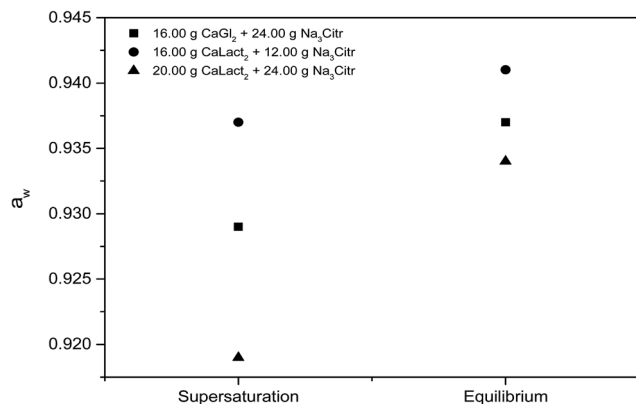
Fig. 2 Water activity, a_w of supersaturated and equilibrated solutions of calcium citrate at 25 °C made by dissolution of calcium L-lactate and sodium citrate or by dissolution of calcium D-gluconate and sodium citrate in 100 mL of water.

supersaturation for increasing added sodium citrate may be seen in Fig. 3. As may be seen from this figure, the supersaturation is rather significant especially for calcium L-lactate. For calcium D-gluconate the supersaturation was found less dependent on excess citrate due to the smaller difference between the association constant for binding of calcium to gluconate relative to binding to citrate compared to the difference between the association constant for binding of calcium to lactate relative to binding to citrate. For calcium citrate this thermodynamic factor almost vanishes, and the supersaturation depends on kinetics as from the smaller degree of supersaturation.

The lag phase for initiation of precipitation was studied by visual inspection for calcium L-lactate, for which the largest supersaturation was detected, see Fig. 3. The length of the lag phase seems to decrease exponentially with an increasing degree of supersaturation, see Fig. 4. For extrapolation to
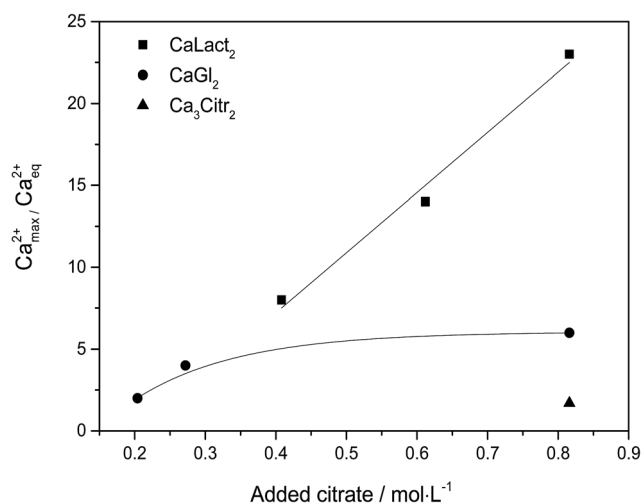
Fig. 3 Calcium citrate supersaturation expressed as a degree of supersaturation $Ca^{2+}_{max}/Ca^{2+}_{eq}$ after adding solid sodium citrate to calcium L-lactate, calcium D-gluconate, or to calcium citrate.
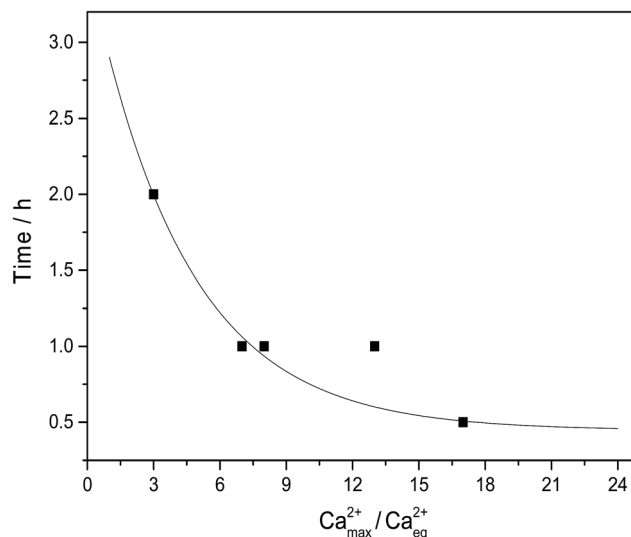
Fig. 4 Lag phase for initiation of precipitation of calcium citrate in supersaturated solutions made by dissolution of calcium L-lactate by sodium citrate in water at 25 °C. $Ca^{2+}_{max}/Ca^{2+}_{eq}$ is the degree of supersaturation determined by titration of Ca^{2+} in maximal supersaturated solution. Curve is based on fitting to an exponential equation to yield: time = 3.09 exp($-Ca^{2+}_{max}/Ca^{2+}_{eq}/4.33$) + 0.44 (all points except point for supersaturation degree of 12).

infinity supersaturation the length of the lag phase gets close to zero with an extrapolated value of 0.4 ± 0.1 hours, as would be expected. Similarly an extrapolation to little or no supersaturation yield a very long lag phase tending to approach infinity as also is to be expected. For calcium D-gluconate sodium citrate solutions, the length of the lag phase was larger and apparently less dependent on the degree of supersaturation. This observation, which could indicate formation of mixed D-gluconate/citrate complexes of calcium could be important for formulation of supplements with high bioavailability and will later be studied in more details.

The maximal supersaturation of calcium citrate found for dissolution of calcium L-lactate by citrate depends linearly on the concentration of sodium citrate used for the dissolution, see Fig. 3. Dissolution of calcium L-lactate by citrate is suggested to depend on a mechanism entailing binding of citrate to the surface of solid calcium L-lactate and accordingly to appear as a zero-order reaction with a constant rate depending on the excess concentration of sodium citrate used

$$CaLact_2(s) + Citr^{3-} \rightarrow CaCitr^- + 2Lact^- \quad (31)$$

The total calcium concentration, $c_{Ca^{2+}}$, accordingly increases linearly from the initial calcium concentration, $c^o_{Ca^{2+}}$, with time as

$$c_{Ca^{2+}} = c^o_{Ca^{2+}} = kc_{Citr^{3-}}t \quad (32)$$

where k is an unknown constant depending on surface properties of the calcium salt and t is a time of dissolution. The length of the lag phase for initiation of precipitation of calcium citrate decreases exponentially with increasing total calcium dissolved, see Fig. 4. The initiation of precipitation will limit the
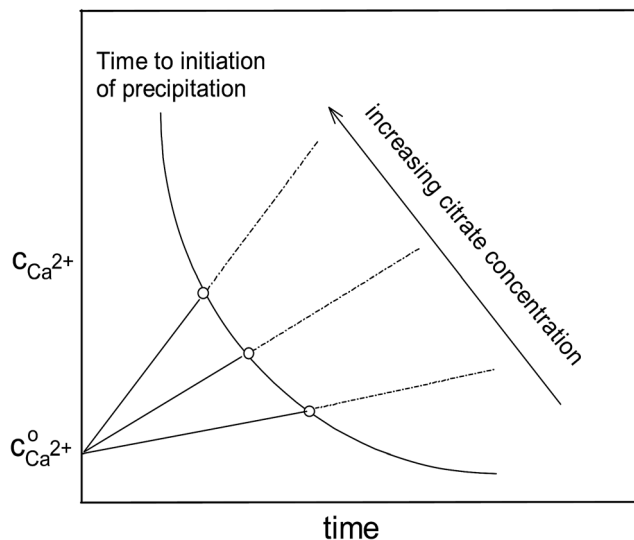
Fig. 5 Increasing calcium concentration during dissolution of calcium L-lactate in aqueous solution of sodium citrate with three different concentrations. The intersection with the time curve for initiation of precipitation as dependent on calcium concentration indicates the maximal supersaturation for each concentration of citrate.

degree of supersaturation. The information from Fig. 3 combined with the information from Fig. 4 in a more qualitative way yields the over-all picture as shown in Fig. 5. In this figure the linear increase of calcium in citrate assisted dissolution above the initial solubility of calcium lactate, $c^o_{Ca^{2+}}$, is depicted for three citrate concentrations. The time for initiation of precipitation increasing with decreasing calcium concentration intersect with the dissolution curves defining the maximal supersaturation possible for this specific citrate concentration. To a fair approximation, this supersaturation depends linearly on the citrate concentration as confirmed by the experimental data shown in Fig. 3 for calcium L-lactate. The situation for calcium D-gluconate is different as the lag time for initiation of precipitation is longer and the supersaturation seems to be less dependent on the added citrate concentration, see Fig. 3.

Conclusions

Citrate has been shown to assist dissolution of calcium hydroxycarboxylates forming supersaturated solution of calcium citrate. This effect is most remarkable for dissolution of calcium citrate and helps to explain the high bioavailability of calcium from this sparingly soluble calcium salt. The effect is, however, more dramatic for dissolution of calcium L-lactate and calcium D-gluconate for which very high degrees of robust supersaturation were demonstrated. The robustness of the supersaturated solutions seems to depend on a slow precipitation of calcium citrate. The presence of citrate in calcified tissue has now been recognized.[7,8] The demonstration of the assistance of citrate in spontaneous supersaturation phenomena occurring by isothermal dissolution against a concentration gradient explains important part of biomineralization dynamics. This perspective of spontaneous supersaturation

needs also to be studied for higher temperatures as they are relevant for physiological conditions in the human body. The temperature dependence for these phenomena should also be extended to the elevated temperatures as are used during dairy processing. Other factors could also be considered and further investigated such as pH as they could affect solubility of calcium salts.[22] The recognition of this unique role of citrate also opens up for novel design of better calcium supplements and foods for special needs for individuals with low calcium uptake, like elderly with high risk of developing osteoporosis.

Acknowledgements

References

1 C. Y. C. Pak, J. A. Harvey and M. C. Hsu, Enhanced Calcium Bioavailability from A Solubilized Form of Calcium Citrate, *J. Clin. Endocrinol. Metab.*, 1987, **65**(4), 801–805.

2 P. Tondapu, D. Provost, B. Adams-Huet, T. Sims, C. Chang and K. Sakhaee, Comparison of the Absorption of Calcium Carbonate and Calcium Citrate after Roux-en-Y Gastric Bypass, *Obes. Surg.*, 2009, **19**(9), 1256–1261.

3 J. M. Hess, S. S. Jonnalagadda and J. L. Slavin, Dairy Foods: Current Evidence of their Effects on Bone, Cardiometabolic, Cognitive, and Digestive Health, *Compr. Rev. Food Sci. Food Saf.*, 2016, **15**, 251–268.

4 L. M. Wang, W. Wang, X. C. Li, L. Peng, Z. Q. Lin and H. Z. Xv, Calcium citrate: a new biomaterial that can enhance bone formation *in situ*, *Chin. J. Traumatol.*, 2012, **15**(5), 291–296.

5 L. C. Costello, R. B. Franklin, M. A. Reynolds and M. Chellaiah, The Important Role of Osteoblasts and Citrate Production in Bone Formation: 'Osteoblast Citration' as a New Concept for an Old Relationship, *Open Bone J.*, 2013, **4**, 1–17.

6 M. Iafisco, G. B. Ramirez-Rodriguez, Y. Sakhno, A. Tampieri, G. Martra, J. Gomez-Morales and J. M. Delgado-Lopez, The growth mechanism of apatite nanocrystals assisted by citrate: relevance to bone biomineralization, *CrystEngComm*, 2015, **17**(3), 507–511.

7 Y. Y. Hu, A. Rawal and K. Schmidt-Rohr, Strongly bound citrate stabilizes the apatite nanocrystals in bone, *Proc. Natl. Acad. Sci. U. S. A.*, 2010, **107**(52), 22425–22429.

8 D. G. Reid, M. J. Duer, G. E. Jackson, R. C. Murray, A. L. Rodgers and C. M. Shanahan, Citrate Occurs Widely in Healthy and Pathological Apatitic Biomineral: Mineralized Articular Cartilage, and Intimal Atherosclerotic Plaque and Apatitic Kidney Stones, *Calcif. Tissue Int.*, 2013, **93**(3), 253–260.

9 M. Vavrusova and L. H. Skibsted, Aqueous solubility of calcium citrate and interconversion between the

tetrahydrate and the hexahydrate as a balance between endothermic dissolution and exothermic complex formation, *Int. Dairy J.*, 2016, **57**, 20–28.

10 M. Vavrusova and L. H. Skibsted, Spontaneous supersaturation of calcium D-gluconate during isothermal dissolution of calcium L-lactate in aqueous sodium D-gluconate, *Food Funct.*, 2014, **5**(1), 85–91.

11 A. L. Márquez, G. N. Salvatore, R. G. Otero, J. R. Wagner and G. G. Palazolo, Impact of freeze–thaw treatment on the stability of calcium-fortified soy beverages, *LWT–Food Sci. Technol.*, 2015, **62**(1), 474–481.

12 A. Irshad, B. D. Sharma, S. R. Ahmed, S. Talukder, O. P. Malav and A. Kumar, Effect of incorporation of calcium lactate on physico-chemical, textural, and sensory properties of restructured buffalo meat loaves, *Vet. World*, 2016, **9**(2), 151–159.

13 K. Sakhaee and C. Pak, Superior calcium bioavailability of effervescent potassium calcium citrate over tablet formulation of calcium citrate after Roux-en-Upsilon gastric bypass, *Surg. Obes. Relat. Dis.*, 2013, **9**(5), 743–748.

14 C. Holt, S. Lenton, T. Nylander, E. S. Sorensen and S. C. Teixeira, Mineralisation of soft and hard tissues and the stability of biofluids, *J. Struct. Biol.*, 2014, **185**(3), 383–396.

15 M. Vavrusova, R. Liang and L. H. Skibsted, Thermodynamics of Dissolution of Calcium Hydroxycarboxylates in Water, *J. Agric. Food Chem.*, 2014, **62**(24), 5675–5681.

16 C. W. Davies, *Ion Association*, Butterworth & Co, Ltd, London, UK, 1962.

17 K. P. Chatterjee and N. R. Dhar, Studies of sparingly soluble salts, readily obtained from hot solutions of reacting substances I, *J. Phys. Chem.*, 1924, **28**, 1009–1028.

18 R. H. Stokes and R. A. Robinson, Ionic Hydration and Activity in Electrolyte Solutions, *J. Am. Chem. Soc.*, 1948, **70**(5), 1870–1878.

19 R. G. Bates, B. R. Staples and R. A. Robinson, Ionic Hydration and Single Ion Activities in Unassociated Chlorides at High Ionic Strengths, *Anal. Chem.*, 1970, **42**(8), 867–871.

20 M. Vavrusova, M. B. Munk and L. H. Skibsted, Aqueous Solubility of Calcium L-Lactate, Calcium D-Gluconate, and Calcium D-Lactobionate: Importance of Complex Formation for Solubility Increase by Hydroxycarboxylate Mixtures, *J. Agric. Food Chem.*, 2013, **61**(34), 8207–8214.

21 A. C. Garcia, M. Vavrusova and L. H. Skibsted, Calcium D-Saccharate: Aqueous Solubility, Complex Formation, and Stabilization of Supersaturation, *J. Agric. Food Chem.*, 2016, **64**(11), 2352–2360.

22 S. L. Goss, K. A. Lemons, J. E. Kerstetter and R. H. Bogner, Determination of calcium salt solubility with changes in pH and P-CO_2, simulating varying gastrointestinal environments, *J. Pharm. Pharmacol.*, 2007, **59**(11), 1485–1492.

Original Article

Codissolution of calcium hydrogenphosphate and sodium hydrogencitrate in water. Spontaneous supersaturation of calcium citrate increasing calcium bioavailability

Martina Vavrusova [a], Bente Pia Danielsen [a], André Castilho Garcia [a,b], Leif Horsfelt Skibsted [a,]*

[a] *Department of Food Science, University of Copenhagen, Rolighedsvej 30, DK-1958, Frederiksberg C, Denmark*
[b] *Instituto Federal de Educação, Ciência e Tecnologia de São Paulo, Campus Capivari. Avenida Doutor Ênio Pires de Camargo, 2971 — São João Batista, CEP: 13360-000, Capivari, SP, Brazil*

ABSTRACT

The sparingly soluble calcium hydrogenphosphate dihydrate, co-dissolving in water during dissolution of freely soluble sodium hydrogencitrate sesquihydrate as caused by proton transfer from hydrogencitrate to hydrogenphosphate, was found to form homogenous solutions supersaturated by a factor up to 8 in calcium citrate tetrahydrate. A critical hydrogencitrate concentration for formation of homogeneous solutions was found to depend linearly on dissolved calcium hydrogenphosphate: $[HCitr^{2-}] = 14[CaHPO_4] - 0.05$ at 25 °C. The lag phase for precipitation of calcium citrate tetrahydrate, as identified from FT-IR spectra, from these spontaneously formed supersaturated solutions was several hours, and the time to reach solubility equilibrium was several days. Initial calcium ion activity was found to be almost independent of the degree of supersaturation as determined electrochemically. The supersaturated solutions had a pH around 4.7, and calcium binding to hydrogencitrate as the dominant citrate species during precipitation was found to be exothermic with a determined association constant of 357 L mol^{-1} at 25 °C for unit ionic strength, and $\Delta H° = -22 \pm 2$ kJ mol^{-1}, $\Delta S° = -26 \pm 8$ J K^{-1} mol^{-1}. Calcium binding to hydrogencitrate and, more importantly, to citrate is suggested to decrease the rate of precipitation by lowering the driving force of precipitation, and becoming important for the robust spontaneous supersaturation with perspectives for design of functional foods with increased calcium bioavailability.

1. Introduction

Osteoporosis, as caused by calcium malabsorption often also for individuals with a high dietary calcium intake, affects 75 million people worldwide and is specially a problem for the elderly [1]. Current theories do not offer explanations for the apparent paradox of low bioavailability of calcium even from foods for which the dietary calcium is known to dissolve in the gastric juice as calcium ions during digestion [2].

Calcium absorption mainly occurs in the intestines (i) through transcellular, saturable transport through cells, as regulated by vitamin D, and (ii) through paracellular, non-saturable transport between cells as regulated by diffusion [3]. Both of these absorption processes depend, however, on the concentration of free calcium, and calcium absorption is hampered by precipitation by phosphates, oxalate, phytates and carbonate for the conditions of increasing pH in the intestines. The paracellular path seems quantitatively the most important although the two absorption paths seem to interact depending on individual physiological conditions [4].

Complex binding of calcium by peptides, amino acids and hydroxycarboxylates may prevent precipitation, but will also lower the free calcium concentration below the critical value for spontaneous diffusion [2]. Supersaturation of calcium salts in the intestine may, accordingly, be important for the calcium gradient from the chyme in the intestines to the free calcium level around 10^{-3} mol L^{-1} in the extracellular fluid behind the epithelium.

Hydroxycarboxylates like gluconate and citrate are known to form supersaturated calcium salt solutions [5,6]. Isothermal dissolution of combinations of sparingly soluble calcium salts and sodium salts of potential ligands for calcium have been shown spontaneously to form highly supersaturated solutions of remarkable robustness. Such solubility overshooting could explain the positive effect of citrate on calcium absorption, bone formation and fracture healing in bones through increased calcium mobility despite the low solubility of calcium citrate [7−10].

Injection fluids for veterinary calcium therapy have been formulated as supersaturated aqueous calcium gluconate solutions made by heating and stabilized through addition of other hydroxycarboxylates for long term storage apparently without a detailed understanding of the mechanism behind the surprising robustness of supersaturation at ambient temperatures [11]. A breakthrough in such understanding seems, however, possible expanding the kinetic models recently published for spontaneous supersaturation of calcium hydroxycarboxylates in the presence of citrate [6]. A further step forwards in the development of novel functional foods with high mineral bioavailability and of food supplements for treatment of calcium deficiency especially for the elderly seems to depend on combining calcium phosphates and citrates [12]. Results of studies of such combinations are now reported, which will hopefully lead to development of new functional foods and novel drug products.

2. Methods and materials

2.1. Materials

Calcium hydrogenphosphate dihydrate, sodium hydrogencitrate sesquihydrate and nitric acid were from Sigma Aldrich (Steinheim, Germany). Calcium chloride dihydrate was from Merck (Darmstadt, Germany). All aqueous solutions were made from purified water from Milli-Q Plus (Millipore Corporation, Bedford, MA).

2.2. Electrochemical measurement of calcium ion activity

Calcium ion activity, a_{Ca}^{2+}, was measured using a calcium ion selective electrode ISE25Ca with a reference REF251 electrode from Radiometer (Copenhagen, Denmark). The calibration solutions used for calibration of electrode were prepared as aqueous $CaCl_2$ solutions with concentration of 1.00×10^{-4}, 1.00×10^{-3}, 1.00×10^{-2} mol L^{-1} prepared from a 1.000 mol L^{-1} $CaCl_2$ stock solution at 10, 20, 25 °C, and 30 °C. Calcium ion activity, a_{Ca}^{2+}, in the standard solutions was calculated based on the relationship between activity and concentration according to

$$a_{Ca^{2+}} = c_{Ca^{2+}} \gamma^{2+} \tag{1}$$

where γ^{2+} is the activity coefficient calculated from the Davies' equation as described previously [13]

$$\log \gamma^{2+} = -A_{DH} z^2 \left(\frac{\sqrt{I}}{1 + \sqrt{I}} - 0.30I \right) \tag{2}$$

where A_{DH} is the Debye-Hückel constant with the numerical value of $A_{DH} = 0.498, 0.506, 0.510$, and 0.515, at 10 °C, 20 °C, 25 °C, and 30 °C, respectively, and $z = 2$ for calcium ions [14]. The calcium ion activity in the test solutions was calculated as described previously [13].

2.3. ICP-OES determination of total calcium and total phosphate

The samples were filtered (589/3, Whatman, Dassel, Germany) and 10 μL were added to 9.99 mL of HNO_3 5%. The samples were analysed by inductively coupled plasma-optical emission spectroscopy using an Agilent 5100 ICP-OES (Santa Clara, CA, USA) and the wavelengths of 396.847 nm and 177.434 nm were monitored to quantify total calcium and total phosphorus, respectively.

2.4. FTIR of precipitates

The precipitates collected from the experiments after equilibrium was reached were characterized by infrared spectroscopy using a FT-IR spectrometer (Bomen MB100, ABB, Quebec, Canada) equipped with ATR attachment. All the spectra were obtained by accumulation of 64 scans, with resolution of 4 cm^{-1}, at 550-4000 cm^{-1}.

2.5. Dissolution of solid calcium hydrogenphosphate dihydrate and sodium hydrogencitrate sesquihydrate and determination of the critical ratio

Several combinations of calcium hydrogenphosphate dihydrate and sodium hydrogencitrate sesquihydrate were investigated in order to determine the critical amount of sodium hydrogencitrate sesquihydrate required to dissolve a specified amount of calcium hydrogenphosphate dihydrate resulting in supersaturated solutions of calcium citrate tetrahydrate. The following combinations of sodium hydrogencitrate sesquihydrate and calcium hydrogenphosphate dihydrate resulted in supersaturated (homogeneous) solutions: 1.00, 2.00, 2.50, and 3.00 g (5.81, 11.6, 14.5, and 17.4 mmol) of solid calcium hydrogenphosphate dihydrate combined with 10.00, 30.00, 40.00, and 55.00 g ($3.80 \cdot 10^{-2}$, 0.114, 0.152, and 0.209 mol) of solid sodium hydrogencitrate sesquihydrate, respectively. To each of these combinations of solids, 100 mL of water was added. The samples (A, B, C, and D) were stored at 25 °C under constant stirring, pH was measured using a 713 pH Meter (Metrohm, Herisau, Switzerland), and the samples were analysed for calcium ion activity using a calcium ion selective electrode up to 144 h while precipitation occurred. The sample made from 11.6 mmol of calcium hydrogenphosphate and 0.114 mol of sodium hydrogencitrate in 100 mL of water was further analysed for total calcium and total phosphorus, both quantified by ICP during precipitation. All these analyses were made periodically starting when the solutions became supersaturated and continued until equilibrium was reached in the samples. All the samples and analyses were made in duplicates.

2.6. Potentiometric determination of association constant

Aqueous solutions of hydrogencitrate were prepared from sodium hydrogencitrate sesquihydrate in concentrations of 0.00100 mol L^{-1} and 0.0100 mol L^{-1}. Solution of $CaCl_2$ was added to each sample with the final concentration of 0.000500 mol L^{-1} of calcium in the samples. All samples remained homogenous during equilibration for 1 h at 10.0 °C, 20.0 °C, 25.0 °C, and 30.0 °C. The calcium ion activity was determined by the calcium ion selective electrode at each of the four investigated temperatures. The calcium ion activity was used for calculation of an association constant. All samples were prepared in duplicates.

3. Results and discussion

Supersaturated homogeneous solutions appeared after 30–60 min after the addition of water to mixtures of solid calcium hydrogenphosphate dihydrate and sodium hydrogencitrate sesquihydrate under constant stirring at 25 °C for certain combinations of the two salts. The higher the amount of the salts, the longer period of time was needed for complete dissolution of the solids. Among the different combinations of these two salts, the critical mass of Na_2HCitr required to completely dissolve a certain mass of $CaHPO_4$, as determined by visual inspection, was found to depend linearly on the

mass of $CaHPO_4$ dissolved. By linear regression, the critical hydrogencitrate concentration for formation of homogenous solutions was found to depend on dissolved calcium hydrogencitrate according to $[HCitr^{2-}] = 14[CaHPO_4] - 0.05$, as may be seen from Fig. 1.

Extrapolation of the linear curve to zero in relation to the amount of Na_2HCitr leads to 3.51 ± 1.61 mmol (35.1 mmol L^{-1}), indicating supersaturation, since the solubility of $CaHPO_4$ $2H_2O$, has been reported to be approximately 1.5 mmol L^{-1} [15].

Different from our previous results involving spontaneous supersaturated solutions [6], the robustness of the supersaturation of the calcium hydrogencitrate/hydrogenphosphate system seems to be independent of the degree of supersaturation in the concentration range studied. Fig. 2 shows total calcium, total phosphate, and calcium ion activity for one of the studied samples (B).

The rate of precipitation of calcium citrate could be describe by a first order reaction as determined for experiment B by the decreasing calcium ion concentration (Fig. 2 A): $[Ca^{2+}] = 0.137 \cdot e^{-(0.12t)} + 0.0236$ and for the decreasing calcium ion activity (Fig. 2 B): $a_{Ca^{2+}} = 1.79 \cdot 10^{-4} \cdot e^{-(0.11t)} + 1.78 \cdot 10^{-5}$. Practically identical values for the pseudo first order rate constant based on concentration of calcium and calcium ion activity were obtained and the electrochemical method based on calcium ion activity is, accordingly, to be recommended for characterization of supersaturation as this method does not required individual sampling for each analysis. Rate constants based on electrochemical registrations of calcium ion activity during precipitation were determined for each experiment by exponential fitting as seen in Fig. 3.

The first order rate constants for precipitation of calcium citrate was found to increase linearly for increasing amount of $CaHPO_4$ dissolved, see insert in Fig. 3. In order to identify the factors controlling the precipitation and precipitation rate,
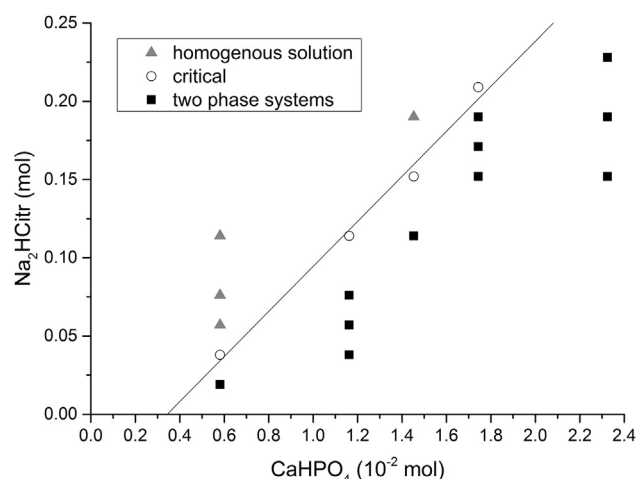
Fig. 1 — Different combinations of sodium hydrogencitrate sesquihydrate and calcium hydrogenphosphate dihydrate in 100 mL of water. The black squares represent the samples in which the dissolution was not complete resulting in two phase systems, the grey triangles represent the samples that formed homogenous supersaturated solutions, and the white circles represent the samples for which complete dissolution just occurred.
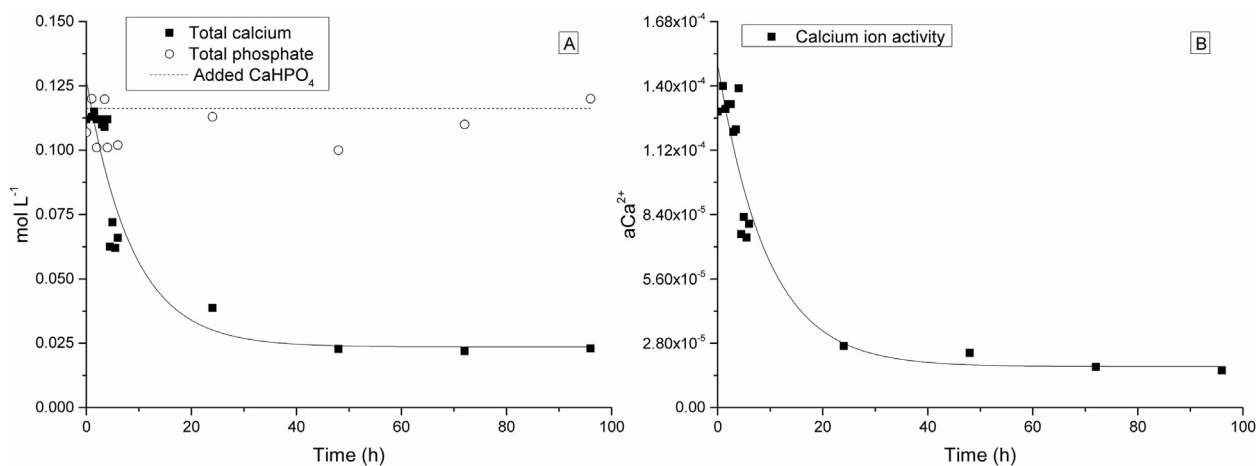
Fig. 2 — Time evolution during precipitation of calcium citrate tetrahydrate for total calcium, total phosphate and calcium ion activity for sample B, consisting of 2.00 g of CaHPO$_4$ (11.6 mmol) and 30.00 g of Na$_2$HCitr (0.114 mol) in 100 mL of water.
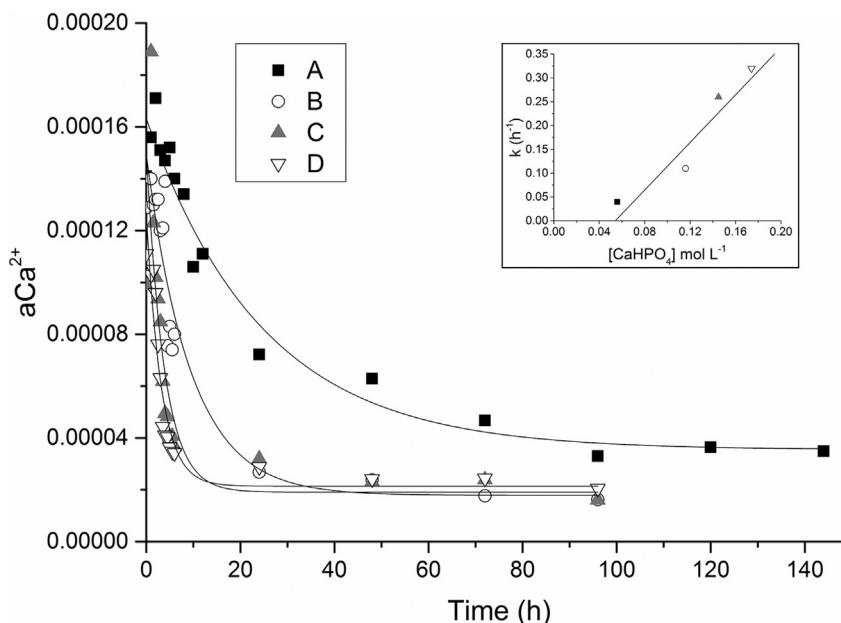
Fig. 3 — Calcium ion activity during precipitation for samples A, B, C and D, consisting of 1.00, 2.00, 2.50, and 3.00 g (5.81, 11.6, 14.5, and 17.4 mmol) of CaHPO$_4$ combined with 10.00, 30.00, 40.00, and 55.00 g (3.80 10^{-2}, 0.114, 0.152, and 0.209 mol) of Na$_2$HCitr in 100 mL of water, respectively. First order rate constants for precipitation determined by exponential fitting for increasing concentration of CaHPO$_4$, are seen in insert.

speciation of calcium in the supersaturated solutions were established.

The thermodynamic equilibrium constant for binding of calcium to citrate has previously been determined [16] to have the value of 3.6 10^4 at 25 °C. In the current work we have corrected this activity based equilibrium constant to a concentration based constant valid for an ionic strength of 1.0 M using Davies' equation (2) leading to a value of 2.72 10^3 L mol^{-1}. The association constant for binding calcium to hydrogencitrate was studied electrochemically at four temperatures and the activity base constant has also been corrected to concentration under the same conditions. Fig. 4 shows the

van't Hoff plot for the concentration based association constant for calcium hydrogencitrate. From the plot, the association constant between calcium and hydrogencitrate at 25 °C is found to have a value of 357 L mol^{-1}, which is reasonable when compared to the value reported by Davies [17] of 1.2 10^3 for the thermodynamic association constant at low ionic strength.

The results from determination of total phosphorus in solution during precipitation show that phosphate remains in solution, see Fig. 2. In agreement with this, the precipitate formed was identified by FT-IR to be calcium citrate tetrahydrate, see Fig. 5.
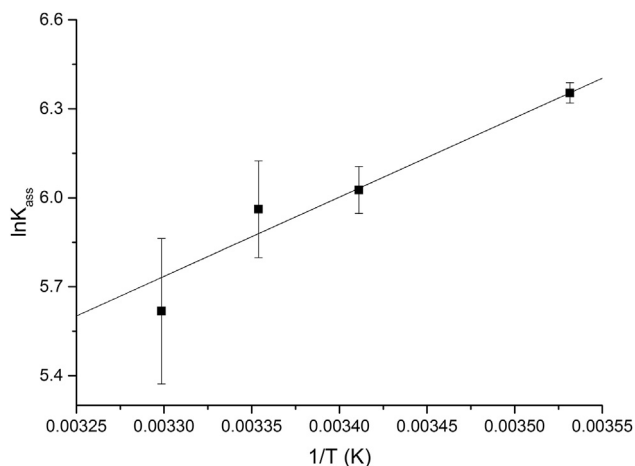
Fig. 4 — van't Hoff plot for calcium hydrogencitrate association constant in water based on concentration at 1.0 M of ionic strength. Enthalpy and entropy have the values $\Delta H° = -22 \pm 2$ kJ mol^{-1} and $\Delta S° = -26 \pm 8$ J K^{-1} mol^{-1}, respectively.

Calcium ion activity was similar in all supersaturated systems studied; this is strong evidence that only a small fraction of calcium is found as free calcium ions in the supersaturated solutions, but is rather associated to the ligands present. To calculate the calcium speciation in the supersaturated solutions several equations were taken into account:

$$H_2PO_4^- + H_2O \rightleftharpoons H_3O^+ + HPO_4^{2-} \qquad (3)$$

corresponding to the second dissociation of phosphoric acid, equal to $2.51 \ 10^{-7}$ mol L^{-1} for ionic strength equals to 1.0 M [18], defined as

$$K_{a_2}^{H_3PO_4} = \frac{[H_3O^+][HPO_4^{2-}]}{[H_2PO_4^-]} \qquad (4)$$

$$HCitr^{2-} + H_2O \rightleftharpoons H_3O^+ + Citr^{3-} \qquad (5)$$

corresponding to the third dissociation of citric acid, equal to $6.34 \ 10^{-6}$ mol L^{-1} for ionic strength equals to 3.2 M [19], defined as

$$K_{a_3}^{H_3Citr} = \frac{[H_3O^+][Citr^{3-}]}{[HCitr^{2-}]} \qquad (6)$$

$$Ca^{2+} + HPO_4^{2-} \rightleftharpoons CaHPO_4 \qquad (7)$$

corresponding to an equilibrium constant, equal to 76 L mol^{-1} corrected to a concentration constant adjusted to ionic strength equal to 1.0 M from the thermodynamic constant of 500 reported by Davies [17], defined as

$$K_1 = \frac{[CaHPO_4]}{[Ca^{2+}][HPO_4^{2-}]} \qquad (8)$$

$$Ca^{2+} + HCitr^{2-} \rightleftharpoons CaHCitr \qquad (9)$$

corresponding to the equilibrium constant, equal to 357 L mol^{-1}, defined as

$$K_2 = \frac{[CaHCitr]}{[Ca^{2+}][HCitr^{2-}]} \qquad (10)$$

$$Ca^{2+} + Citr^{3-} \rightleftharpoons CaCitr^- \qquad (11)$$

corresponding to the equilibrium constant, equal to $2.72 \ 10^3$ L mol^{-1}, defined as
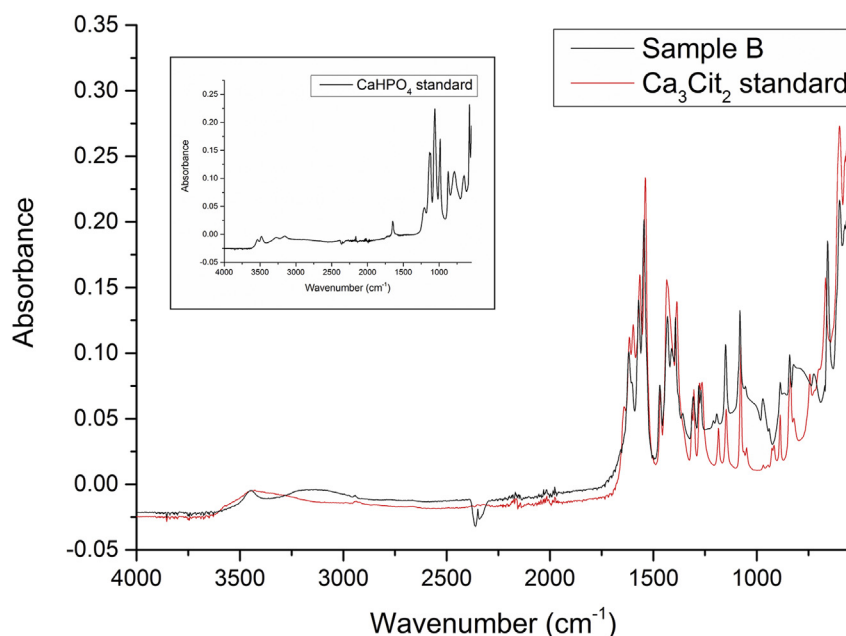
Fig. 5 — FT-IR spectra of the solid collect from experiment B, calcium citrate tetrahydrate standard and, in the insert, the spectrum of calcium hydrogenphosphate dihydrate standard.

$$K_3 = \frac{[CaCitr^-]}{[Ca^{2+}][Citr^{3-}]} \qquad (12)$$

and the three mass balance equations

$$t_{Ca} = [CaHPO_4] + [CaHCitr] + [CaCitr^-] + [Ca^{2+}] \qquad (13)$$

$$t_P = [CaHPO_4] + [H_2PO_4^-] + [HPO_4^{2-}] \qquad (14)$$

$$t_{Citr} = [CaHCitr] + [CaCitr^+] + [HCitr^{2-}] + [Citr^{3-}] \qquad (15)$$

from which t_{Ca} correspond to total calcium concentration, t_P corresponds to total phosphorus, both equal to the concentration of added $CaHPO_4$, and t_{Citr} correspond to total citrate, which is equal to the concentration of added Na_2HCitr. All the equilibria and mass balance equations contain eight unknowns, $[H_2PO_4^-]$, $[HPO_4^{2-}]$, $[HCitr^{2-}]$, $[Citr^{3-}]$, $[CaHPO_4]$, $[CaHCitr]$, $[CaCitr^-]$, and $[Ca^{2+}]$, which were calculated neglecting the variation in the volume of the samples due to the added salts. All the equilibrium constants used for these calculations were valid at an ionic strength of 1.0 M. For many electrolytes, the activity coefficients are constant in an ionic strength interval around unity. The speciation is, accordingly, not sensitive to the somewhat higher ionic strength of the most concentrated supersaturated solutions. Table 1 shows the ion speciation in experiments A, B, C, and D prior to precipitation. The supersaturation factor is the ratio between calcium ion activity in supersaturated solutions and in the equilibrium solutions, I is the ionic strength of the samples, γ^{2+} is the coefficient of activity of calcium ions, calculated as the ratio between measured calcium ion activity and the calculated ion concentration, equation (1), and Q is the ionic product of Ca_3Citr_2, which can be compared to the solubility product, K_{sp}, reported to be $(7 \pm 2)\ 10^{-14}$ $mol^5\ L^{-5}$ at ionic strength of 1.0 M [6]. The calculated coefficient of activity is close to unit in the supersaturated solutions, which is in agreement with the mean of the coefficients reported for calcium chloride solutes of high ionic strength, conforming the validity of the calculation method [20].

From the results reported in Table 1, it is seen that the calculated ion product is larger than or close to the solubility product. However, the ratio between $Q_{Ca_3Citr_2}/K_{sp(Ca_3Citr_2)}$ is smaller than the apparent supersaturation as calculated from the activity of calcium ions in the supersaturated solutions and the equilibrium calcium ion activity, see Fig. 3. This provides an explanation for the robustness of the supersaturation. The driving force for precipitation is becoming smaller due to the complexation of calcium by hydrogencitrate and especially citrate. The supersaturated homogenous solutions resulting from dissolution of $CaHPO_4\ 2H_2O$ and Na_2HCitr $1\tfrac{1}{2}H_2O$ may contain up to approximately 10 times as much calcium as compared to the equilibrated solutions, providing a unique example of solubilization of an inorganic nutrient by complexation, which could form the basis for development of novel foods with high calcium bioavailability.

Bioavailability of mineral nutrients always needs to be confirmed in human intervention studies. Citrate has already been found to increase calcium absorption in several studies [7,8]. The method developed in the present study may thus serve as a convenient preclinical test of new mineral drug formulations or of novel mineral supplements, but will need

Table 1 – Ion speciation in supersaturated systems A, B, C and D. All concentrations are expressed as mol L^{-1}. Calcium activity, $a_{Ca^{2+}}$, corresponds to the average of the first four measurements.

System	Added CaHPO₄	Added Na₂HCitr	$a_{Ca^{2+}}$	Supersaturation factor	pH	$[H_2PO_4^-]$	$[HPO_4^{2-}]$	$[HCitr^{2-}]$	$[Citr^{3-}]$	$[CaHPO_4]$	$[CaHCitr]$	$[CaCitr^-]$	$[Ca^{2+}]$	I	γ^{2+a}	$Q^b_{Ca_3Citr_2}$
A	$5.81\ 10^{-2}$	$3.80\ 10^{-1}$	$(1.55 \pm 0.13)\ 10^{-4}$	4.4	4.80 ± 0.01	$5.72\ 10^{-2}$	$9.06\ 10^{-4}$	$2.41\ 10^{-1}$	$8.14\ 10^{-2}$	$1.30\ 10^{-5}$	$1.62\ 10^{-2}$	$4.17\ 10^{-2}$	$1.88\ 10^{-4}$	1.24	0.82	$4.4\ 10^{-14}$
B	$1.16\ 10^{-1}$	1.14	$(1.31 \pm 0.07)\ 10^{-4}$	8.1	4.62 ± 0.01	$1.15\ 10^{-1}$	$1.21\ 10^{-3}$	$8.36\ 10^{-1}$	$1.88\ 10^{-1}$	$1.32\ 10^{-5}$	$4.28\ 10^{-2}$	$7.33\ 10^{-2}$	$1.43\ 10^{-4}$	3.66	0.92	$1.0\ 10^{-13}$
C	$1.45\ 10^{-1}$	1.52	$(1.28 \pm 0.42)\ 10^{-4}$	8.0	4.61 ± 0.01	$1.44\ 10^{-1}$	$1.45\ 10^{-3}$	1.13	$2.44\ 10^{-1}$	$1.50\ 10^{-5}$	$5.49\ 10^{-2}$	$9.03\ 10^{-2}$	$1.36\ 10^{-4}$	4.88	0.94	$1.5\ 10^{-13}$
D	$1.74\ 10^{-1}$	2.09	$(1.04 \pm 0.06)\ 10^{-4}$	5.1	4.58 ± 0.01	$1.73\ 10^{-1}$	$1.66\ 10^{-3}$	1.59	$3.25\,10^{-1}$	$1.51\ 10^{-5}$	$6.81\ 10^{-2}$	$1.06\ 10^{-1}$	$1.20\ 10^{-4}$	6.72	0.87	$1.8\ 10^{-13}$

a $\gamma^{2+} = a_{Ca^{2+}}/[Ca^{2+}]$.
b $Q_{Ca_3Citr_2} = [Ca^{2+}]^3[Citr^{3-}]^2$.

to be followed up by intervention studies [21]. Such clinical studies should also include effects of other food or beverage components, since calcium is known to interact with browning products formed during heating of foods like shrimp or with antibacterial drugs [21,22]. Oligosaccharides are also known to interfere with calcium absorption [23,24].

Conflicts of interest

All authors declare no conflicts of interest.

Acknowledgements

REFERENCES

[1] Thorpe MP, Evans EM. Dietary protein and bone health: harmonizing conflicting theories. Nutr Rev 2011;69:215—30.
[2] Skibsted LH. Mineral nutrient interaction: improving bioavailability of calcium and iron. Food Sci Biotechnol 2016;25:1233—41.
[3] Bronner F. Intestinal calcium absorption: mechanisms and applications. J Nutr 1987;117:1347—52.
[4] Diaz de Barboza G, Guizzardi S, Tolosa de Talamoni N. Molecular aspects of intestinal calcium absorption. World J Gastroentero 2015;21:7142—54.
[5] Vavrusova M, Skibsted LH. Spontaneous supersaturation of calcium D-gluconate during isothermal dissolution of calcium L-lactate in aqueous sodium d-gluconate. Food Func 2014;5:85—91.
[6] Vavrusova M, Garcia AC, Danielsen BP, Skibsted LH. Spontaneous supersaturation of calcium citrate from simultaneous isothermal dissolution of sodium citrate and sparingly soluble calcium hydroxycarboxylates in water. RSC Adv 2017;7:3078—88.
[7] Pak CY, Harvey JA, Hsu MC. Enhanced calcium bioavailability from a solubilized form of calcium citrate. J Clin Endocrinol Metab 1987;65:801—5.
[8] Tondapu P, Provost D, Adams-Huet B, Sims T, Chang C, Sakhaee K. Comparison of the absorption of calcium carbonate and calcium citrate after Roux-en-Y gastric bypass. Obes Surg 2009;19:1256—61.
[9] Wang L, Wang W, Li X, Peng L, Lin Z, Xü H. Calcium citrate: a new biomaterial that can enhance bone formation in situ. Chin J Traumatol 2012;15:291—6.
[10] Costello LC, Franklin RB, Reynolds MA, Chellaiah M. The important role of osteoblasts and citrate production in bone formation: "osteoblast citration" as a new concept for an old relationship. Open Bone J 2012;4:27—34.
[11] Siegrist VH. Kalziumglukonat-injektionslösungen mit zusats von kalziumlaevulinat bzw. Kalzium-d-saccharat Pharm Acta Helv 1949;24:430—40 [In German].
[12] Baugreet S, Hamill RM, Kerry JP, McCarthy SN. Mitigating nutrition and health deficiencies in older adults: a role for food innovation? J Food Sci 2017;4:848—55.
[13] Vavrusova M, Liang R, Skibsted LH. Thermodynamics of dissolution of calcium hydroxycarboxylates in water. J Agric Food Chem 2014;62:5675—81.
[14] Davies CW. Ion association. Washington: Butterworths; 1962.
[15] Pan HB, Darvell BW. Solubility of dicalcium phosphate dihydrate by solid titration. Caries Res 2009;43:254—60.
[16] Vavrusova M, Skibsted LH. Aqueous solubility of calcium citrate and interconversion between the tetrahydrate and the hexahydrate as a balance between endothermic dissolution and exothermic complex formation. Int Dairy J 2016;57:20—8.
[17] Davies CW, Hoyle BE. The interaction of calcium ions with some phosphate and citrate buffers. J Chem Soc 1953:4134—6.
[18] Green AA. The preparation of acetate and phosphate buffer solutions of known pH and ionic strength. J Am Chem Soc 1933;55:2331—6.
[19] Crea F, De Stefano C, Millero FJ, Sharma VK. Dissociation constants for citric acid in NaCl and KCl solutions and their mixtures at 25 °C. J Solut Chem 2004;33:1349—66.
[20] Robinson RA, Stokes RH. Electrolyte solutions. 2nd ed. London: Butterworths; 1959.
[21] Cheng C, Chen M-L, Tseng C, Uang Y-S, Huang C-L, Hsu K-Y. A relative bioavailability study of 500 mg calcium p-aminosalicylate film coating tablet in healthy individuals. J Food Drug Anal 2014;22:242—7.
[22] Chen T-Y, Luo H-M, Hsu P-H, Sung W-C. Effects of calcium supplements on the quality and acrylamide content of puffed shrimp chips. J Food Drug Anal 2016;24:164—72.
[23] Whisner CM, Martin BR, Schoterman MHC, Nakatsu CH, McCabe LD, McCabe GP, et al. Galacto-oligosaccharides increase calcium absorption and gut bifidobacteria in young girls: a double-blind cross-over trial. Br J Nutr 2013;110:1292—303.
[24] van den Heuvel EGHM, Muys T, van Dokkum W, Schaafsma G. Oligofructose stimulates calcium absorption in adolescents. Am J Clin Nutr 1999;69:544—8.

Supersaturation of calcium citrate as a mechanism behind enhanced availability of calcium phosphates by presence of citrate

André C. Garcia[a,b], Martina Vavrusova[a], Leif H. Skibsted[a,*]

[a] *Department of Food Science, University of Copenhagen, Rolighedsvej 30, DK -1958 Frederiksberg C, Denmark*
[b] *Instituto Federal de Educação, Ciência e Tecnologia de São Paulo, Campus Capivari. Avenida Doutor Ênio Pires de Camargo, 2971 – São João Batista, – CEP: 13360-000 –Capivari, SP, Brazil*

ARTICLE INFO

ABSTRACT

Dissolution of amorphous calcium phosphate (ACP) in aqueous citrate at varying pH has been studied with perspective of increasing availability of calcium from sidestreams of whey protein, lactose and/or cheese production or on development of new functional foods. ACP formed as an initial precipitate in $0.10 \, mol \, L^{-1}$ equimolar aqueous calcium chloride, sodium citrate, and sodium hydrogenphosphate was used as model for mineral residues formed during milk processing. Upon acidification of the ACP suspension by hydrochloric acid decreasing pH from 6.5 to 4.5, the transformations of ACP occurred through an 8 h period of supersaturation prior to a slow precipitation of calcium citrate tetrahydrate. This robust supersaturation, which may explain increased availability of calcium phosphates in presence of citrate, presented a degree of supersaturation of 7.1 and was characterized by precipitation rates for $0.10 \, mol \, L^{-1}$ equimolar aqueous calcium chloride, sodium hydrogencitrate, and sodium hydrogenphosphate with pH 5.5, and for $0.10 \, mol \, L^{-1}$ equimolar aqueous calcium chloride, sodium hydrogencitrate, and sodium dihydrogenphosphate with pH 4.1, with a degree of supersaturation of 2.7. The crystallization processes were similar according to Avrami's model with a half-life for precipitation of approximately 5 h independent of the degree of supersaturation. Ion speciation based on measurement of pH, and total concentrations of calcium, phosphate and citrate, and of conductivity and calcium ion activity during precipitation indicates a low driving force for precipitation with calcium citrate complex dominating at pH 5.5 and calcium hydrogencitrate complex dominating at pH 4.1. Calcium hydrogencitrate is suggested to be the species involved in the crystal growth followed by solid state transformation to calcium citrate tetrahydrate.

1. Introduction

Milk and dairy products are import sources of calcium in human diet and also have a significant content of citrate (Garnsworthy et al., 2006; Hess et al., 2016). Despite of the low aqueous solubility, calcium citrate is often prescribed as supplement for individuals affected by osteoporosis due to a high calcium bioavailability from calcium citrate, which can provide the adequate levels of calcium to stimulate osteoblasts proliferation and differentiation in vivo (Adluri et al., 2010; Wang et al., 2012).

Calcium absorption occurs mainly in the intestines through two sets of events: a saturable transcellular pathway regulated by vitamin D, and a non-saturable paracellular pathway, which consists in the Ca^{2+} transport through transmembrane proteins (Bronner, 1987; Diaz de Barboza et al., 2015). Although the mechanisms are different, the calcium absorption depends on the concentration of free calcium, which is affected by calcium precipitation by carbonate, oxalate, phytates or phosphates. On the other hand, calcium binding to organic molecules, like peptides, amino acids and hydroxycarboxylates may prevent the precipitation of calcium, but may also avert the spontaneous diffusion due to the reduction on the free calcium concentration (Kutus et al., 2017; Skibsted, 2016).

In this context, the supersaturation of certain calcium salts resulting from solubility overshooting phenomena may provide the key to explain the increased bioavailability presented by some calcium compounds, such as calcium hydroxycarboxylates, which are used for calcium fortification of foods and beverages, like calcium L-lactate, calcium D-gluconate, and calcium citrate (Márquez et al., 2015; Rasyid & Hansen, 1991). Spontaneous supersaturation of calcium D-gluconate in water by a factor of seven was observed during the isothermal dissolution of calcium L-lactate in aqueous sodium D-gluconate (Vavrusova & Skibsted, 2014). Similarly calcium citrate is also involved

in robust supersaturated solutions formed spontaneously by the iso-thermal dissolution of sodium citrate in saturated aqueous solutions of calcium hydroxycarboxylates, like L-lactate, D-gluconate and citrate (Vavrusova, Danielsen, Garcia & Skibsted, 2018; Vavrusova, Garcia, Danielsen & Skibsted, 2017). The more recent observation that calcium hydrogenphosphate dissolves readily in water together with sodium hydrogencitrate forming solutions strongly supersaturated in calcium citrate may even be of more importance for understanding the high bioavailability of calcium from dairy products. A prerequisite for in-creased calcium absorption in the intestines is a non-equilibrium si-tuation where calcium salts, like the citrate and phosphates remain dissolved at concentrations higher than the equilibrium solubility concentration. Precipitation rates of calcium citrate and of calcium phosphates clearly become crucial for a better understanding of calcium bioavailability from dairy products and from calcium supplements based on milk minerals. Similarly, citrate assisted dissolution of spar-ingly soluble calcium phosphates together with slow precipitation of calcium citrate may also explain the observations of positive effects of calcium citrate on bone healing (Costello et al., 2012; Iafisco et al., 2015; Wang et al., 2012). We have accordingly studied the dynamics of transformation between calcium phosphate and calcium citrate from mixtures of calcium chloride, sodium citrate and sodium phosphate in order to inspire the design of calcium supplements based on milk mi-nerals.

2. Material and methods

2.1. Chemicals

Calcium chloride dihydrate was from Merck (Darmstadt, Germany), sodium citrate dihydrate, sodium hydrogencitrate sesquihydrate, so-dium hydrogenphosphate anhydrous and sodium dihydrogenphosphate anhydrous were from Sigma-Aldrich (Steinheim, Germany). All re-agents were of analytical grade and the aqueous solutions were made from purified water from Milli-Q Plus (Millipore Corporation, Bedford, MA).

2.2. Samples

All the investigated samples contained equimolar concentrations ($0.10 \, mol \, L^{-1}$) of calcium, phosphate and/or citrate and were prepared by mixing stock solutions ($0.30 \, mol \, L^{-1}$) of $CaCl_2$, Na_2HPO_4, NaH_2PO_4, Na_3Citr and/or Na_2HCitr. Binary systems containing calcium chloride and only one of the sodium phosphates or citrates were initially ana-lysed for calcium ion activity, conductivity and pH in function of time. Afterwards three different combinations of solutions were studied: the first experiment was prepared by mixing 500 mL of each stock solutions of $CaCl_2$, Na_3Citr and Na_2HPO_4; in the second experiment stock solu-tions of $CaCl_2$, Na_2HCitr and Na_2HPO_4 were mixed, and $CaCl_2$, Na_2HCitr and NaH_2PO_4 in the third experiment. The studied solutions were mixed in a reactor Atlas Potassium (Syrris, Royston, United Kingdom) equipped with a 2.0 L thermostatic bath adjusted to 25 °C with mechanical agitation, pH, transmittance based turbidity and re-fraction index probes, used to monitor the formation of precipitate from the samples. Periodically, aliquots were collected in duplicates from the reactor and centrifuged. The supernatant was filtered and analysed for total calcium, total phosphate, and total citrate, while the precipitate was characterized via FT-IR. The reactor was equipped with two syringe pumps that added HCl or NaOH ($2.0 \, mol \, L^{-1}$ at $0.80 \, mL \, min^{-1}$) to adjust the pH to the desired value.

2.3. Total calcium and total phosphorus determination

The samples were initially filtered through a 0.22 μm cellulose acetate syringe filter (Q-Max RR, Knebel, Denmark) and 10 μL were added to 9.99 mL of nitric acid 5% using micropipettes from Thermo

Scientific (Espoo, Finland). The samples were analysed by using an Agilent 5100 ICP-OES (Santa Clara, CA, USA) monitoring the wave-lengths of 396.847 and 177.434 nm to quantify total calcium and total phosphorus, respectively. All samples were prepared in duplicates.

2.4. Spectrophotometric determination of citrate

Total citrate was quantified based on the middle-UV absorption of the carbonyl groups of protonated carboxyl groups (Krukowski et al., 2017), using a Shimadzu UV-1280 UV–vis spectrophotometer to mea-sure absorbance between 190 and 300 nm, with a λ_{max} of 209 nm, with a quartz cuvette with 1.0 cm of optical path length. Sodium citrate standards and filtrated samples were acidified with HCl to a final concentration of $0.13 \, mol \, L^{-1}$ (pH < 1.0). To verify any possible in-terference of phosphates to the analyses, standard stock solutions of sodium hydrogenphosphate and sodium dihydrogenphosphate of con-centrations 0.1 and $0.05 \, mol \, L^{-1}$ were also analysed following the same procedure as the samples.

2.5. Infrared spectra

Fourier transformed infrared spectroscopy (FT-IR) was used to characterize the precipitates. The spectra were obtained in a FT-IR spectrometer (Bomem, MB100, ABB, Quebec, Canada) equipped with a ATR attachment, by accumulation of 64 scans, with resolution of $4 \, cm^{-1}$, at $550–2000 \, cm^{-1}$.

2.6. Electrochemical measurement of calcium ion activity

Calcium ion activity, $a_{Ca^{2+}}$, was determined using a calcium ion selective electrode ISE25Ca with a reference REF 251 electrode (Radiometer, Copenhagen, Denmark). The electrode calibration was performed with calcium chloride standard solutions with concentra-tions of 1.00×10^{-4}, 1.00×10^{-3} and $1.00 \times 10^{-2} \, mol \, L^{-1}$, prepared from a $1.000 \, mol \, L^{-1}$ stock solution. The calcium ion activity was calculated according to the Nernst equation, which relates the electrode potential and $-\log(a_{Ca^{2+}})$, as previously described (Vavrusova et al., 2014) and considering the relation between activity and concentration given as

$$a_{Ca^{2+}} = [Ca^{2+}]\gamma^{2\pm} \tag{1}$$

where $\gamma^{2\pm}$ is the activity coefficient calculated from Davies' equation

$$\log\gamma^{z\pm} = -A_{DH}z^2\left(\frac{\sqrt{I}}{I + \sqrt{I}} - 0.30I\right) \tag{2}$$

in which A_{DH} corresponds to the Debye-Hückel constant with the nu-merical value of 0.510 at 25 °C (Davies, 1962).

2.7. Conductivity

The conductivity measurements were performed at 25 °C using a 4-pole conductivity cell, model CDC866T (Radiometer, Copenhagen, Denmark) calibrated with a 0.01 D (demal) potassium chloride stan-dard solution ($1408 \, \mu S \, cm^{-1}$) (Shreiner & Pratt, 2004).

2.8. pH measurements

A pH meter (713 pH Meter, Metrohm, Denmark) equipped with a glass electrode (602 Combined Metrosensor glass electrode, Metrohm, Denmark), standardized before each measurement against NBS inter-national activity pH-standard with pH 4.000, 7.000, and 9.240 was used for the pH measurements using the relation: $pH = -\log a_{H_3O^+}$.
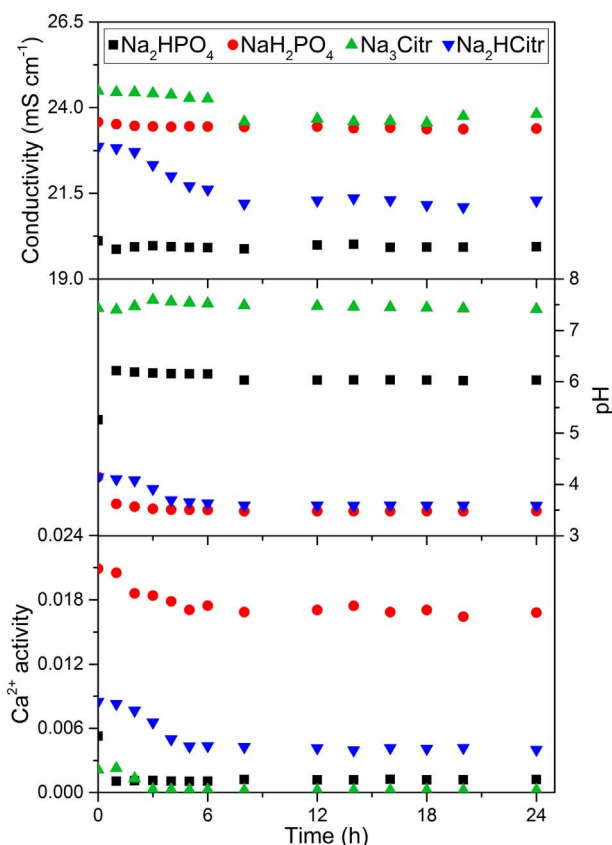
Fig. 1. Calcium ion activity, pH and conductivity in binary systems of equimolar concentrations ($0.10 \, mol \, L^{-1}$) of calcium chloride and sodium hydrogenphosphate (black), sodium dihydrogenphosphate (red), sodium citrate (green) or sodium hydrogencitrate (blue). (For interpretation of the references to colour in this figure legend, the reader is referred to the web version of this article.)

2.9. Statistical analysis

Free calcium concentrations obtained through the thermodynamic model based on the ion speciation were compared to the free calcium concentrations obtained through conductivity and calcium ion activity by evaluating paired *t*-test values at 5% level of significance. The correlation between the two methods was analysed by Pearson's correlation.

3. Results and discussion

3.1. Binary systems

Binary systems were initially investigated by mixing equimolar concentrations ($0.10 \, mol \, L^{-1}$) of $CaCl_2$ with Na_2HPO_4, NaH_2PO_4, Na_3Citr or Na_2HCitr. The samples were kept stirring at 25 °C and were analysed periodically for calcium ion activity, pH and conductivity; results are shown in Fig. 1. The formation of precipitate, verified by visual inspection, was noticed instantly for $CaCl_2$ and Na_2HPO_4, within the first hour for $CaCl_2$ and NaH_2PO_4, within 3 h for $CaCl_2$ and Na_3Citr and within 4 h for $CaCl_2$ and Na_2HCitr. Even though there were no external pH adjustments, precipitation of some form of calcium salt was observed for all the combinations with different rates and yields, as can be observed on the distinct variations of pH, calcium ion activity and conductivity of these samples.

3.2. Dissolution experiments and characterization of the precipitates

The equimolar ($0.10 \, mol \, L^{-1}$) combination of $CaCl_2$, Na_3Citr, and
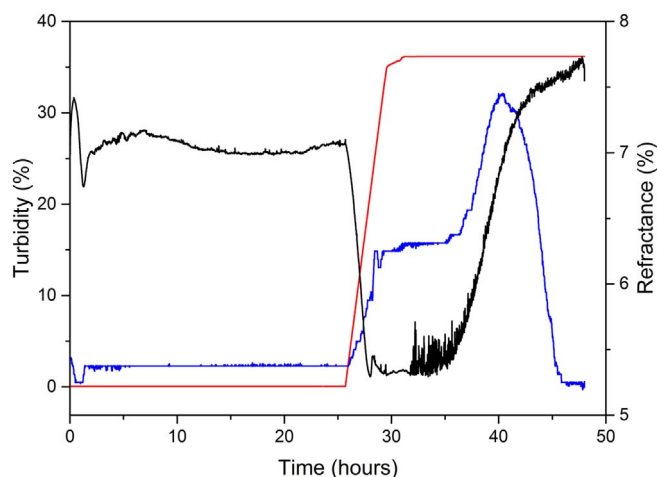
Fig. 2. Turbidity (black) and refraction index (blue) as function of time for equimolar solution ($0.10 \, mol \, L^{-1}$) of $CaCl_2$ Na_3Citr, and Na_2HPO_4. The curve in red indicates the cumulative volume of added HCl at constant rate ($2.0 \, mol \, L^{-1}$ in a total of 35 mL). (For interpretation of the references to colour in this figure legend, the reader is referred to the web version of this article.)

Na_2HPO_4 resulted in immediate formation of precipitate upon mixing of the stock solutions. An initial pH of 6.8 was measured in the mixture, which is similar to mineral precipitates from evaporators of whey permeates (Vavrusova, Johansen, Garcia & Skibsted, 2017). The system was equilibrated under constant stirring at 25 °C during 25 h, period in which the pH slighted dropped from 6.8 to 6.5, after that HCl was added to the system until pH 4.5 was reached. Fig. 2 shows the turbidity and refraction index as function of time.

By adding HCl to the system, the equilibrium was disturbed. The decrease in turbidity as well the increase in the refraction index happened between pH 6.0 and 5.0. It was possible to observe that around 28 h of reaction the sample became clear, with turbidity close to zero and refraction index constant around 6.4%. Another precipitation process was observed after 36 h of reaction, when turbidity started to increase and a peak in refraction index was observed. Total calcium, total citrate and total phosphorous were quantified in filtrated aliquots collected at 20, 28 and 48 h of reaction and the results are shown in Table 1, along with the results of the other experimental setups. Fig. 3 shows the FT-IR spectra of precipitates collect at 20 and 48 h of reaction.

For equimolar ($0.10 \, mol \, L^{-1}$) combinations of $CaCl_2$, Na_2HCitr, and Na_2HPO_4, in a second experiment and $CaCl_2$, Na_2HCitr, and NaH_2PO_4, in a third experiment, similar behaviors were observed, different from the first experiment. There was no immediate formation of precipitate when the stock solutions were mixed and the solution of the second experiment remained clear for a period of 5 h, while the solution of the third experiment remained clear for 10 h. The second experiment was equilibrated under constant stirring at 25 °C for 20 h, while the pH remained stable around 5.5, after that NaOH was added to the system until pH 8.5 was reached. The third experiment was the most acid combination with initial pH of 4.1 dropping to 3.7 within the first 18 h. The system was equilibrated under constant stirring at 25 °C for 25 h, after that NaOH was added to the system in two steps until pH 8.5 was reached. Turbidity and refraction index as function of time are shown in Fig. 4 for the second and third experiments.

In both experiments the precipitation started after a period of more than 5 h, with a peak on the refraction index indicating a crystallization process followed by an increase in turbidity. During the addition of NaOH it is possible to observe a sharp increase in turbidity around 25 h for the second experiment and around 52 h for the third experiment, which happened in both experiments between pH 6.5 and 7.0. These sharp increases in turbidity, followed by increases also in the refraction index indicate that the changes in the composition of the samples were

Table 1
Concentrations of total calcium, total citrate and total phosphorous, quantified in filtrated aliquots and the ratio between calcium/phosphorous and calcium/citrate in the precipitates, by the difference between the filtrated sample and the initial concentration of 0.10 mol L^{-1}.

Experimental set	Reaction time (h)	pH	Calcium (mol L^{-1})	Citrate (mol L^{-1})	Phosphorous (mol L^{-1})	Ca/Citr	Ca/P
CaCl$_2$, Na$_3$Citr, and Na$_2$HPO$_4$	20	6.3	$(4.20 \pm 0.06) \times 10^{-2}$	$(9.31 \pm 0.01) \times 10^{-2}$	$(5.88 \pm 0.04) \times 10^{-2}$	8.37	1.41
	28	4.9	$(8.23 \pm 0.08) \times 10^{-2}$	$(9.20 \pm 0.03) \times 10^{-2}$	$(8.40 \pm 0.09) \times 10^{-2}$	2.21	1.11
	48	4.0	$(3.78 \pm 0.04) \times 10^{-2}$	$(6.02 \pm 0.04) \times 10^{-2}$	$(9.01 \pm 0.08) \times 10^{-2}$	1.56	6.28
CaCl$_2$, Na$_2$HCitr, and Na$_2$HPO$_4$	20	5.8	$(1.59 \pm 0.09) \times 10^{-2}$	$(4.39 \pm 0.07) \times 10^{-2}$	$(9.51 \pm 0.02) \times 10^{-2}$	1.50	17.16
	27	7.9	$(9.33 \pm 0.11) \times 10^{-3}$	$(8.62 \pm 0.03) \times 10^{-2}$	$(3.65 \pm 0.05) \times 10^{-2}$	6.57	1.43
	45	8.3	$(5.11 \pm 0.08) \times 10^{-3}$	$(8.67 \pm 0,01) \times 10^{-2}$	$(3.33 \pm 0.07) \times 10^{-2}$	7.13	1.42
CaCl$_2$, Na$_2$HCitr, and NaH$_2$PO$_4$	20	3.7	$(3.53 \pm 0.02) \times 10^{-2}$	$(5.76 \pm 0.02) \times 10^{-2}$	$(9.38 \pm 0.06) \times 10^{-2}$	1.53	10.44
	43	5.8	$(1.48 \pm 0.05) \times 10^{-2}$	$(4.12 \pm 0.04) \times 10^{-2}$	$(8.81 \pm 0.01) \times 10^{-2}$	1.45	7.16
	67	8.3	$(2.24 \pm 0.09) \times 10^{-3}$	$(8.09 \pm 0.04) \times 10^{-2}$	$(3.06 \pm 0.03) \times 10^{-2}$	5.12	1.41
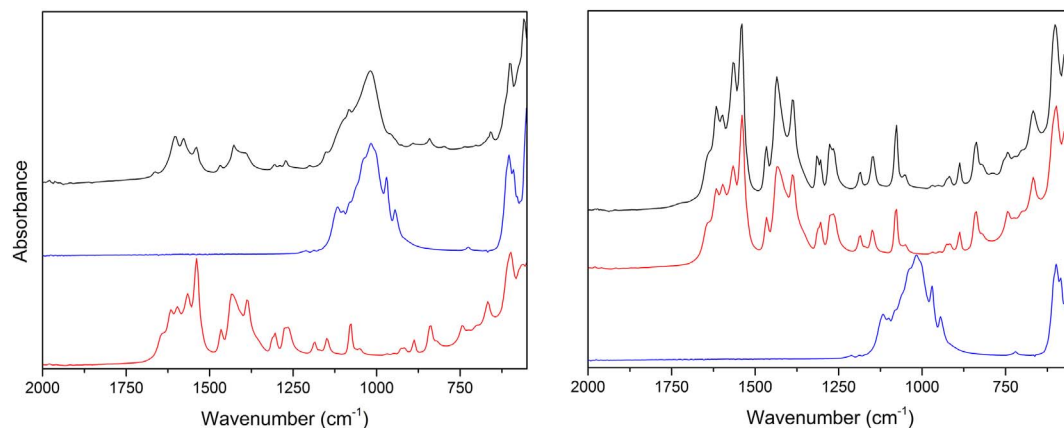
Fig. 3. FT-IR spectra of the precipitates (in black) collected after 20 h of reaction, left, and after 48 h of reaction, right, for equimolar (0.10 mol L^{-1}) CaCl$_2$, Na$_3$Citr, and Na$_2$HPO$_4$ in comparison with spectra of standard calcium citrate tetrahydrate (in red) and calcium phosphate anhydrous (in blue). (For interpretation of the references to colour in this figure legend, the reader is referred to the web version of this article.)
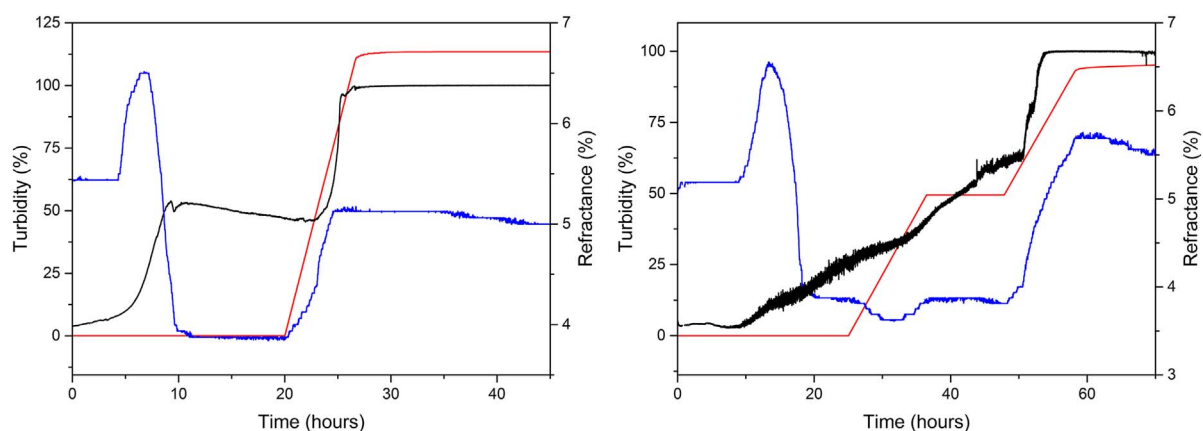

Fig. 4. Turbidity (black) and refraction index (blue) as function of time for equimolar solutions (0.10 mol L^{-1}) of CaCl$_2$, Na$_2$HCitr, and Na$_2$HPO$_4$, right and CaCl$_2$, Na$_2$HCitr, and NaH$_2$PO$_4$, left. The curve in red indicates the cumulative volume of added NaOH at constant rate (2.0 mol L^{-1} a total of 75 mL for the second experiment and 170 mL for the third experiment). (For interpretation of the references to colour in this figure legend, the reader is referred to the web version of this article.)

induced by the pH increase. Aliquots of the second experiment were collected at 20, 27 and 45 h of reaction and filtrated for quantification of total calcium, total citrate and total phosphorous. The same analyses were made for the third system with aliquots collected at 20, 43 and 67 h of reaction. The results are summarized in Table 1. Precipitates were collected for FT-IR analyses at 20 and 45 h for the second experiment and at 20 and 67 h for the third experiment. The FT-IR spectra collected at two moments of both experiments presented the same profile and are shown in Fig. 5.

In all the three experiments, by the FT-IR spectra and the quantification of total calcium, total citrate and total phosphorus it is clear that

the nature of the formed precipitate depends on pH and that it can be reverted by pH changes. The first experiment (CaCl$_2$, Na$_3$Citr and Na$_2$HPO$_4$) provided the conditions for the formation of calcium phosphate, probably amorphous calcium phosphate (ACP), since citrate ions can act as stabilizer for the formation of ACP at the pH around 6.5 (Holt et al., 1989). The verified Ca/P ratio of 1.41 found in the precipitate, Table 1, is also consistent with the Ca/P found for ACP, reported to be between 1.18 and 1.50 (Lenton et al., 2015). The FT-IR spectrum of the precipitate collected at 20 h presents a broad band in the region of 1000 cm^{-1}, typical of P−O bonds, indicating the predominance of calcium phosphate in the precipitate, but two small broad bands around
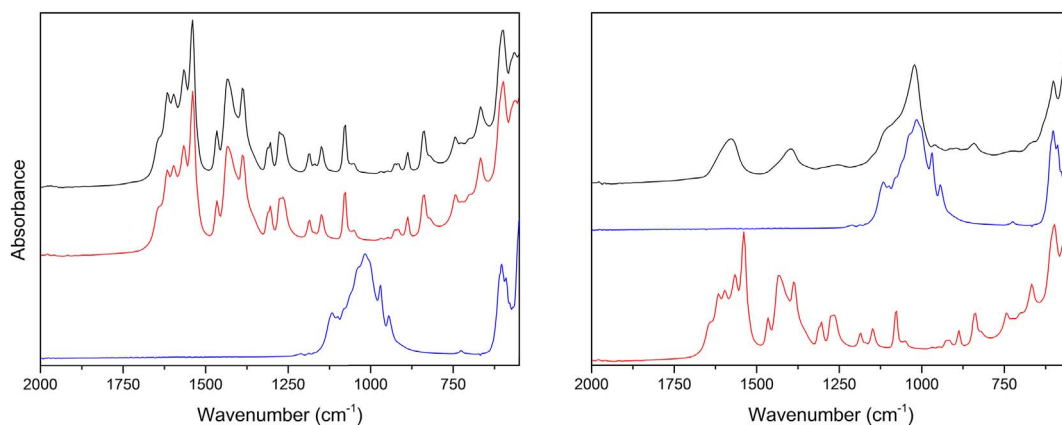
Fig. 5. FT-IR spectra of the precipitates (in black) after 20 h of experiment, left, and after 45 h of reaction, right, for equimolar (0.10 mol L^{-1}) CaCl$_2$, Na$_2$HCitr, and NaH$_2$PO$_4$ in comparison with spectra of standard calcium citrate tetrahydrate (in red) and calcium phosphate anhydrous (in blue). The spectra collected for the precipitates after 20 and 67 h for CaCl$_2$, NaH$_2$Citr, and NaH$_2$PO$_4$ presented the same profile. (For interpretation of the references to colour in this figure legend, the reader is referred to the web version of this article.)

1600 and 1400 cm^{-1} regions, characteristics of the asymmetric and symmetric C−O bonds, suggests some low co-precipitation of citrate, reinforce by the slight decrease in citrate concentration in the filtrate in relation to the stock solution (Table 1). By the decrease of pH to 4.5 the precipitated calcium phosphate was solubilized, as observed on the turbidity decrease and the change in refraction index between 25 and 30 h, both shown in Fig. 2, and reinforced by the increase in the concentration of total calcium and total phosphorus quantified in the filtrated aliquot of the sample at 28 h (Table 1). The second precipitation process, initiated around 36 h, after a period in which the sample was clear, as can be observed in Fig. 2 by the increase in turbidity and the peak on refraction index, was characterized as calcium citrate. In the aliquot collected at 48 h, most of the phosphorous remained in solution and the difference in the concentration of calcium and citrate due to the precipitation leads to a Ca/Citr relation of 1.56 (Table 1), very close to what is expected for Ca$_3$Citr$_2$, besides that the FT-IR spectrum of the precipitate matches perfectly the spectrum of the standard of calcium citrate tetrahydrate, as can be seen in Fig. 3.

The second and third experiments presented very similar behaviors, with a period of clear solution in acidic conditions with further precipitation of calcium citrate, as was also observed and previously described for the first system after the acidification. The filtrated aliquots collected at 20 h of reaction from both systems show that most of the phosphate remained in solution and that the Ca/Citr relation in the precipitates were of 1.50 and 1.53 (Table 1) for the second and third experiments, respectively, as it is expected for Ca$_3$Citr$_2$. The precipitates collected at 20 h presented very similar FT-IR spectra that matched the spectrum of calcium citrate standard as can be seen in Fig. 5. The increase in pH promoted by the addition of NaOH led to the precipitation of calcium phosphate and dissolution of calcium citrate, as can be observed in the aliquots collect at 45 h of the second experiment and at 67 h of the third experiment. The Ca/P relation were of 1.42 and 1.41 for the second and third experiment respectively, as shown in Table 1, ratio consistent with ACP, as previously mentioned for the first system. It is important to notice that some calcium citrate remained precipitated, as can be verified in the citrate concentration in the filtrates and also in the FT-IR spectra of the precipitates that show broad bands around 1600 and 1400 cm^{-1}, regions in which calcium citrate spectrum typically present bond stretching signals. The intermediate aliquots collected from the second and third experiments show different moments of these two similar systems: for the second experiment, the aliquot was collect at 27 h of reaction, pH 7.9, after the sharp increase in turbidity due to the precipitation of calcium citrate. The Ca/P ratio was 1.43 and most of the precipitated citrate was solubilized. The aliquot of the third experiment, however, was collected at 43 h of reaction, pH 4.8, before the sharp increase in turbidity. The phosphate

concentration in the filtrate was lower than in the first aliquot, indicating that some precipitation of phosphate have started, but the Ca/P was 7.16, while the Ca/Citr was 1.45, so the precipitate was still mainly composed of calcium citrate, considering that the interconversion to calcium phosphate happens in the pH range between 6.5 and 7.0, when the sharp increase in turbidity was observed for both third and second experiments.

3.3. Thermodynamic and kinetic modelling

In order to further investigate the thermodynamics and kinetics behind the slow precipitation of calcium citrate, the second and third experiments were repeated in laboratory scale and aliquots were periodically collected, filtrated and analysed for calcium ion activity, conductivity, pH, total calcium, total citrate and total phosphorous concentrations. These results are summarized in Tables 2 and 3 and were used to calculate the ion speciation of these systems according to the equilibria and mass balances exhibited in Tables 4 and 5.

The calculations were performed by iterations. An estimated value of 0.5 mol L^{-1} for ionic strength was used for the initial set of calculations for the samples at 0 h of reaction, either to calculate the value of thermodynamic constants and/or to calculate the value of activity coefficients using Davies Eq. (2). From the results of the first calculations, the obtained concentrations of the ions in solution were used to calculate the ionic strength according to

$$I = \frac{1}{2} \sum c_i z_i^2 \tag{3}$$

in which c$_i$ corresponds to the ion concentration of an ion and z$_i$ to the ion's valence. With the new value for the ionic strength, new thermodynamic constants and activity coefficients were calculated in order to repeat the ion speciation. The iterations were repeated until constant values of ionic strength were obtained, this constant value was then used as initial ionic strength for the iterative calculations for the subsequent hour of reaction. Tables 6 and 7 show the results for the ions speciation for both experiments.

Calcium ion activity and conductivity, exhibited in Tables 2 and 3, were used to estimate the free calcium concentration, which was compared to the free calcium concentration obtained from the thermodynamic model based on the ion speciation, exhibited in Tables 6 and 7. Griffin and Jurinak (Griffin & Jurinak, 1973) proposed a linear relationship between ionic strength and conductivity at 25 °C given by

$$I \cong 0.013 \, \lambda \tag{4}$$

in which I is the ionic strength, given in mol L^{-1}, and λ is the conductivity, given in mS cm^{-1}. The obtained values for ionic strength from the experimental conductivity were used to calculate the activity

Table 2
Calcium ion activity, conductivity (λ), total calcium, total citrate and pH for aqueous solution composed of $CaCl_2$, Na_2HCitr, and Na_2HPO_4 ($0.10\,mol\,L^{-1}$) as function of time. Concentrations expressed in $mol\,L^{-1}$.

Time (h)	Calcium activity	λ ($mS\,cm^{-1}$)	Total calcium	Total citrate	Total phosphorus	pH	$a_{H_3O^+}$
0	$(2.85 \pm 0.10) \times 10^{-3}$	27.53 ± 0.05	$(1.01 \pm 0.02) \times 10^{-1}$	$(1.01 \pm 0.02) \times 10^{-1}$	$(1.02 \pm 0.02) \times 10^{-1}$	5.52 ± 0.01	3.05×10^{-6}
1	$(2.62 \pm 0.28) \times 10^{-3}$	28.43 ± 0.05	$(1.01 \pm 0.02) \times 10^{-1}$	$(1.01 \pm 0.02) \times 10^{-1}$	$(1.05 \pm 0.01) \times 10^{-1}$	5.52 ± 0.01	3.00×10^{-6}
2	$(2.06 \pm 0.26) \times 10^{-3}$	28.48 ± 0.25	$(1.00 \pm 0.04) \times 10^{-1}$	$(9.83 \pm 0.08) \times 10^{-2}$	$(1.04 \pm 0.03) \times 10^{-1}$	5.56 ± 0.04	2.75×10^{-6}
3	$(1.03 \pm 0.33) \times 10^{-3}$	28.13 ± 0.08	$(8.77 \pm 0.50) \times 10^{-2}$	$(8.38 \pm 0.68) \times 10^{-2}$	$(1.02 \pm 0.01) \times 10^{-1}$	5.61 ± 0.03	2.43×10^{-6}
4	$(6.09 \pm 1.02) \times 10^{-4}$	27.52 ± 0.69	$(5.35 \pm 0.45) \times 10^{-2}$	$(6.40 \pm 0.73) \times 10^{-2}$	$(1.04 \pm 0.03) \times 10^{-1}$	5.61 ± 0.01	2.45×10^{-6}
8	$(3.49 \pm 0.05) \times 10^{-4}$	27.09 ± 0.27	$(1.71 \pm 0.01) \times 10^{-2}$	$(4.48 \pm 0.01) \times 10^{-2}$	$(1.04 \pm 0.02) \times 10^{-1}$	5.63 ± 0.01	2.32×10^{-6}
12	$(3.19 \pm 0.15) \times 10^{-4}$	27.13 ± 0.59	$(1.61 \pm 0.02) \times 10^{-2}$	$(4.40 \pm 0.01) \times 10^{-2}$	$(1.04 \pm 0.02) \times 10^{-1}$	5.65 ± 0.01	2.24×10^{-6}
16	$(2.94 \pm 0.18) \times 10^{-4}$	27.28 ± 0.09	$(1.54 \pm 0.01) \times 10^{-2}$	$(4.29 \pm 0.04) \times 10^{-2}$	$(1.05 \pm 0.02) \times 10^{-1}$	5.65 ± 0.01	2.26×10^{-6}
20	$(2.99 \pm 0.22) \times 10^{-4}$	27.35 ± 0.01	$(1.52 \pm 0.01) \times 10^{-2}$	$(4.27 \pm 0.06) \times 10^{-2}$	$(1.03 \pm 0.01) \times 10^{-1}$	5.64 ± 0.01	2.27×10^{-6}
24	$(2.91 \pm 0.06) \times 10^{-4}$	27.25 ± 0.06	$(1.45 \pm 0.01) \times 10^{-2}$	$(4.23 \pm 0.07) \times 10^{-2}$	$(1.01 \pm 0.01) \times 10^{-1}$	5.65 ± 0.01	2.25×10^{-6}
28	$(2.88 \pm 0.01) \times 10^{-4}$	27.30 ± 0.07	$(1.43 \pm 0.01) \times 10^{-2}$	$(4.28 \pm 0.02) \times 10^{-2}$	$(1.03 \pm 0.02) \times 10^{-1}$	5.65 ± 0.01	2.25×10^{-6}
32	$(2.91 \pm 0.11) \times 10^{-4}$	27.13 ± 0.09	$(1.44 \pm 0.01) \times 10^{-2}$	$(4.27 \pm 0.03) \times 10^{-2}$	$(1.03 \pm 0.01) \times 10^{-1}$	5.65 ± 0.01	2.22×10^{-6}
36	$(2.93 \pm 0.04) \times 10^{-4}$	27.32 ± 0.13	$(1.41 \pm 0.01) \times 10^{-2}$	$(4.28 \pm 0.06) \times 10^{-2}$	$(1.02 \pm 0.04) \times 10^{-1}$	5.65 ± 0.01	2.22×10^{-6}
40	$(2.84 \pm 0.01) \times 10^{-4}$	27.32 ± 0.15	$(1.39 \pm 0.01) \times 10^{-2}$	$(4.33 \pm 0.16) \times 10^{-2}$	$(1.02 \pm 0.01) \times 10^{-1}$	5.65 ± 0.01	2.22×10^{-6}
44	$(2.78 \pm 0.05) \times 10^{-4}$	27.11 ± 0.13	$(1.39 \pm 0.01) \times 10^{-2}$	$(4.12 \pm 0.17) \times 10^{-2}$	$(1.02 \pm 0.01) \times 10^{-1}$	5.65 ± 0.01	2.22×10^{-6}

Samples were prepared in duplicates.

Table 3
Calcium ion activity, conductivity (λ), total calcium, total citrate and pH for aqueous solution composed of $CaCl_2$, Na_2HCitr, and NaH_2PO_4 ($0.10\,mol\,L^{-1}$) as function of time. Concentrations expressed in $mol\,L^{-1}$.

Time (h)	Calcium activity	λ ($mS\,cm^{-1}$)	Total calcium	Total citrate	Total phosphorus	pH	$a_{H_3O^+}$
0	$(7.12 \pm 0.09) \times 10^{-3}$	26.52 ± 0.01	$(1.03 \pm 0.01) \times 10^{-1}$	$(9.78 \pm 0.55) \times 10^{-2}$	$(1.09 \pm 0.01) \times 10^{-1}$	4.13 ± 0.01	7.50×10^{-5}
1	$(7.30 \pm 0.07) \times 10^{-3}$	26.07 ± 0.03	$(1.04 \pm 0.01) \times 10^{-1}$	$(9.84 \pm 0.49) \times 10^{-2}$	$(1.05 \pm 0.01) \times 10^{-1}$	4.11 ± 0.01	7.74×10^{-5}
2	$(6.70 \pm 0.31) \times 10^{-3}$	25.91 ± 0.02	$(1.02 \pm 0.01) \times 10^{-1}$	$(9.46 \pm 0.03) \times 10^{-2}$	$(1.07 \pm 0.01) \times 10^{-1}$	4.05 ± 0.03	8.91×10^{-5}
3	$(5.14 \pm 0.51) \times 10^{-3}$	25.75 ± 0.01	$(9.85 \pm 0.52) \times 10^{-2}$	$(9.29 \pm 0.04) \times 10^{-2}$	$(1.06 \pm 0.01) \times 10^{-1}$	3.90 ± 0.05	1.26×10^{-4}
4	$(5.12 \pm 0.34) \times 10^{-3}$	26.17 ± 0.01	$(7.92 \pm 0.34) \times 10^{-2}$	$(8.01 \pm 0.40) \times 10^{-2}$	$(1.05 \pm 0.02) \times 10^{-1}$	3.88 ± 0.05	1.31×10^{-4}
8	$(4.26 \pm 0.03) \times 10^{-3}$	25.14 ± 0.32	$(4.16 \pm 0.02) \times 10^{-2}$	$(5.84 \pm 0.03) \times 10^{-2}$	$(1.07 \pm 0.03) \times 10^{-1}$	3.70 ± 0.01	2.00×10^{-4}
12	$(3.86 \pm 0.01) \times 10^{-3}$	25.10 ± 0.04	$(4.02 \pm 0.03) \times 10^{-2}$	$(5.92 \pm 0.03) \times 10^{-2}$	$(1.09 \pm 0.01) \times 10^{-1}$	3.68 ± 0.01	2.07×10^{-4}
16	$(3.84 \pm 0.02) \times 10^{-3}$	25.21 ± 0.06	$(3.86 \pm 0.07) \times 10^{-2}$	$(5.67 \pm 0.28) \times 10^{-2}$	$(1.03 \pm 0.01) \times 10^{-1}$	3.68 ± 0.01	2.10×10^{-4}
20	$(3.86 \pm 0.08) \times 10^{-3}$	25.29 ± 0.09	$(3.87 \pm 0.01) \times 10^{-2}$	$(5.63 \pm 0.12) \times 10^{-2}$	$(1.08 \pm 0.02) \times 10^{-1}$	3.67 ± 0.01	2.13×10^{-4}
24	$(4.08 \pm 0.03) \times 10^{-3}$	25.30 ± 0.40	$(3.90 \pm 0.05) \times 10^{-2}$	$(5.72 \pm 0.08) \times 10^{-2}$	$(1.03 \pm 0.02) \times 10^{-1}$	3.67 ± 0.01	2.16×10^{-4}
28	$(4.02 \pm 0.05) \times 10^{-3}$	25.28 ± 0.04	$(3.86 \pm 0.04) \times 10^{-2}$	$(5.66 \pm 0.12) \times 10^{-2}$	$(1.06 \pm 0.02) \times 10^{-1}$	3.66 ± 0.01	2.18×10^{-4}
32	$(3.99 \pm 0.06) \times 10^{-3}$	25.03 ± 0.27	$(3.84 \pm 0.07) \times 10^{-2}$	$(5.67 \pm 0.16) \times 10^{-2}$	$(1.03 \pm 0.02) \times 10^{-1}$	3.66 ± 0.01	2.18×10^{-4}
36	$(4.05 \pm 0.12) \times 10^{-3}$	25.23 ± 0.15	$(3.85 \pm 0.03) \times 10^{-2}$	$(5.77 \pm 0.08) \times 10^{-2}$	$(1.04 \pm 0.01) \times 10^{-1}$	3.66 ± 0.01	2.19×10^{-4}
40	$(3.89 \pm 0.04) \times 10^{-3}$	25.20 ± 0.05	$(3.79 \pm 0.03) \times 10^{-2}$	$(5.40 \pm 0.15) \times 10^{-2}$	$(1.06 \pm 0.01) \times 10^{-1}$	3.66 ± 0.01	2.20×10^{-4}
44	$(3.89 \pm 0.07) \times 10^{-3}$	25.23 ± 0.14	$(3.75 \pm 0.03) \times 10^{-2}$	$(5.65 \pm 0.20) \times 10^{-2}$	$(1.02 \pm 0.03) \times 10^{-1}$	3.66 ± 0.01	2.19×10^{-4}

Samples were prepared in duplicates.

coefficient for calcium ion using Davies' Eq. (2) and then used to calculate the free calcium concentration using the experimental results from calcium ion activity and the relationship between calcium activity and activity coefficient (Eq. (1)). Fig. 6 shows the comparison between free calcium concentrations from both methods for the two experimental systems.

The initial hours of the experiments are characterized by a period of supersaturation in relation to calcium citrate, with degrees of supersaturation of 7.1 for the system composed of $CaCl_2$, Na_2HCitr and Na_2HPO_4 and of 2.7 for the system composed of $CaCl_2$, Na_2HCitr and NaH_2PO_4, determined by the ratio between maximum calcium concentration and calcium concentration in equilibrium. The concentrations of free calcium obtained by different methods (Fig. 6) were compared using a paired t-test and were shown to be significantly different at $\alpha = 0.05$, but with good correlation. The samples composed of $CaCl_2$, Na_2HCitr and Na_2HPO_4 presented a P-value of 0.011 and Pearson's correlation (r) of 0.909 and the sample composed of $CaCl_2$, Na_2HCitr and NaH_2PO_4 presented a P-value of 0.004 and Pearson's correlation (r) of 0.890. The already expected discrepancies in free calcium concentrations obtained from both methods were attributed mainly to the initial hours of the experiments, characterized by the supersaturation period. It is possible to observe in Fig. 6 that the results from both methods are in good accordance after 8 h of reaction, when both systems are in equilibrium. The thermodynamic model might not

give a complete accurate description of these samples in metastable conditions, since it is based on ion speciation calculated with equilibrium constants, but the values showing the tendency of the systems towards equilibrium are still reasonable. In previous work, we have verified for calcium D-saccharate that the ratio between total calcium concentrations in supersaturated and saturated solutions was higher than the ratio between free calcium concentrations in supersaturated and saturated solutions (Garcia et al., 2016). We have also verified that free calcium concentration is not directly dependent on the degree of supersaturation (Vavrusova et al., 2018). All these findings corroborates that free calcium concentration is slowly adjusted in supersaturated solutions.

From the experiments monitoring turbidity, it was observed that when the conditions were favorable for the formation of calcium citrate, the precipitation was not immediate, the samples remained clear for hours (Figs. 2, and 4). From the thermodynamic model, the ionic products were higher than the solubility product for calcium citrate (7.60×10^{-17} (Vavrusova & Skibsted, 2016)) in the first 4 h (Tables 6 and 7), confirming the supersaturation. The ionic product approaches the solubility product slowly during the precipitation and is comparable after 8 h for the less acidic experiment, with higher degree of supersaturation, and after 4 h for the more acidic experiment, with lower degree of supersaturation.

For mixtures of hydroxycarboxylates supersaturated in relation to

Table 4

Equilibria and mass balances used for calculation of ion speciation for aqueous solution of $CaCl_2$, Na_2HCitr, and Na_2HPO_4.

Chemical equilibrium	Thermodynamic equilibrium constant equation	Conversion from activity to concentration
$H_2PO_4^- + H_2O \rightleftharpoons H_3O^+ + HPO_4^{2-}$	$K_{aP2} = \frac{a_{H_3O^+}a_{HPO_4^{2-}}}{a_{H_2PO_4^-}}$	$\frac{K_{aP2}}{a_{H_3O^+}}\left(\frac{\gamma^\pm}{\gamma^{2\pm}}\right) = \frac{[HPO_4^{2-}]}{[H_2PO_4^-]}$
$H_2Citr^- + H_2O \rightleftharpoons H_3O^+ + HCitr^{2-}$	$K_{aCitr2} = \frac{a_{H_3O^+}a_{HCitr^{2-}}}{a_{H_2Citr^-}}$	$\frac{K_{aCitr2}}{a_{H_3O^+}}\left(\frac{\gamma^\pm}{\gamma^{2\pm}}\right) = \frac{[HCitr^{2-}]}{[H_2Citr^-]}$
$HCitr^{2-} + H_2O \rightleftharpoons H_3O^+ + Citr^{3-}$	$K_{aCitr3} = \frac{a_{H_3O^+}a_{Citr^{3-}}}{a_{HCitr^{2-}}}$	$\frac{K_{aCitr3}}{a_{H_3O^+}}\left(\frac{\gamma^{2\pm}}{\gamma^{3\pm}}\right) = \frac{[Citr^{3-}]}{[HCitr^{2-}]}$
$Ca^{2+} + HCitr^{2-} \rightleftharpoons CaHCitr$	$K_1 = \frac{a_{CaHCitr}}{a_{Ca^{2+}}a_{HCitr^{2-}}}$	$K_1(\gamma^{2\pm}\gamma^{2\pm}) = \frac{[CaHCitr]}{[Ca^{2+}][HCitr^{2-}]}$
$Ca^{2+} + Citr^{3-} \rightleftharpoons CaCitr^-$	$K_2 = \frac{a_{CaCitr^-}}{a_{Ca^{2+}}a_{Citr^{3-}}}$	$K_2\left(\frac{\gamma^{2\pm}\gamma^{3\pm}}{\gamma^\pm}\right) = \frac{[CaCitr^-]}{[Ca^{2+}][Citr^{3-}]}$
$Ca^{2+} + HPO_4^{2-} \rightleftharpoons CaHPO_4$	$K_3 = \frac{a_{CaHPO_4}}{a_{Ca^{2+}}a_{HPO_4^{2-}}}$	$K_3(\gamma^{2\pm}\gamma^{2\pm}) = \frac{[CaHPO_4]}{[Ca^{2+}][PO_4^{2-}]}$
$Na^+ + HCitr^{2-} \rightleftharpoons NaHCitr^-$	$K_4 = \frac{a_{NaHCitr^-}}{a_{Na^+}a_{HCitr^{2-}}}$	$K_4(\gamma^{2\pm}) = \frac{[NaHCitr^-]}{[Na^+][HCitr^{2-}]}$
$Na^+ + Citr^{3-} \rightleftharpoons NaCitr^{2-}$	$K_5 = \frac{a_{NaCitr^{2-}}}{a_{Na^+}a_{Citr^{3-}}}$	$K_5\left(\frac{\gamma^\pm\gamma^{3\pm}}{\gamma^{2\pm}}\right) = \frac{[NaCitr^{2-}]}{[Na^+][Citr^{3-}]}$

Mass balances
Total calcium $\quad t_{Ca} = [Ca^{2+}] + [CaHPO_4] + [CaHCitr] + [CaCitr^-]$
Total phosphate $\quad t_P = [H_2PO_4^-] + [HPO_4^{2-}] + [CaHPO_4]$
Total citrate $\quad t_{Citr} = [H_2Citr^-] + [HCitr^{2-}] + [Citr^{3-}] + [CaHCitr] + [CaCitr^-]$
Total sodium $\quad t_{Na} = [Na^+] + [NaHCitr^-] + [NaCitr^{2-}]$

$K_{aP2} = 10^{-(7.198 - 1.404\sqrt{I} + 0.6168I - 0.08114I^{3/2})}$, (Hershey et al., 1989).
$K_{aCitr2} = 1.7338 \ 10^{-5}$, (Bates & Pinching, 1949).
$K_{aCitr3} = 4.0179 \ 10^{-7}$, (Bates & Pinching, 1949).
$K_1 = 2600$, (Vavrusova, Danielsen, et al., 2018).
$K_2 = 49600$, (Vavrusova & Skibsted, 2016).
$K_3 = 500$, (Davies & Hoyle, 1953).
$K_4 = 8.7$, (Daniele et al., 2008).
$K_5 = 34.7$, (Daniele et al., 2008).

Table 5

Equilibria and mass balances used for calculation of ion speciation for aqueous solution of $CaCl_2$, Na_2HCitr, and NaH_2PO_4.

Chemical equilibrium	Thermodynamic equilibrium constant equation	Conversion from activity to concentration
$H_3PO_4 + H_2O \rightleftharpoons H_3O^+ + H_2PO_4^-$	$K_{aP1} = \frac{a_{H_3O^+}a_{H_2PO_4^-}}{a_{H_3PO_4}}$	$\frac{K_{aP1}}{a_{H_3O^+}}\left(\frac{1}{\gamma^\pm}\right) = \frac{[H_2PO_4^-]}{[H_3PO_4]}$
$H_2PO_4^- + H_2O \rightleftharpoons H_3O^+ + HPO_4^{2-}$	$K_{aP2} = \frac{a_{H_3O^+}a_{HPO_4^{2-}}}{a_{H_2PO_4^-}}$	$\frac{K_{aP2}}{a_{H_3O^+}}\left(\frac{\gamma^\pm}{\gamma^{2\pm}}\right) = \frac{[HPO_4^{2-}]}{[H_2PO_4^-]}$
$H_3Citr + H_2O \rightleftharpoons H_3O^+ + H_2Citr^-$	$K_{aCitr1} = \frac{a_{H_3O^+}a_{H_2Citr^-}}{a_{H_3Citr}}$	$\frac{K_{aCitr1}}{a_{H_3O^+}}\left(\frac{1}{\gamma^\pm}\right) = \frac{[H_2Citr^-]}{[H_3Citr]}$
$H_2Citr^- + H_2O \rightleftharpoons H_3O^+ + HCitr^{2-}$	$K_{aCitr2} = \frac{a_{H_3O^+}a_{HCitr^{2-}}}{a_{H_2Citr^-}}$	$\frac{K_{aCitr2}}{a_{H_3O^+}}\left(\frac{\gamma^\pm}{\gamma^{2\pm}}\right) = \frac{[HCitr^{2-}]}{[H_2Citr^-]}$
$HCitr^{2-} + H_2O \rightleftharpoons H_3O^+ + Citr^{3-}$	$K_{aCitr3} = \frac{a_{H_3O^+}a_{Citr^{3-}}}{a_{HCitr^{2-}}}$	$\frac{K_{aCitr3}}{a_{H_3O^+}}\left(\frac{\gamma^{2\pm}}{\gamma^{3\pm}}\right) = \frac{[Citr^{3-}]}{[HCitr^{2-}]}$
$Ca^{2+} + HCitr^{2-} \rightleftharpoons CaHCitr$	$K_1 = \frac{a_{CaHCitr}}{a_{Ca^{2+}}a_{HCitr^{2-}}}$	$K_1(\gamma^{2\pm}\gamma^{2\pm}) = \frac{[CaHCitr]}{[Ca^{2+}][HCitr^{2-}]}$
$Ca^{2+} + Citr^{3-} \rightleftharpoons CaCitr^-$	$K_2 = \frac{a_{CaCitr^-}}{a_{Ca^{2+}}a_{Citr^{3-}}}$	$K_2\left(\frac{\gamma^{2\pm}\gamma^{3\pm}}{\gamma^\pm}\right) = \frac{[CaCitr^-]}{[Ca^{2+}][Citr^{3-}]}$
$Ca^{2+} + HPO_4^{2-} \rightleftharpoons CaHPO_4$	$K_3 = \frac{a_{CaHPO_4}}{a_{Ca^{2+}}a_{HPO_4^{2-}}}$	$K_3(\gamma^{2\pm}\gamma^{2\pm}) = \frac{[CaHPO_4]}{[Ca^{2+}][PO_4^{2-}]}$
$Na^+ + HCitr^{2-} \rightleftharpoons NaHCitr^-$	$K_4 = \frac{a_{NaHCitr^-}}{a_{Na^+}a_{HCitr^{2-}}}$	$K_4(\gamma^{2\pm}) = \frac{[NaHCitr^-]}{[Na^+][HCitr^{2-}]}$
$Na^+ + Citr^{3-} \rightleftharpoons NaCitr^{2-}$	$K_5 = \frac{a_{NaCitr^{2-}}}{a_{Na^+}a_{Citr^{3-}}}$	$K_5\left(\frac{\gamma^\pm\gamma^{3\pm}}{\gamma^{2\pm}}\right) = \frac{[NaCitr^{2-}]}{[Na^+][Citr^{3-}]}$

Mass balances
Total calcium $\quad t_{Ca} = [Ca^{2+}] + [CaHPO_4] + [CaHCitr] + [CaCitr^-]$
Total phosphate $\quad t_P = [CaHPO_4] + [H_3PO_4] + [H_2PO_4^-] + [HPO_4^{2-}]$
Total citrate $\quad t_{Citr} = [CaHCitr] + [CaCitr^-] + [H_3Citr] + [H_2Citr^-] + [HCitr^{2-}] + [Citr^{3-}]$
Total sodium $\quad t_{Na} = [Na^+] + [NaHCitr^-] + [NaCitr^{2-}]$

$K_{aP1} = 10^{-(2.146 - 0.5136\sqrt{I} + 0.1606I)}$, (Hershey et al., 1989).
$K_{aP2} = 10^{-(7.198 - 1.404\sqrt{I} + 0.6168I - 0.08114I^{3/2})}$, (Hershey et al., 1989).
$K_{aCitr1} = 7.4473 \ 10^{-4}$, (Bates & Pinching, 1949).
$K_{aCitr2} = 1.7338 \ 10^{-5}$, (Bates & Pinching, 1949).
$K_{aCitr3} = 4.0179 \ 10^{-7}$, (Bates & Pinching, 1949).
$K_1 = 2600$, (Vavrusova, Danielsen, et al., 2018).
$K_2 = 49600$, (Vavrusova & Skibsted, 2016).
$K_3 = 500$, (Davies & Hoyle, 1953).
$K_4 = 8.7$, (Daniele et al., 2008).
$K_5 = 34.7$, (Daniele et al., 2008).

Table 6
Ion speciation for aqueous solution of $CaCl_2$, Na_2HCitr, and Na_2HPO_4 ($0.10\,mol\,L^{-1}$) as function of time. Concentrations expressed in $mol\,L^{-1}$.

Time (h)	$H_2PO_4^-$	HPO_4^{2-}	H_2Citr^-	$HCitr^{2-}$	$Citr^{3-}$	Ca^{2+}	$CaHCitr$	$CaCitr^-$	$CaHPO_4$	Na^+	$NaHCitr^-$	$NaCitr^{2-}$	I	Q^a
0	8.79×10^{-2}	8.94×10^{-3}	2.20×10^{-4}	4.38×10^{-3}	3.77×10^{-3}	1.52×10^{-2}	1.41×10^{-2}	6.65×10^{-2}	5.55×10^{-3}	3.88×10^{-1}	7.76×10^{-3}	4.23×10^{-3}	0.451	4.17×10^{-15}
1	9.03×10^{-2}	9.36×10^{-3}	2.20×10^{-4}	4.44×10^{-3}	3.89×10^{-3}	1.47×10^{-2}	1.39×10^{-2}	6.66×10^{-2}	5.65×10^{-3}	3.88×10^{-1}	8.01×10^{-3}	4.29×10^{-3}	0.453	4.06×10^{-15}
2	8.78×10^{-2}	9.89×10^{-3}	1.79×10^{-4}	3.94×10^{-3}	3.75×10^{-3}	1.52×10^{-2}	1.27×10^{-2}	6.62×10^{-2}	6.15×10^{-3}	3.88×10^{-1}	7.74×10^{-3}	3.81×10^{-3}	0.452	4.13×10^{-15}
3	8.52×10^{-2}	1.08×10^{-2}	1.27×10^{-4}	3.17×10^{-3}	3.43×10^{-3}	1.44×10^{-2}	9.70×10^{-3}	5.72×10^{-2}	6.33×10^{-3}	3.90×10^{-1}	7.09×10^{-3}	3.08×10^{-3}	0.443	2.93×10^{-15}
4	8.99×10^{-2}	1.10×10^{-2}	1.62×10^{-4}	4.01×10^{-3}	4.31×10^{-3}	7.37×10^{-3}	6.25×10^{-3}	3.66×10^{-2}	3.31×10^{-3}	3.87×10^{-1}	8.82×10^{-3}	3.86×10^{-3}	0.428	6.11×10^{-16}
8	9.12×10^{-2}	1.17×10^{-2}	2.13×10^{-4}	5.58×10^{-3}	6.35×10^{-3}	1.72×10^{-3}	2.03×10^{-3}	1.26×10^{-2}	8.20×10^{-4}	3.82×10^{-1}	1.28×10^{-2}	5.29×10^{-3}	0.419	1.69×10^{-17}
12	9.09×10^{-2}	1.21×10^{-2}	2.02×10^{-4}	5.48×10^{-3}	6.45×10^{-3}	1.60×10^{-3}	1.85×10^{-3}	1.18×10^{-2}	7.85×10^{-4}	3.82×10^{-1}	1.30×10^{-2}	5.19×10^{-3}	0.419	1.39×10^{-17}
16	9.21×10^{-2}	1.21×10^{-2}	2.02×10^{-4}	5.43×10^{-3}	6.33×10^{-3}	1.55×10^{-3}	1.78×10^{-3}	1.13×10^{-2}	7.63×10^{-4}	3.82×10^{-1}	1.28×10^{-2}	5.15×10^{-3}	0.418	1.22×10^{-17}
20	9.04×10^{-2}	1.18×10^{-2}	2.03×10^{-4}	5.42×10^{-3}	6.30×10^{-3}	1.54×10^{-3}	1.76×10^{-3}	1.12×10^{-2}	7.40×10^{-4}	3.82×10^{-1}	1.27×10^{-2}	5.14×10^{-3}	0.417	1.18×10^{-17}
24	8.89×10^{-2}	1.17×10^{-2}	2.00×10^{-4}	5.42×10^{-3}	6.37×10^{-3}	1.46×10^{-3}	1.66×10^{-3}	1.06×10^{-2}	6.94×10^{-4}	3.82×10^{-1}	1.28×10^{-2}	5.14×10^{-3}	0.416	1.02×10^{-17}
28	9.01×10^{-2}	1.19×10^{-2}	2.05×10^{-4}	5.54×10^{-3}	6.51×10^{-3}	1.42×10^{-3}	1.66×10^{-3}	1.06×10^{-2}	6.86×10^{-4}	3.82×10^{-1}	1.31×10^{-2}	5.25×10^{-3}	0.418	9.82×10^{-18}
32	9.01×10^{-2}	1.21×10^{-2}	2.00×10^{-4}	5.48×10^{-3}	6.51×10^{-3}	1.42×10^{-3}	1.64×10^{-3}	1.06×10^{-2}	6.94×10^{-4}	3.82×10^{-1}	1.31×10^{-2}	5.19×10^{-3}	0.418	9.86×10^{-18}
36	8.96×10^{-2}	1.20×10^{-2}	2.01×10^{-4}	5.51×10^{-3}	6.57×10^{-3}	1.39×10^{-3}	1.61×10^{-3}	1.05×10^{-2}	6.78×10^{-4}	3.82×10^{-1}	1.32×10^{-2}	5.21×10^{-3}	0.417	9.38×10^{-18}
40	8.92×10^{-2}	1.19×10^{-2}	2.06×10^{-4}	5.64×10^{-3}	6.70×10^{-3}	1.34×10^{-3}	1.60×10^{-3}	1.03×10^{-2}	6.52×10^{-4}	3.81×10^{-1}	1.35×10^{-2}	5.34×10^{-3}	0.418	8.89×10^{-18}
44	8.95×10^{-2}	1.20×10^{-2}	1.93×10^{-4}	5.28×10^{-3}	6.28×10^{-3}	1.42×10^{-3}	1.58×10^{-3}	1.02×10^{-2}	6.89×10^{-4}	3.82×10^{-1}	1.27×10^{-2}	5.01×10^{-3}	0.416	9.15×10^{-18}

[a] Thermodynamic ionic product based on ions speciation $(([Ca^{2+}]\gamma^{2\pm})^3([Citr^{3-}]\gamma^{3\pm})^2)$, to be compared to the thermodynamic solubility product $K_{SP(Ca_3Citr_2)} = 7.60 \times 10^{-17}$ (Vavrusova & Skibsted, 2016).

calcium citrate, time elapsing prior to precipitation of calcium citrate is shorter as higher is the degree of supersaturation (Vavrusova, Garcia et al., 2017). In the present work though, the studied concentrations of calcium, citrate and phosphate were the same, but the pH resulting from the combinations of salts were different. The kinetics behind the precipitation from supersaturated solutions can be a complex matter, sugars crystallization, for example can change from a second to first order reaction (Hartel & Shastry, 1991). The precipitations of calcium citrate were investigated using the Avrami's model for crystallization (Avrami, 1939, 1940, 1941), which describes the changes in the volume of the crystals as a function of time. To use the Avrami model, the amount of calcium citrate precipitated in equilibrium was considered to be unity in the degree of crystallization. The results are shown in Fig. 7.

By the Avrami fits, the crystallization process of calcium citrate is very similar in both systems due to the values of the Avrami constant (k) of $0.229 \pm 0.003\,h^{-n}$ and $0.196 \pm 0.003\,h^{-n}$ for the second and third experiments, respectively, which are related to the crystals nucleation and growth rate, and Avrami exponents (n) of 4.1 ± 0.3 and 3.7 ± 0.3 for the second and third experiments, respectively, which indicates the growth morphology of the crystals (Sun et al., 1996); a k of 4 indicates a spherical growth (in all dimensions) for the crystals of calcium citrate.

A surprisingly robust supersaturation of calcium citrate is evident as an intermediate state during transformation of amorphous calcium phosphate to calcium citrate. The precipitation of calcium citrate takes place with a half-life of approximate 5 h for both investigated conditions. As may be seen from Tables 6 and 7, the calcium hydrogencitrate complex is dominating at pH 4.1, while the calcium citrate complex dominates at pH 5.5. Still a common precipitation reaction may be rate determining. According to the Avrami model for phase transition, the crystals growth occurs at the same rate in all directions and is independent of the degree of transformation. The rate determining reaction is suggested to be

$$CaHCitr_{(aq)} \rightarrow CaHCitr_{(s)} \tag{5}$$

followed by a solid state transformation to $Ca_3Citr_2 \cdot 4H_2O$. Such an initial precipitation of a less stable salt is further in agreement with Ostwald's rule of stages (Nývlt, 1995). For higher pH values, rapid ion equilibria may then reform CaHCitr in solution prior to precipitation.

Whey proteins and lactose are important sidestream products from whey processing. Better knowledge of the precipitation kinetics of calcium citrate and calcium phosphates, as obtained in the present study may help improve whey processing to avoid mineral coprecipitation with lactose and whey proteins, although more studies are clearly needed. The effect of citrate on the solubility of calcium phosphates from dairy products seems also of importance for the transformations of calcium salts during digestion. Most calcium compounds dissolves or dissociates in the gastric acid, but calcium salts may subsequently precipitate during the increasing pH of the intestines. The transformations between amorphous calcium phosphate and precipitated calcium citrate may also be relevant for understanding the function of citrate as a promoter of calcium absorption, since the long lag phase for calcium citrate precipitation would allow calcium absorption in the intestines.

4. Conclusions

A mechanism based on supersaturation and slow precipitation of calcium citrate is suggested to explain a possible high bioavailability, at least from physical chemical point of view, from the acidification of amorphous calcium phosphate in presence of citrate. This supersaturation phenomenon might occur in the organism during digestion, especially in the acidic stomach environment, and might also explain the increased calcium mobility in other physiological processes, like bone healing and biomineralization. These positive results are an incentive to investigate the supersaturation in more complexes systems

Table 7
Ion speciation for aqueous solution of $CaCl_2$, Na_2HCitr, and NaH_2PO_4 ($0.10 \, mol \, L^{-1}$) as function of time. Concentrations expressed in $mol \, L^{-1}$.

Time (h)	H_3PO_4	$H_2PO_4^-$	HPO_4^{2-}	H_3Citr	H_2Citr^-	$HCitr^{2-}$	$Citr^{3-}$	Ca^{2+}
0	6.20×10^{-4}	1.08×10^{-1}	4.22×10^{-4}	5.81×10^{-4}	1.08×10^{-2}	8.78×10^{-3}	3.09×10^{-4}	3.19×10^{-2}
1	6.12×10^{-4}	1.03×10^{-1}	3.90×10^{-4}	6.16×10^{-4}	1.11×10^{-2}	8.75×10^{-3}	2.99×10^{-4}	3.23×10^{-2}
2	7.19×10^{-4}	1.05×10^{-1}	3.47×10^{-4}	7.51×10^{-4}	1.18×10^{-2}	8.03×10^{-3}	2.38×10^{-4}	3.43×10^{-2}
3	1.01×10^{-3}	1.05×10^{-1}	2.43×10^{-4}	1.40×10^{-3}	1.55×10^{-2}	7.47×10^{-3}	1.56×10^{-4}	3.56×10^{-2}
4	1.05×10^{-3}	1.03×10^{-1}	2.27×10^{-4}	1.48×10^{-3}	1.57×10^{-2}	7.29×10^{-3}	1.47×10^{-4}	2.92×10^{-2}
8	1.64×10^{-3}	1.05×10^{-1}	1.46×10^{-4}	2.91×10^{-3}	2.03×10^{-2}	6.16×10^{-3}	8.13×10^{-5}	1.73×10^{-2}
12	1.73×10^{-3}	1.07×10^{-1}	1.44×10^{-4}	3.17×10^{-3}	2.13×10^{-2}	6.27×10^{-3}	7.99×10^{-5}	1.66×10^{-2}
16	1.66×10^{-3}	1.01×10^{-1}	1.33×10^{-4}	3.12×10^{-3}	2.07×10^{-2}	5.99×10^{-3}	7.53×10^{-5}	1.64×10^{-2}
20	1.76×10^{-3}	1.06×10^{-1}	1.38×10^{-4}	3.14×10^{-3}	2.06×10^{-2}	5.89×10^{-3}	7.31×10^{-5}	1.66×10^{-2}
24	1.71×10^{-3}	1.01×10^{-1}	1.30×10^{-4}	3.27×10^{-3}	2.11×10^{-2}	5.93×10^{-3}	7.25×10^{-5}	1.66×10^{-2}
28	1.78×10^{-3}	1.04×10^{-1}	1.32×10^{-4}	3.28×10^{-3}	2.10×10^{-2}	5.85×10^{-3}	7.07×10^{-5}	1.66×10^{-2}
32	1.73×10^{-3}	1.01×10^{-1}	1.29×10^{-4}	3.29×10^{-3}	2.11×10^{-2}	5.88×10^{-3}	7.12×10^{-5}	1.65×10^{-2}
36	1.75×10^{-3}	1.02×10^{-1}	1.29×10^{-4}	3.39×10^{-3}	2.16×10^{-2}	5.98×10^{-3}	7.20×10^{-5}	1.64×10^{-2}
40	1.80×10^{-3}	1.04×10^{-1}	1.32×10^{-4}	3.15×10^{-3}	2.00×10^{-2}	5.52×10^{-3}	6.62×10^{-5}	1.69×10^{-2}
44	1.72×10^{-3}	1.01×10^{-1}	1.27×10^{-4}	3.33×10^{-3}	2.12×10^{-2}	5.90×10^{-3}	7.13×10^{-5}	1.61×10^{-2}

Time (h)	$CaHCitr$	$CaCitr^-$	$CaHPO_4$	$NaHCitr^-$	Na^+	$NaCitr^{2-}$	I	Q^a
0	5.90×10^{-2}	1.13×10^{-2}	5.45×10^{-4}	4.88×10^{-4}	2.99×10^{-1}	6.52×10^{-3}	0.405	2.51×10^{-16}
1	5.96×10^{-2}	1.11×10^{-2}	5.11×10^{-4}	4.72×10^{-4}	2.99×10^{-1}	6.50×10^{-3}	0.404	2.45×10^{-16}
2	5.81×10^{-2}	9.36×10^{-3}	4.82×10^{-4}	3.77×10^{-4}	3.00×10^{-1}	5.98×10^{-3}	0.406	1.86×10^{-16}
3	5.61×10^{-2}	6.38×10^{-3}	3.51×10^{-4}	2.48×10^{-4}	3.01×10^{-1}	5.57×10^{-3}	0.407	8.96×10^{-17}
4	4.49×10^{-2}	4.90×10^{-3}	2.68×10^{-4}	2.32×10^{-4}	3.01×10^{-1}	5.44×10^{-3}	0.393	4.33×10^{-17}
8	2.25×10^{-2}	1.62×10^{-3}	1.02×10^{-4}	1.29×10^{-4}	3.02×10^{-1}	4.62×10^{-3}	0.368	2.80×10^{-18}
12	2.20×10^{-2}	1.52×10^{-3}	9.69×10^{-5}	1.27×10^{-4}	3.02×10^{-1}	4.69×10^{-3}	0.368	2.38×10^{-18}
16	2.07×10^{-2}	1.42×10^{-3}	8.87×10^{-5}	1.20×10^{-4}	3.02×10^{-1}	4.49×10^{-3}	0.364	2.04×10^{-18}
20	2.06×10^{-2}	1.39×10^{-3}	9.30×10^{-5}	1.17×10^{-4}	3.02×10^{-1}	4.42×10^{-3}	0.366	1.99×10^{-18}
24	2.09×10^{-2}	1.39×10^{-3}	8.77×10^{-5}	1.15×10^{-4}	3.02×10^{-1}	4.45×10^{-3}	0.364	1.98×10^{-18}
28	2.05×10^{-2}	1.35×10^{-3}	8.92×10^{-5}	1.13×10^{-4}	3.02×10^{-1}	4.38×10^{-3}	0.365	1.87×10^{-18}
32	2.05×10^{-2}	1.35×10^{-3}	8.63×10^{-5}	1.14×10^{-4}	3.02×10^{-1}	4.41×10^{-3}	0.364	1.86×10^{-18}
36	2.07×10^{-2}	1.35×10^{-3}	8.55×10^{-5}	1.15×10^{-4}	3.02×10^{-1}	4.48×10^{-3}	0.364	1.86×10^{-18}
40	1.97×10^{-2}	1.28×10^{-3}	9.02×10^{-5}	1.06×10^{-4}	3.02×10^{-1}	4.14×10^{-3}	0.365	1.72×10^{-18}
44	2.01×10^{-2}	1.32×10^{-3}	8.31×10^{-5}	1.14×10^{-4}	3.02×10^{-1}	4.43×10^{-3}	0.363	1.73×10^{-18}

[a] Thermodynamic ionic product based on ions speciation ($([Ca^{2+}]\gamma^{2\pm})^3([Citr^{3-}]\gamma^{3\pm})^2$), to be compared to the thermodynamic solubility product $K_{SP(Ca_3Citr_2)} = 7.60 \times 10^{-17}$ (Vavrusova & Skibsted, 2016).
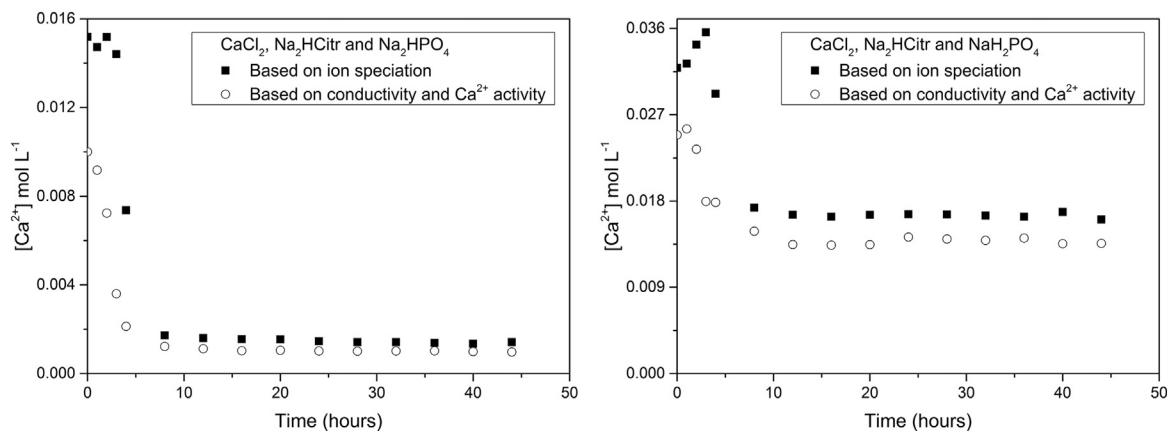
Fig. 6. Free calcium concentrations based on the ion speciation from the thermodynamic model (filled points) and based on experimental conductivity and calcium ion activity (open points).
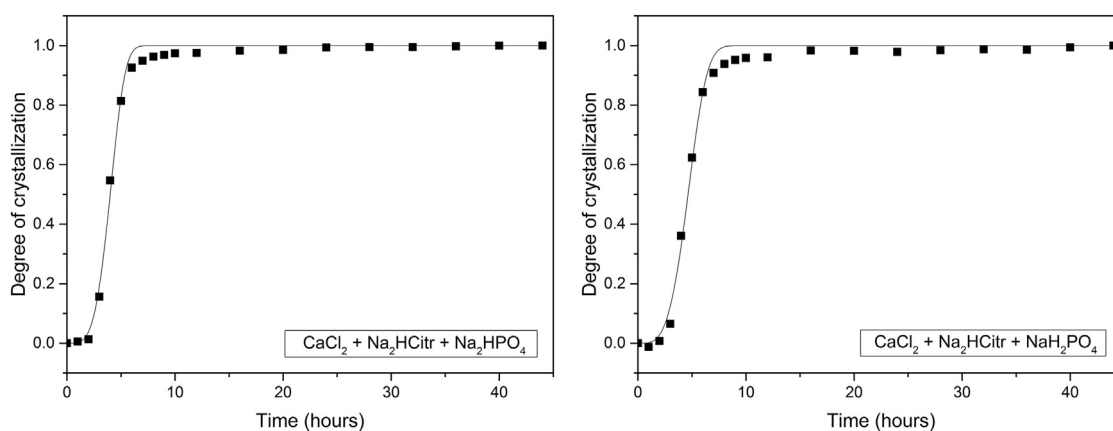

Fig. 7. Plots of degree of crystallization of calcium citrate as function of time using Avrami model ($F = 1 - e^{(-(kt)^a)}$).

with presence of biomolecules, such as whey proteins. Besides that, this phenomenon could be an inspiration for the development of new functional foods and/or supplements with higher contents of available calcium, taking into account that the inadequate intake or malabsorption of calcium is a major concern related to bone diseases, such as osteoporosis, especially in elderly populations.

Conflict of interest

The authors declare no competing interests.

References

Adluri, R. S., Zhan, L., Bagchi, M., Maulik, N., & Maulik, G. (2010). Comparative effects of a novel plant-based calcium supplement with two common calcium salts on proliferation and mineralization in human osteoblast cells. *Molecular and Cellular Biochemistry, 340*(1), 73–80.

Avrami, M. (1939). Kinetics of phase change. I general theory. *The Journal of Chemical Physics, 7*(12), 1103–1112.

Avrami, M. (1940). Kinetics of phase change. II transformation - time relations for random distribution of nuclei. *The Journal of Chemical Physics, 8*(2), 212–224.

Avrami, M. (1941). Granulation, phase change, and microstructure kinetics of phase change. III. *The Journal of Chemical Physics, 9*(2), 177–184.

Bates, R. G., & Pinching, G. D. (1949). Resolution of the dissociation constants of citric acid at 0 to 50°, and determination of certain related thermodynamic functions. *Journal of the American Chemical Society, 71*(4), 1274–1283.

Bronner, F. (1987). Intestinal calcium absorption: Mechanisms and applications. *The Journal of Nutrition, 117*(8), 1347–1352.

Costello, L. C., Franklin, R. B., Reynolds, M. A., & Chellaiah, M. (2012). The important role of osteoblasts and citrate production in bone formation: "Osteoblast citration" as a new concept for an old relationship. *The Open Bone Journal, 4*, 27–34.

Daniele, P. G., Foti, C., Gianguzza, A., Prenesti, E., & Sammartano, S. (2008). Weak alkali and alkaline earth metal complexes of low molecular weight ligands in aqueous solution. *Coordination Chemistry Reviews, 252*(10), 1093–1107.

Davies, C. W. (1962). *Ion association.* Washington: Butterworths.

Davies, C. W., & Hoyle, B. E. (1953). The interaction of calcium ions with some phosphate and citrate buffers. *Journal of the Chemical Society,* 4134–4136 (0).

Diaz de Barboza, G., Guizzardi, S., & Tolosa de Talamoni, N. (2015). Molecular aspects of intestinal calcium absorption. *World Journal of Gastroenterology, 21*(23), 7142–7154.

Garcia, A. C., Vavrusova, M., & Skibsted, L. H. (2016). Calcium d-saccharate: Aqueous solubility, complex formation, and stabilization of supersaturation. *Journal of Agricultural and Food Chemistry, 64*(11), 2352–2360.

Garnsworthy, P. C., Masson, L. L., Lock, A. L., & Mottram, T. T. (2006). Variation of milk citrate with stage of lactation and de novo fatty acid synthesis in dairy cows. *Journal of Dairy Science, 89*(5), 1604–1612.

Griffin, B. A., & Jurinak, J. J. (1973). Estimation of activity coefficients from electrical conductivity of natural systems and soil extracts. *Soil Science, 116*(1), 26–30.

Hartel, R. W., & Shastry, A. V. (1991). Sugar crystallization in food products. *Critical Reviews in Food Science and Nutrition, 30*(1), 49–112.

Hershey, P. J., Fernandez, M., & Millero, F. J. (1989). The dissociation of phosphoric acid in NaCl and NaMgCl solutions at 25 °C. *Journal of Solution Chemistry, 18*(9), 875–891.

Hess, J. M., Jonnalagadda, S. S., & Slavin, J. L. (2016). Dairy foods: Current evidence of their effects on bone, cardiometabolic, cognitive, and digestive health. *Comprehensive Reviews in Food Science and Food Safety, 15*(2), 251–268.

Holt, C., Van Kemenade, M. J. J. M., Nelson, L. S., Hukins, D. W. L., Bailey, R. T., Harries, J. E., ... De Bruyn, P. L. (1989). Amorphous calcium phosphates prepared at pH 6.5 and 6.0. *Materials Research Bulletin, 24*(1), 55–62.

Iafisco, M., Ramirez-Rodriguez, G. B., Sakhno, Y., Tampieri, A., Martra, G., Gomez-Morales, J., & Delgado-Lopez, J. M. (2015). The growth mechanism of apatite nanocrystals assisted by citrate: Relevance to bone biomineralization. *CrystEngComm, 17*(3), 507–511.

Krukowski, S., Karasiewicz, M., & Kolodziejski, W. (2017). Convenient UV-spectrophotometric determination of citrates in aqueous solutions with applications in the pharmaceutical analysis of oral electrolyte formulations. *Journal of Food and Drug Analysis, 25*(3), 717–722.

Kutus, B., Ozsvar, D., Varga, N., Palinko, I., & Sipos, P. (2017). ML and ML$_2$ complex formation between ca(ii) and d-glucose derivatives in aqueous solutions. *Dalton Transactions, 46*(4), 1065–1074.

Lenton, S., Nylander, T., Teixeira, S. C. M., & Holt, C. (2015). A review of the biology of calcium phosphate sequestration with special reference to milk. *Dairy Science & Technology, 95*(1), 3–14.

Márquez, A. L., Salvatore, G. N., Otero, R. G., Wagner, J. R., & Palazolo, G. G. (2015). Impact of freeze-thaw treatment on the stability of calcium-fortified soy beverages. *LWT - Food Science and Technology, 62*(1, Part 2), 474–481.

Nývlt, J. (1995). The Ostwald rule of stages. *Crystal Research and Technology, 30*(4), 443–449.

Rasyid, F., & Hansen, P. M. T. (1991). Stabilization of soy milk fortified with calcium gluconate. *Food Hydrocolloids, 4*(5), 415–422.

Shreiner, R. H., & Pratt, K. W. (2004). *Standard reference materials: Primary standards and standard reference materials for electrolytic conductivity.* Washington: NIST: National Institute of Standards and Technology.

Skibsted, L. H. (2016). Mineral nutrient interaction: Improving bioavailability of calcium and iron. *Food Science and Biotechnology, 25*(5), 1233–1241.

Sun, N. X., Liu, X. D., & Lu, K. (1996). An explanation to the anomalous Avrami exponent. *Scripta Materialia, 34*(8), 1201–1207.

Vavrusova, M., Danielsen, B. P., Garcia, A. C., & Skibsted, L. H. (2018). Codissolution of calcium hydrogenphosphate and sodium hydrogencitrate in water. Spontaneous supersaturation of calcium citrate increasing calcium bioavailability. *Journal of Food and Drug Analysis, 26*, 330–336.

Vavrusova, M., Garcia, A. C., Danielsen, B. P., & Skibsted, L. H. (2017). Spontaneous supersaturation of calcium citrate from simultaneous isothermal dissolution of sodium citrate and sparingly soluble calcium hydroxycarboxylates in water. *RSC Advances, 7*(6), 3078–3088.

Vavrusova, M., Johansen, N. P., Garcia, A. C., & Skibsted, L. H. (2017). Aqueous citric acid as a promising cleaning agent of whey evaporators. *International Dairy Journal, 69*, 45–50.

Vavrusova, M., Liang, R., & Skibsted, L. H. (2014). Thermodynamics of dissolution of calcium hydroxycarboxylates in water. *Journal of Agricultural and Food Chemistry, 62*(24), 5675–5681.

Vavrusova, M., & Skibsted, L. H. (2014). Spontaneous supersaturation of calcium D-gluconate during isothermal dissolution of calcium L-lactate in aqueous sodium d-gluconate. *Food & Function, 5*(1), 85–91.

Vavrusova, M., & Skibsted, L. H. (2016). Aqueous solubility of calcium citrate and interconversion between the tetrahydrate and the hexahydrate as a balance between endothermic dissolution and exothermic complex formation. *International Dairy Journal, 57*, 20–28.

Wang, L., Wang, W., Li, X., Peng, L., Lin, Z., & Xü, H. (2012). Calcium citrate: A new biomaterial that can enhance bone formation in situ. *Chinese Journal of Traumatology, 15*(5), 291–296.